DISSERTATION

Two-body sfermion decays at full one-loop level within the MSSM [1]

Verfasserin

Mgr. Hana Hluchá

---

[1] corrected version

Declaration

I honestly declare that I have written the submitted PhD thesis myself and I have used only the literature mentioned in the bibliography.

....
Mgr. Hana Hluchá

Kurzfassung

Der LHC hat seinen Betrieb aufgenommen. Somit sind wir in der Lage die Teilchenphysik auf der TeV Skala zu untersuchen, womit aller Wahrscheinlichkeit nach die Entdeckung neuer Teilchen einhergeht. Daher sind theoretische Vorhersagen von Wirkungsquerschnitten, Zerfallsbreiten sowie Massen unerlässlich.

Das Ziel dieser Arbeit war die Berechechnung von Zweikörperzerfällen von Sfermionen, welche von der minimal supersymmetrischen Erweiterung des Standardmodells (MSSM) vorausgesagt werden. Die Arbeit wurde in Übereinstimmung mit der Supersymmetry Parameter Analysis (SPA) Konvention durchgeführt, welche eine klares Regelwerk für die zu verwendenden Parameter darstellet. Dadurch sind die Resultate verschiedener Gruppen wesentlich einfacher miteinander zu vergleichen.

Das in der SPA Konvention definierte Renormierungsschema ist das sogenannte modifizierte minimale Subtraktionschema (DRbar), in der dimensionale Reduktion anstatt dimensionaler Regularisierung verwendet wird. Dieses Renormierungsschema ist konsistent mit Supersymmetrie, da die äquivalente Beschreibung von fermionischen und bosonischen Freiheitsgraden erhalten bleibt. Die Eingabeparameter werden im DRbar Schema auf einer Skala von 1 TeV definiert.

Da sich auf vollem Einschleifenniveau eine sehr groe Anzahl von Feymangraphen ergibt, ist die Verwendung von Computerprogrammen für deren Berechung erforderlich. Für die Generation der Feynman Amplituden wurde das Programmpaket FeynArts benützt. Die folgende tensorielle Reduktion und Übersetzung zu Fortran Programmcode wurde mit Hilfe des Programmpakets FormCalc durchgeführt, welches auf Mathetmatica und Form basiert. Die Numerische Auswertung der Passarino-Veltman Integrale erfolgte mit LoopTools. Der resultierende Programmcode wurde anschliessend in ein eigenes Programm implementiert. Für die Renormierungsprozedur mussten aller erforderlichen Counterterme inkludiert werden, um UV konvergente Resultate zu erhalten. Um auch IR konvergent Resultate zu erzielen musste die Photon- sowie Gluonabstrahlung berücksichtigt werden. Die Ergebnisse werden in dem Programmpaket SFOLD(Sfermion Full One Loop Decays) öffentlich verfügbar gemacht.

Das erste Kapitel der Dissertation führt das minimal supersymmetrische Standardmodell ein. Weiters werden kurz das CMSSM Model, das AMSB und GMSB

Model sowie deren experimentelle Limits diskutiert. Im zweiten Kapitel wird die Renommierung des gesamten MSSM abgehandelt. Im dritten Kapitel werden alle relevanten Sfermion - Zweikörperzerflle erläutert. Das letzte Kapitel stellt den eigentlichen Kern dieser Dissertation dar, in dem ausführlich Szenarien präsentiert werden, in denen die elektroschwachen Korrekturen nicht vernachlässigbar sind. Dies betrifft die bosonischen Sfermionzerfaelle.

Abstract

The Large Hadron Collider has started its operation. We are thus able to probe particle physics at the Tera scale at which new particles may be discovered. Therefore, theoretical predictions for their properties are mandatory. Many observables in many new theories have been calculated including masses, decay widths, cross-sections and other measurable quantities. The aim of this thesis is the calculation of the widths of all two-body sfermion decays predicted by the Minimal Supersymmetric extension of the Standard Model (MSSM) at the full one loop level.

This work is done within the Supersymmetry Paramter Analysis (SPA) framework, based on a consistent set of conventions and input parameters. Such a unified scheme enables cross-checking of results from different calculations and minimizes possible confusion.

The renormalization scheme defined in the SPA convention is the so-called modified minimal subtraction (DRbar) using dimensional reduction scheme instead of dimensional regularization. This scheme is applicable to supersymmetric theories and preserves the equality of bosonic and fermionic degrees of freedom. The DRbar running input parameters are defined in the SPA convention at 1 TeV.

In order to deal with such a huge number of one-loop Feynman graphs it is inevitable to use packages for automatic calculations. For the creation of the Feynman graphs the Mathematica package FeynArts was used.

For the translation of the amplitudes to Fortran I used the package FormCalc which is based on Mathematica and Form. The occurring one-loop Passarino-Veltman integrals were evaluated using LoopTools.

The numerical code produced in this way was put into an own program. Doing the renormalization procedure all necessary counterterms had to be included to get an ultraviolet finite result. For the result to be also infrared convergent, photon and gluon bremsstrahlung were considered. In two-particle decays the so-called bremsstrahlung integrals were used.

The author of this work provides a numerical package named SFOLD (Sfermion Full One Loop Decays).

The thesis is organized as follows. The first chapter introduces the MSSM, its lagrangian and the mass spectrum. Furthermore, it also briefly discusses the

CMSSM model, the GMSB model, the AMSB model as well as the experimental constraints for all four above mentioned models. The second chapter focuses on the renormalization of the whole MSSM model. The third chapter discusses two-body sfermion decays and the three basic configurations. I provide also results for the hard photon radiation. The core of this thesis is the fourth chapter presenting many plots including those where we clearly can see that the electroweak corrections cannot be neglected. This applies also to the bosonic decays.

Acknowledgments

First of all, I wish to thank my supervisor Prof. Walter Majeroto for giving me helpful comments and for proofreading my thesis.

I would like to thank Dr. Helmut Eberl for many discussions and for being my second thesis father.

My thanks also goes to my theory colleagues and friends Sebastian Frank, Wolfgang Frisch, Elena Ginina, Robert Schoefback and Bernard Schrausser.

I am also very thankful to all workers at the HEPHY institute, especially to our administrators.

Last but not least, I would like to thank my parents for always being there, my two brothers, my fiance Tomas and Bujnak family which became my second family.

Contents

List of Figures

List of Tables

Chapter 1

Introduction

1.1 Why supersymmetry?

Supersymmetry (SUSY) has been around since 1971-74 [1, 2, 3]. It was not introduced to solve any of the problems of the Standard Model (SM). Symmetry considerations have often in the past led to success. When fermionic generators (they transform a bosonic state into fermionic and vice versa) appeared on the scene, Haag, Lopuszanski and Sohnius found a way around the *Coleman-Mandula no-go theorem* [4] which states that any symmetry compatible with an interacting relativistic quantum field theory is of the form of a direct product of the Poincaré algebra with an internal symmetry (such as gauge symmetry). However, Coleman and Mandula considered only bosonic generators. *Haag-Lopuszanski-Sohnius theorem* [5] extends the Poincaré algebra in a non-trivial way to the super Poincaré algebra. The simplest superalgebra involves only one set of the fermionic generators Q_α [6, 7, 8]:

$$[P^\mu, P^\nu] = 0 \tag{1.1}$$

$$[M^{\mu\nu}, P^\lambda] = i(\eta^{\nu\lambda}P^\mu - \eta^{\mu\lambda}P^\nu) \tag{1.2}$$

$$[M^{\mu\nu}, M^{\rho\sigma}] = i(\eta^{\nu\rho}M^{\mu\sigma} + \eta^{\mu\sigma}M^{\nu\rho} - \eta^{\mu\rho}M^{\nu\sigma} - \eta^{\nu\sigma}M^{\mu\rho}) \tag{1.3}$$

$$[P^\mu, Q_a] = 0 = [P^\mu, Q_{\dot{a}}] \tag{1.4}$$

$$[M^{\mu\nu}, Q_a] = -i(\sigma^{\mu\nu})_a{}^b Q_b \tag{1.5}$$

$$[M^{\mu\nu}, Q^{\dot{a}}] = -i(\bar{\sigma}^{\mu\nu})^{\dot{a}}{}_{\dot{b}} Q^{\dot{b}} \tag{1.6}$$

$$\{Q_a, Q_b\} = 0 = \{Q_{\dot{a}}, Q_{\dot{b}}\} \tag{1.7}$$

$$\{Q_a, Q_{\dot{b}}\} = 2\sigma^\mu_{a\dot{b}} P_\mu \tag{1.8}$$

Already the purely theoretical considerations provide a strong motivation for supersymmetry. Nature seems to respect symmetries, particularly the Poincaré symmetry. At the same time, the only way how to increase this symmetry is supersymmetry.

On top of that, the existence of space-time supersymmetry is suggested by the string theory [9].

There are a number of theoretical and phenomenological issues that the SM fails to address adequately, contrary to the supersymmetric theories [10]:

- *Unification with gravity*
  The supersymmetry algebra (1.8) contains the generator of translations P_μ. One can therefore consider translations varying from point to point in space-time. This 'local supersymmetry' is then a theory of general coordinate transformations of space-time and so a theory of gravity [11].

- *Gauge coupling unification*
  In contrast to SM, SUSY allows for the gauge coupling unification. The extrapolation of the low energy values of the gauge couplings using renormalization group equations shows that the gauge couplings unify at the scale 10^{16} GeV [12]. This quality lends credence to the picture of grand unified theories (GUTs) and certain string theories. Precise measurements of the low energy values of the gauge coupling demonstrated that the SM cannot describe gauge coupling unification.

- *Hierarchy problem*
  Phenomenologically, the mass of the Higgs boson associated with the electroweak symmetry breaking must be in the electroweak range. However, radiative corrections to the Higgs mass are quadratically dependent on the UV cutoff Λ, since the masses of the fundamental scalar fields are not protected by chiral or gauge symmetries. The "natural" value of the Higgs mass is therefore of $O(\Lambda)$ rather than $O(100 GeV)$, which leads to a destabilization of the hierarchy of the mass scales in the SM.
  SUSY introduces new particles into the theory that couple to the Higgs and appear in the loop. These particles cancel the quadratic divergence due to an additional factor (-1) coming from Fermi statistics. The cancelation is true up to the SUSY breaking scale, M_{susy}, since

  $$\sum_{\text{bosons}} m^2 - \sum_{\text{fermions}} m^2 = M_{\text{susy}}^2 \tag{1.9}$$

  which should not be very large (≤ 1 TeV) to make the fine-tuning natural. Thus SUSY provides a solution to the hierarchy problem by protecting the electroweak scale from large radiative corrections [13].

- *Electroweak symmetry breaking (EWSB)*
  In the SM, electroweak symmetry breaking is parametrized by the Higgs boson h and its potential $V(h)$. However, the Higgs sector is not constrained by any

2

symmetry principles, the negativeness of the parameter μ^2 is put into the theory by hand.

In supersymmetry, at least one of the mass parameters from the Higgs potential decreases while running from the GUT scale to the electroweak scale and may even change the sign. This leads to the potential with a non-trivial minimum. The phenomenon is known as *radiative electroweak symmetry breaking*. The Higgs field vacuum expectation values have nonzero values and provide masses to fermions, gauge bosons and masses to their superpartners [14].

- *Dark matter*
  In supersymmetric theories with conserved R-parity the lightest superpartner (LSP) is stable. The LSP particle provides a very good candidate for the non-baryonic cold dark matter [15]. This was noticed even before the need for cold dark matter was established.

Supersymmetry has already made several correct predictions:

- Supersymmetry predicted that the top quark would be heavy [16]. This is a necessary condition for the explanation of the electroweak symmetry breaking.

- Supersymmetric grand unified theories with a high fundamental scale predicted the present experimental value of $\sin^2 \theta_W$ [17].

- Supersymmetry requires the existence of a light Higgs boson [18] which is consistent with current precision measurements.

1.2 Supersymmetric Lagrangian

The fully supersymmetric and locally gauge invariant lagragian that describes the renormalized interactions of scalar, spinor and vector fields reads [19, 20]

$$\mathcal{L} = \frac{1}{16kg^2}\text{Tr}\left(W^a W_a\Big|_{\theta\theta} + W_{\dot{a}} W^{\dot{a}}\Big|_{\bar{\theta}\bar{\theta}}\right) + \Phi^\dagger e^{2gV}\Phi\Big|_{\theta\theta\bar{\theta}\bar{\theta}} + \left(W + \text{h.c.}\right) \qquad (1.10)$$

where W is called the superpotential and represents the products of chiral superfields Φ. $W_a, W_{\dot{a}}$ are called field strength superfields and are given by

$$
\begin{aligned}
W_a &= -\frac{1}{4}(\bar{D}\bar{D})D_a V \\
W_{\dot{a}} &= -\frac{1}{4}(DD)D_{\dot{a}} V
\end{aligned}
\qquad (1.11)
$$

where $D_a, D^{\dot{a}}$ are the covariant derivatives

$$
\begin{aligned}
D_a &= \partial_a - i(\sigma^\mu)_{a\dot{b}}\theta^{\dot{b}}\partial_\mu \\
D^{\dot{a}} &= \partial^{\dot{a}} - i(\bar{\sigma}^\mu)^{\dot{a}b}\theta_b\partial_\mu
\end{aligned}
\qquad (1.12)
$$

3

and V is a vector superfield in the so-called Wess-Zumino gauge

$$V_{WZ}(x,\theta,\bar{\theta}) = \theta\sigma^{\mu}\bar{\theta}V_{\mu}(x) + i(\theta\theta)\bar{\theta}\bar{\lambda}(x) - i(\bar{\theta}\bar{\theta})\theta\lambda(x) + \frac{1}{2}(\theta\theta)(\bar{\theta}\bar{\theta})D(x) \qquad (1.13)$$

Finally, the (left-handed) chiral superfield reads

$$\begin{aligned}
\Phi(x,\theta,\bar{\theta}) &= \phi(x) + \sqrt{2}\theta\psi(x) + (\theta\theta)F(x) - i\partial_{\mu}\phi(x)\theta\sigma^{\mu}\bar{\theta} \\
&+ \frac{i}{\sqrt{2}}(\theta\theta)\partial_{\mu}\psi(x)\sigma^{\mu}\bar{\theta} - \frac{1}{4}(\theta\theta)(\bar{\theta}\bar{\theta})\partial_{\mu}\partial^{\mu}\phi(x) \qquad (1.14)
\end{aligned}$$

The component field $\psi(x)$ is a Weyl spinor and $\phi(x)$ is its scalar superpartner (fermion and sfermion). The component field $V_{\mu}(x)$ is a vector field and $\lambda(x)$ is its fermionic superpartner (gauge boson and gaugino). The fields $F(x)$ and $D(x)$ are auxialiary fields having no kinetic term in the lagrangian. The component expansion of the supersymmetric and gauge invariant lagrangian for a renormalizable nonabelian theory (not considering superpotential) is

$$\begin{aligned}
\mathcal{L} &= i\lambda^{(a)}\sigma^{\mu}\mathscr{D}_{\mu}\bar{\lambda}^{(a)} - \frac{1}{4}F_{\mu\nu}^{(a)}F^{(a)\,\mu\nu} + \frac{1}{2}D^{(a)}D^{(a)} + i(\bar{\psi}_{i}\bar{\sigma}^{\mu}\mathscr{D}_{\mu}\psi_{i}) + F_{i}^{*}F_{i} \\
&+ (\mathscr{D}_{\mu}\phi_{i})^{*}(\mathscr{D}^{\mu}\phi_{i}) + i\sqrt{2}gT_{ij}^{(a)}[\phi_{i}^{*}(\lambda^{(a)}\psi_{j}) - (\bar{\lambda}^{(a)}\bar{\psi}_{i})\phi_{j}] \\
&+ gD^{(a)}T_{ij}^{(a)}\phi_{i}^{*}\phi_{j} \qquad (1.15)
\end{aligned}$$

where the covariant derivatives and the non-abelian field strength tensor are

$$\begin{aligned}
\mathscr{D}_{\mu}\bar{\lambda}^{(a)} &= \partial_{\mu}\bar{\lambda}^{(a)} - gf^{abc}V_{\mu}^{(b)}\bar{\lambda}^{(c)} \\
F_{\mu\nu}^{(a)} &= \partial_{\mu}V_{\nu}^{(a)} - \partial_{\nu}V_{\mu}^{(a)} - gf^{abc}V_{\mu}^{(b)}V_{\nu}^{(c)} \\
\mathscr{D}_{\mu}\psi &= \partial_{\mu}\psi + igV_{\mu}\psi \\
\mathscr{D}_{\mu}\phi &= \partial_{\mu}\phi + igV_{\mu}\phi \qquad (1.16)
\end{aligned}$$

1.3 The MSSM

The Minimal Supersymmetric Standard Model (MSSM) extends the Standard Model in a minimal manner. That means, incorporating only one set of SUSY generators into the theory. Moreover, in the MSSM one makes the minimal choice of the Higgs sector. In supersymmetric theories one needs two complex Higgs doublets to give mass to both the up-type and down-type fermions. This is because the superpotential must consist of the combinations of chiral superfields of the same handedness. One cannot simply use the complex conjugate of the Higgs doublet as in the Standard Model otherwise the lagrangian would not be invariant under the supersymmetric transformations. The MSSM field content is summarized in the

Superfield	Particle	Spin	G	Superpartner	Spin
$\hat{V}_1$	B_μ	1	(1, 1, 0)	$\tilde{B}$	$\frac{1}{2}$
$\hat{V}_2$	W_μ^i	1	(1, 3, 0)	$\tilde{W}^i$	$\frac{1}{2}$
$\hat{V}_3$	G_μ^a	1	(8, 1, 0)	$\tilde{g}^a$	$\frac{1}{2}$
$\hat{Q}$	$Q = (u_L, d_L)$	$\frac{1}{2}$	$(3, 2, \frac{1}{3})$	$\tilde{Q} = (\tilde{u}_L, \tilde{d}_L)$	0
$\hat{U}^c$	$U^c = \bar{u}_R$	$\frac{1}{2}$	$(3^*, 1, -\frac{4}{3})$	$\tilde{U}^c = \tilde{u}_R^*$	0
$\hat{D}^c$	$D^c = \bar{d}_R$	$\frac{1}{2}$	$(3^*, 1, \frac{2}{3})$	$\tilde{D}^c = \tilde{d}_R^*$	0
$\hat{L}$	$L = (\nu_L, e_L)$	$\frac{1}{2}$	(1, 2, -1)	$\tilde{L} = (\tilde{\nu}_L, \tilde{e}_L)$	0
$\hat{E}^c$	$E^c = \bar{e}_R$	$\frac{1}{2}$	(1, 1, 2)	$\tilde{E}^c = \tilde{e}_R^*$	0
$\hat{H}_1$	$H_1 = (H_1^0, H_1^-)$	0	(1, 2, -1)	$\tilde{H}_1 = (\tilde{H}_1^0, \tilde{H}_1^-)$	$\frac{1}{2}$
$\hat{H}_2$	$H_2 = (H_2^+, H_2^0)$	0	(1, 2, 1)	$\tilde{H}_2 = (\tilde{H}_2^+, \tilde{H}_2^0)$	$\frac{1}{2}$

Table 1.1: Particle content of the MSSM.

following table (Tab. 1.1). G stands for $\mathrm{SU(3)}_C \otimes \mathrm{SU(2)}_W \otimes \mathrm{U(1)}_Y$.

The lagrangian of the MSSM can be written in the following way [21]

$$\mathcal{L}_{\mathrm{MSSM}} = \mathcal{L}_{\mathrm{kinetic}} - V_Y - V_F - V_D - V_{\tilde{G}\psi\tilde{\psi}} + \mathcal{L}_{\mathrm{soft}} \qquad (1.17)$$

where the $\mathcal{L}_{\mathrm{kinetic}}$ contains the standard kinetic terms including gauge interactions with the gauge bosons. The terms $V_Y, V_F, V_D, V_{\tilde{G}\psi\tilde{\psi}}$ stand for all interaction that are allowed in the supersymmetric theory and the $\mathcal{L}_{\mathrm{soft}}$ includes the soft supersymmetry breaking terms.

Superpotential

$$W = -\varepsilon_{ij}\left[h_e \hat{H}_1^i \hat{L}^j \hat{E}^c + h_d \hat{H}_1^i \hat{Q}^j \hat{D}^c + h_u \hat{H}_2^j \hat{Q}^i \hat{U}^c - \mu \hat{H}_1^i \hat{H}_2^j\right] + \mathrm{h.c.} \qquad (1.18)$$

where $\varepsilon_{12} = -1$. By writing the superpotential we have suppressed possible generation indices on superfields. The superpotential gives rise to two kind of interactions described by the Yukawa potential V_Y and the so-called F-term potential V_F.

The Yukawa potential

5

The Yukawa potential is obtained by substituting two of the superfields by their fermionic content and the remaining superfield (if something remains) by its scalar content. The result is

$$
\begin{aligned}
V_Y &= -\varepsilon_{ij}\left[h_e H_1^i L^j E^c + h_d H_1^i Q^j D^c + h_u H_2^j Q^i U^c - \mu \tilde{H}_1^i \tilde{H}_2^j\right] \\
&\quad - \varepsilon_{ij}\left[h_e \tilde{H}_1^i L^j \tilde{E}^c + h_d \tilde{H}_1^i Q^j \tilde{D}^c + h_u \tilde{H}_2^j Q^i \tilde{U}^c\right] \\
&\quad - \varepsilon_{ij}\left[h_e \tilde{H}_1^i \tilde{L}^j E^c + h_d \tilde{H}_1^i \tilde{Q}^j D^c + h_u \tilde{H}_2^j \tilde{Q}^i U^c\right] + \text{h.c.}
\end{aligned}
\tag{1.19}
$$

The F-term potential

The F-term potential arises after using the Lagrange-Euler equations of motion for the auxiliary field F and substituting them back into the lagrangian. The F-term superpotential is then given by

$$
V_F = \sum_i \left|\frac{\partial W(\phi)}{\partial \phi_i}\right|^2
\tag{1.20}
$$

where ϕ_i are the scalar components of the superfields.

The D-term potential

This potential comes, analogously as in the case of F-term potential, from eliminating the auxiliary field D using the equation of motion and substituting back into the lagrangian. The D-term potential is given by

$$
V_D = \frac{1}{2}\sum_a D^a D^a
\tag{1.21}
$$

where

$$
D^a = -g^a \phi_i^* T_{ij}^{(a)} \phi_j
\tag{1.22}
$$

The ϕ_i are the scalar components of the superfields and the $T^{(a)}(\,(a) \leftrightarrow {}', i, a)$ are the generators of the particular gauge symmetry.

The $V_{\tilde{G}\psi\tilde{\psi}}$ potential

This potential represents the interaction of the gauginos.

$$
V_{\tilde{G}\psi\tilde{\psi}} = i\sqrt{2}g T_{ij}^{(a)}(\bar{\lambda}^{(a)}\bar{\psi}_i)\phi_j - i\sqrt{2}g T_{ij}^{(a)}\phi_i^*(\lambda^{(a)}\psi_j)
\tag{1.23}
$$

6

where ϕ, ψ are the scalar, resp. fermionic components of the chiral superfield and $\lambda^{(a)}$ is the gaugino field.

The $\mathcal{L}_{\text{soft}}$ lagrangian

We do know that supersymmetry must be broken since we have not observed SUSY particles at the mass scale of the SM particles. The MSSM does not explain the origin of the SUSY breaking, it only parametrizes our ignorance about the true mechanism by introducing additional terms in the lagrangian breaking the supersymmetry explicitly, but softly, meaning that we do not consider any dimensionless SUSY-breaking couplings which would reintroduce quadratic divergences in the theory.

$$
\begin{aligned}
-\mathcal{L}_{\text{soft}} &= m_{H_1}^2 |H_1|^2 + m_{H_2}^2 |H_2|^2 - m_{12}^2 \varepsilon_{ij}(H_1^i H_2^j + H_1^{\dagger i} H_2^{\dagger j}) \\
&- \varepsilon_{ij}\left(h_e A_e H_1^i \tilde{L}^j \tilde{E}^c + h_d A_d H_1^i \tilde{Q}^j \tilde{D}^c + h_u A_u H_2^j \tilde{Q}^i \tilde{U}^c + \text{h.c.}\right) \\
&+ M_{\tilde{Q}}^2 |\tilde{q}_L|^2 + M_{\tilde{U}}^2 |\tilde{u}_R^c|^2 + M_{\tilde{D}}^2 |\tilde{d}_R^c|^2 + M_{\tilde{L}}^2 |\tilde{l}_L|^2 + M_{\tilde{E}}^2 |\tilde{e}_R^c|^2 \\
&+ \frac{1}{2} m_{\tilde{g}} \tilde{g}^a \tilde{g}^a + \frac{1}{2} M \tilde{W}^i \tilde{W}^i + \frac{1}{2} M' \tilde{B} \tilde{B}
\end{aligned}
\tag{1.24}
$$

where we have introduced the SUSY-breaking mass parameters $m_{H_1}^2$, $m_{H_2}^2$, m_{12}^2, $m_{\tilde{g}}$, M, M', $M_{\tilde{Q}}^2$, $M_{\tilde{U}}^2$, $M_{\tilde{D}}^2$, $M_{\tilde{L}}^2$, $M_{\tilde{E}}^2$ as well as the SUSY-breaking trilinear scalar couplings A_e, A_u, A_d. The price paid is 105 new real constants if we allow for complex parameters.

1.4 Particle spectrum of the MSSM

1.4.1 Higgs sector

The potential for the Higgs fields reads

$$
\begin{aligned}
V &= m_1^2 |H_1|^2 + m_2^2 |H_2|^2 - m_{12}^2 \varepsilon_{ij}(H_1^i H_2^j + H_1^{\dagger i} H_2^{\dagger j}) \\
&+ \frac{1}{8}(g^2 + g'^2)(|H_1|^2 - |H_2|^2)^2 + \frac{1}{2} g^2 |H_1^\dagger H_2|^2
\end{aligned}
\tag{1.25}
$$

where $m_{1,2}^2 = m_{H_{1,2}}^2 + |\mu|^2$. Both neutral Higgs boson fields acquire a non-vanishing vacuum expectation value (VEV)

$$
\langle H_1 \rangle = \begin{pmatrix} \frac{v_1}{\sqrt{2}} \\ 0 \end{pmatrix}, \qquad \langle H_2 \rangle = \begin{pmatrix} 0 \\ \frac{v_2}{\sqrt{2}} \end{pmatrix}
\tag{1.26}
$$

The doublets are parametrized in the following way

$$H_1 \equiv \begin{pmatrix} H_1^0 \\ H_1^- \end{pmatrix} = \begin{pmatrix} (v_1 + \phi_1^0 + i\chi_1^0)/\sqrt{2} \\ \phi_1^- \end{pmatrix}, \qquad Y_{H_1} = -1 \qquad (1.27)$$

$$H_2 \equiv \begin{pmatrix} H_2^+ \\ H_2^0 \end{pmatrix} = \begin{pmatrix} \phi_2^+ \\ (v_2 + \phi_2^0 + i\chi_2^0)/\sqrt{2} \end{pmatrix}, \qquad Y_{H_2} = +1 \qquad (1.28)$$

The gauge bosons are made massive after electro-weak symmetry breaking. Because their masses are functions of v_1, v_2, their experimentally measured values can fix one of the VEVs as can be seen from relations

$$m_Z^2 = \frac{g^2 + g'^2}{4}(v_1^2 + v_2^2), \qquad m_W^2 = \frac{g^2}{4}(v_1^2 + v_2^2) \qquad (1.29)$$

$$v^2 \equiv (v_1^2 + v_2^2) = \frac{4m_Z^2}{g^2 + g'^2} \approx (246\text{GeV})^2 \qquad (1.30)$$

The other VEV remains a free parameter of the theory. Conventionally, physisicts do not work with this parameter but introduce the angle β which is defined as

$$\tan\beta \equiv \frac{v_2}{v_1} \geq 0, \qquad 0 \leq \beta \leq \frac{\pi}{2} \qquad (1.31)$$

However, $\tan\beta$ is not entirely a free parameter. It is restricted by the conditions for the minimum of the Higgs potential

$$0 = T_1 = m_1^2 v_1 + m_{12}^2 v_2 + \frac{1}{8}(g^2 + g'^2)(v_1^2 - v_2^2)v_1$$

$$0 = T_2 = m_2^2 v_2 + m_{12}^2 v_1 + \frac{1}{8}(g^2 + g'^2)(v_2^2 - v_1^2)v_2 \qquad (1.32)$$

The Higgs mass matrix is of the block-diagonal form. The particular blocks are

$$\mathcal{M}_{\phi^0}^2 = \begin{pmatrix} \frac{T_1}{v_1} - m_{12}^2 \tan\beta + m_Z^2 \cos^2\beta & m_{12}^2 - m_Z^2 \sin\beta\cos\beta \\ m_{12}^2 - m_Z^2 \sin\beta\cos\beta & \frac{T_2}{v_2} - m_{12}^2 \cot\beta + m_Z^2 \sin^2\beta \end{pmatrix}$$

$$\mathcal{M}_{\phi^\pm}^2 = \begin{pmatrix} \frac{T_1}{v_1} - m_{12}^2 \tan\beta + m_W^2 \sin^2\beta & m_{12}^2 + m_W^2 \sin\beta\cos\beta \\ m_{12}^2 + m_W^2 \sin\beta\cos\beta & \frac{T_2}{v_2} - m_{12}^2 \cot\beta + m_W^2 \cos^2\beta \end{pmatrix}$$

$$\mathcal{M}_{\chi^0}^2 = \begin{pmatrix} \frac{T_1}{v_1} - m_{12}^2 \tan\beta & -m_{12}^2 \\ -m_{12}^2 & \frac{T_2}{v_2} - m_{12}^2 \cot\beta \end{pmatrix} \qquad (1.33)$$

The diagonalization proceeds in the following way

$$\text{diag}(m_{H^0}^2, m_{h^0}^2) = R(\alpha)\,\mathcal{M}_{\phi^0}^2\,R(\alpha)^\dagger$$

$$\text{diag}(m_{G^\pm}^2, m_{H^\pm}^2) = R(\beta)\,\mathcal{M}_{\phi^\pm}^2\,R(\beta)^\dagger$$

$$\text{diag}(m_{G^0}^2, m_{A^0}^2) = R(\beta)\,\mathcal{M}_{\chi^0}^2\,R(\beta)^\dagger \qquad (1.34)$$

where
$$R(\alpha) = \begin{pmatrix} \cos\alpha & \sin\alpha \\ -\sin\alpha & \cos\alpha \end{pmatrix}, \quad R(\beta) = \begin{pmatrix} -\cos\beta & \sin\beta \\ \sin\beta & \cos\beta \end{pmatrix} \quad (1.35)$$

The relations between the mass eigenstates and the interaction eigenstates are

$$\begin{pmatrix} H^0 \\ h^0 \end{pmatrix} = R(\alpha) \begin{pmatrix} \phi_1^0 \\ \phi_2^0 \end{pmatrix}$$

$$\begin{pmatrix} G^\pm \\ H^\pm \end{pmatrix} = R(\beta) \begin{pmatrix} \phi_1^\pm \\ \phi_2^\pm \end{pmatrix}, \quad \begin{pmatrix} G^0 \\ A^0 \end{pmatrix} = R(\beta) \begin{pmatrix} \chi_1^0 \\ \chi_2^0 \end{pmatrix} \quad (1.36)$$

The mass eigenvalues and the mixing angle α are

$$m_{h^0,H_0}^2 = \frac{1}{2}\left[m_{A^0}^2 + m_Z^2 \mp \sqrt{(m_{A^0}^2 + m_Z^2)^2 - 4m_{A^0}^2 m_Z^2 \cos^2\beta}\right] \quad (1.37)$$

$$m_{H^\pm}^2 = m_{A^0}^2 + m_W^2 \quad (1.38)$$

$$m_{A^0}^2 = -m_{12}^2 \frac{1}{\sin\beta\cos\beta} \quad (1.39)$$

$$\tan 2\alpha = \tan 2\beta \frac{m_{A^0}^2 + m_Z^2}{m_{A^0}^2 - m_Z^2} \quad (1.40)$$

The three free parameters of the Higgs sector are conventionally chosen to be $m_{A^0}, \tan\beta, \mu$.

1.4.2 Sfermion sector

The sfermion mass matrix has its origin in the F-term, D-term potentials, SUSY breaking potential and in the trilinear couplings where the neutral Higgs fields get their VEVs

$$\mathcal{M}_{\tilde{f}}^2 = \begin{pmatrix} m_{\tilde{f}_L}^2 & a_f m_f \\ a_f m_f & m_{\tilde{f}_R}^2 \end{pmatrix} \quad (1.41)$$

where

$$m_{\tilde{f}_L}^2 = M_{\{\tilde{Q},\tilde{L}\}}^2 + (I_f^{3L} - e_f s_W^2)\cos 2\beta m_Z^2 + m_f^2$$

$$m_{\tilde{f}_R}^2 = M_{\{\tilde{U},\tilde{D},\tilde{E}\}}^2 + e_f s_W^2 \cos 2\beta m_Z^2 + m_f^2$$

$$a_f = A_f - \mu(\tan\beta)^{-2I_f^{3L}} \quad (1.42)$$

The term I_f^{3L} denotes the third component of the weak isospin of the fermion, e_f denotes the electric charge in terms of the elementary charge e. The diagonalization proceeds as follows

$$\text{diag}(m_{\tilde{f}_1}^2, m_{\tilde{f}_2}^2) = \left(R^{\tilde{f}}\right) \mathcal{M}_{\tilde{f}}^2 \left(R^{\tilde{f}}\right)^\dagger \quad (1.43)$$

9

where

$$\left(R^{\tilde{f}}\right) = \begin{pmatrix} \cos\theta_{\tilde{f}} & \sin\theta_{\tilde{f}} \\ -\sin\theta_{\tilde{f}} & \cos\theta_{\tilde{f}} \end{pmatrix} \tag{1.44}$$

The relation between the mass eigenstates and the interaction eigenstates is

$$\begin{pmatrix} \tilde{f}_1 \\ \tilde{f}_2 \end{pmatrix} = R^{\tilde{f}} \begin{pmatrix} \tilde{f}_L \\ \tilde{f}_R \end{pmatrix} \tag{1.45}$$

The mass eigenvalues and the mixing angle are

$$m^2_{\tilde{f}_{1,2}} = \frac{1}{2}\left(m^2_{\tilde{f}_L} + m^2_{\tilde{f}_R} \mp \sqrt{(m^2_{\tilde{f}_L} - m^2_{\tilde{f}_R})^2 + 4a^2_f m^2_f}\right) \tag{1.46}$$

$$\cos\theta_{\tilde{f}} = \frac{-a_f m_f}{\sqrt{(m^2_{\tilde{f}_L} - m^2_{\tilde{f}_1})^2 + a^2_f m^2_f}} \qquad (0 \leq \theta_{\tilde{f}} < \pi) \tag{1.47}$$

1.4.3 Neutralino sector

The fermionic superpartners of the gauge bosons (gauginos) and the superpartners of the Higgs bosons (higgsinos) mix to form mass eigenstates called neutralinos (particles with zero charge) and charginos (charged particles).

In the interaction base on can combine the four neutral Weyl states as

$$\psi^0_j = (\tilde{B}, \tilde{W}^0_3, \tilde{H}^0_1, \tilde{H}^0_2) \tag{1.48}$$

where $\tilde{B}, \tilde{W}^0_3 \leftrightarrow -i\lambda$. The mass lagrangian written in terms of the vector ψ^0 is

$$\mathcal{L} = -\frac{1}{2}(\psi^0)^T Y \psi^0 + \text{h.c.} \tag{1.49}$$

where the neutralino mass matrix Y is

$$Y = \begin{pmatrix} M' & 0 & -m_Z s_W \cos\beta & m_Z s_W \sin\beta \\ 0 & M & m_Z c_W \cos\beta & -m_Z c_W \sin\beta \\ -m_Z s_W \cos\beta & m_Z c_W \cos\beta & 0 & -\mu \\ m_Z s_W \sin\beta & -m_Z c_W \sin\beta & -\mu & 0 \end{pmatrix} \tag{1.50}$$

Due to the Majorana nature of the neutralinos, the mass matrix can be diagonalized using only one rotation matrix Z

$$\text{diag}\,(m_{\tilde{\chi}^0_1}, m_{\tilde{\chi}^0_2}, m_{\tilde{\chi}^0_3}, m_{\tilde{\chi}^0_4}) = ZYZ^{-1}$$
$$|m_{\tilde{\chi}^0_1}| \leq |m_{\tilde{\chi}^0_2}| \leq |m_{\tilde{\chi}^0_3}| \leq |m_{\tilde{\chi}^0_4}| \tag{1.51}$$

where we assume that the mixing matrix is real and we also allow the eigenvalues to be negative. The 4-component Majorana spinor for the neutralino fields can be constructed as

$$\tilde{\chi}^0_i = \begin{pmatrix} Z_{ij}\,\psi^0_j \\ Z_{ij}\,\bar{\psi}^0_j \end{pmatrix} \tag{1.52}$$

10

1.4.4 Chargino sector

The superpartners of the charged gauge bosons and charged Higgs bosons mix to create charginos. In the Weyl representation we have

$$\psi^+ = (\tilde{W}^+, \tilde{H}_2^+) \qquad \psi^- = (\tilde{W}^-, \tilde{H}_1^-) \tag{1.53}$$

where $W^\pm = \frac{1}{\sqrt{2}}(W^1 \mp W^2)$ and $W^\pm \leftrightarrow -i\lambda^\pm$. The mass lagrangian in this basis reads

$$\mathcal{L} = -\frac{1}{2}(\psi^+, \psi^-) \begin{pmatrix} 0 & X^T \\ X & 0 \end{pmatrix} \begin{pmatrix} \psi^+ \\ \psi^- \end{pmatrix} + \text{h.c} \tag{1.54}$$

where the chargino mass matrix is

$$X = \begin{pmatrix} M & \sqrt{2}m_W \sin\beta \\ \sqrt{2}m_W \cos\beta & \mu \end{pmatrix} \tag{1.55}$$

This matrix can be diagonalized by using two unitary matrices U and V.

$$UXV^{-1} = \text{diag}(m_{\chi_1^\pm}, m_{\chi_2^\pm}), \qquad |m_{\chi_1^\pm}| \le |m_{\chi_2^\pm}| \tag{1.56}$$

We use a convention in which the matrices U, V are real. It implies that the eigenvalues can be negative. The Dirac spinor is constructed as

$$\tilde{\chi}_i^+ \equiv \begin{pmatrix} V_{ij}\,\psi_j^+ \\ U_{ij}\,\bar{\psi}_j^- \end{pmatrix} \tag{1.57}$$

The mass eigenvalues are given by

$$m_{\tilde{\chi}_{1,2}^\pm}^2 = \frac{1}{2}\Big[M^2 + \mu^2 + 2m_W^2 \mp \sqrt{(M^2 + \mu^2 + 2m_W^2)^2 - 4(m_W^2 \sin 2\beta - \mu M)^2} \Big] \tag{1.58}$$

1.5 The CMSSM, GMSB, AMSB models

It is expected that the MSSM soft terms arise indirectly or radiative [22, 10]. SUSY breaking (SB) occurs in a hidden sector of particles that have no or very small direct couplings to the visible sector. The supersymmetry breaking is then mediated by some interaction resulting in the MSSM soft terms. There have been three main proposals for what the mediating interactions might be. The first is that they are gravitational (gravity-mediated SB). The soft parameters arise due to couplings which vanish as $M_{\text{Planck}} \to \infty$. The second possibility is that they are the ordinary electroweak and QCD gauge interactions (gauge-mediated SB). In gauge mediation, the soft parameters arise from loop diagrams involving new messenger fields with SM quantum numbers. The third possibility of mediation is bulk mediation. In

these models, the hidden and observable sectors reside on different branes separated in extra dimensions, and supersymmetry breaking is mediated by fields which propagate in between them, "in the bulk".

The CMSSM model

The soft terms in the MSSM lagrangian are all determined by five parameters: $m_{1/2}$, m_0, A_0, m_{12}^2, μ . In terms of these, the parameters appearing in (1.24) are

$$
\begin{aligned}
m_{\tilde{g}} &= M = M' = m_{1/2} \\
M_{\tilde{Q}}^2 &= M_{\tilde{U}}^2 = M_{\tilde{D}}^2 = M_{\tilde{L}}^2 = M_{\tilde{E}}^2 = m_0^2 \\
m_{H_1}^2 &= m_{H_2}^2 = m_0^2 \\
A_e &= A_d = A_e = A_0
\end{aligned}
\tag{1.59}
$$

at the scale M_{GUT}. After RG evolving the soft terms down to the electroweak scale, one can demand that the scalar potential gives correct EWSB. This allows the trading of $|\mu|$ and m_{12}^2 for one parameter $\tan\beta$. Then the entire mass spectrum is determined by only four (and a half) unknown parameters m_0^2, $m_{1/2}$, A_0, $\tan\beta$, $\mathrm{sign}(\mu)$.

The GMSB model

In the basic implemenatation of gauge mediated SB, there is the observable sector and the hidden sector, where SUSY is assumed to be broken dynamically such that nonzero F component VEVs of the hidden sector are generated. In addition, there is a messenger sector with messenger fields. The messenger fields couple to the goldstino field of the hidden sector, which generates nonzero F_S.

The free parameters includes at least the effective visible sector breaking parameter Λ, the typical messenger mass scale M_S, the integer number N_5 of copies of the minimal messengers and the Higgs mass parameters m_{12}^2 and μ which are traded for $\tan\beta$. The scale $\Lambda = F_S/M_S$.

The AMSB model

In models with extra-dimensional mediated SB, the MSSM chiral supermultiplets are confined to one four-dimensional spacetime brane and the SB sector confined to a parallel brane separated by a five-dimensional bulk. Concerning the gauge supermultiplets, one possibility is that they propagate in the bulk and thus mediate the breaking. It is also possible that the gauge supermultiplet fields are also confined to the MSSM brane leading to the breaking transition due entirely supergravity effects. The name AMSB derives from the fact that the resulting MSSM soft terms can be

understood in terms of the anomalous violation of a local superconformal invariance, an extension of scale invariance.

There is only one unknown parameter F_ϕ among the MSSM soft terms in AMSB. F_ϕ is the vacuum expectation value of the auxiliary field component of a non-dynamical chiral supermultiplet called the "conformal compensator". However, the AMSB model in its simplest form is not viable since the sleptons acquire negative squared masses. One way to modify the model is to add the common parameter m_0^2 to all of the scalar squared masses at some scale and choose them large enough to allow the sleptons to have masses above the experimental bounds. This allows the phenomenology to be studied in a framework parametrized by just F_ϕ, m_0^2, $\tan\beta$, sign(μ). (Some sources use $m_{3/2}$ or M_{aux} to denote F_ϕ.)

1.6 Experimental constraints

Currently, the most stringent limits on squark and gluino masses come from the LHC [23, 24]. Their results are summarized in Fig. 1.1.
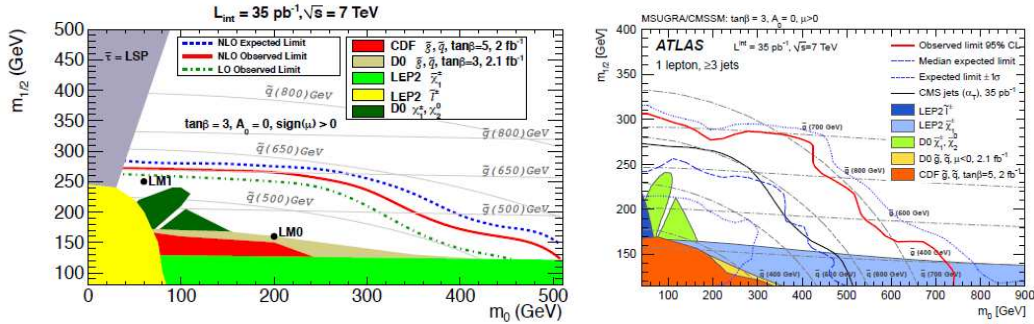
Figure 1.1: **left**: (The CMS Collaboration): Measured (red line) and expected (dashed blue line) 95% CL exclusion contour at NLO in the CMSSM $(m_0, m_{1/2})$ plane for $\tan\beta = 3$, $A_0 = 0$, sign(μ) > 0, taken from [23]; **right**: (The ATLAS Collaboration): Observed and expected 95% CL exclusion limits in the combined electron and muon channels; taken from [24].

The Particle Data Group mass limits at the CL = 95% from the last year [25] are shown in Table 1.2. The assumptions include: 1. $\tilde{\chi}_1^0$ is the lightest supersymmetric particle; 2. R-parity is conserved; 3. With the exception of $\tilde{t}$ and $\tilde{b}$, all scalar quarks are assumed to be degenerate in mass and $m_{\tilde{q}_L} = m_{\tilde{q}_R}$; 4. Limits for sleptons refer to the $\tilde{l}_R$ states; 5. Gaugino mass unification at the GUT scale.

The best-fit points as well as the 68% CL and 95% CL regions for the CMSSM are presented in [26] and shown in Fig. 1.2. The applied phenomenological, experimental and cosmological constraints include: precision electroweak data, $(g-2)_\mu$, B-physics

$m_{\tilde{\chi}_1^0} > 46$ GeV	all $\tan\beta$, all m_0, all $m_{\tilde{\chi}_2^0} - m_{\tilde{\chi}_1^0}$
$m_{\tilde{\chi}_2^0} > 62.4$ GeV	$1 < \tan\beta$, all m_0, all $m_{\tilde{\chi}_2^0} - m_{\tilde{\chi}_1^0}$
$m_{\tilde{\chi}_3^0} > 99.9$ GeV	$1 < \tan\beta < 40$, all m_0, all $m_{\tilde{\chi}_2^0} - m_{\tilde{\chi}_1^0}$
$m_{\tilde{\chi}_4^0} > 116$ GeV	$1 < \tan\beta < 40$, all m_0, all $m_{\tilde{\chi}_2^0} - m_{\tilde{\chi}_1^0}$
$m_{\tilde{\chi}_1^\pm} > 94$ GeV	$\tan\beta < 40$, all m_0, $m_{\tilde{\chi}_1^\pm} - m_{\tilde{\chi}_1^0} > 3$ GeV
$m_{\tilde{\nu}} > 94$ GeV	$1 \le \tan\beta \le 40$, $m_{\tilde{e}_R} - m_{\tilde{\chi}_1^0} > 10$ GeV
$m_{\tilde{e}} > 107$ GeV	all $m_{\tilde{e}_R} - m_{\tilde{\chi}_1^0}$
$m_{\tilde{\mu}} > 94$ GeV	$1 \le \tan\beta \le 40$, $m_{\tilde{\mu}_R} - m_{\tilde{\chi}_1^0} > 10$ GeV
$m_{\tilde{\tau}} > 81.9$ GeV	$m_{\tilde{\tau}_R} - m_{\tilde{\chi}_1^0} > 15$ GeV, all θ_τ
$m_{\tilde{q}} > 379$ GeV	$\tan\beta = 3, \mu < 0, A = 0$, any $m_{\tilde{g}}$
$m_{\tilde{b}} > 89$ GeV	$m_{\tilde{b}_1} - m_{\tilde{\chi}_1^0} > 8$ GeV, all θ_b
$m_{\tilde{t}} > 95.7$ GeV	$\tilde{t} \to c\tilde{\chi}_1^0$, $m_{\tilde{t}} - m_{\tilde{\chi}_1^0} > 10$ GeV, all θ_t
$m_{\tilde{g}} > 308$ GeV	any $m_{\tilde{q}}$
$m_{h^0} > 92.8$ GeV	
$m_{A^0} > 93.4$ GeV	$\tan\beta > 0.4$ GeV
$m_{H^\pm} > 79.3$ GeV	

Table 1.2: PDG mass limits, July 2010

observables (the rates for BR($b \to s\gamma$) and BR($B_\mu \to \tau\nu_\tau$), B_s mixing and the upper limit on BR($B_s \to \mu^+\mu_-$)), the bound on the lightest MSSM Higgs boson mass M_h, the cold dark matter (CDM) density inferred from astrophysical and cosmological data, assuming that this is dominated by the relic density of the lightest neutralino, and the recent limits from SUSY searches at CMS and ATLAS [23, 24].

The likelihood function for the lightest MSSM Higgs mass M_h in the CMSSM [26] is displayed in Fig. 1.3. We can see that the LHC constraints increase the consistency of the model prediction with the direct LEP limit.

An analysis of the AMSB paramerer space constraints from flavour physics and cosmological relic density was performed in [28]. The result is summarized in Fig. 1.4.
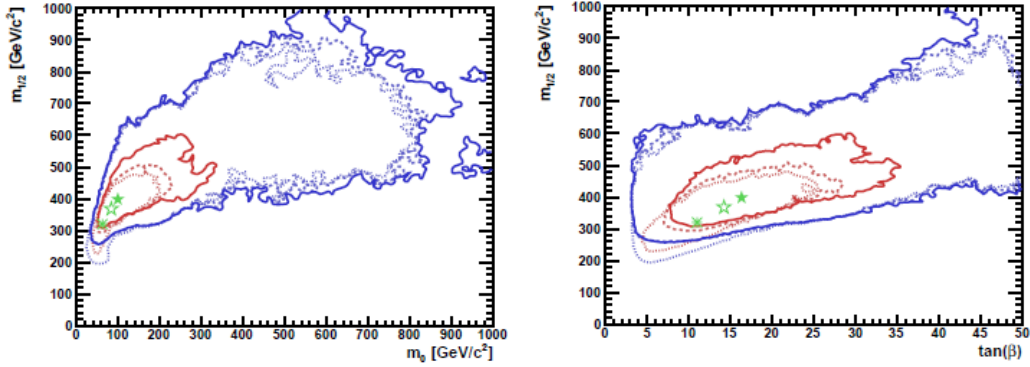
Figure 1.2: **left**: The $(m_0, m_{1/2})$ plane in the CMSSM. The 68% CL and 95% CL contours are shown (red and blue, respectively) both after applying the CMS and ATLAS constraints (dashed and solid lines respectively) and beforehand (dotted lines). Also shown as open (solid) green stars are the best-fit points found after applying the CMS (ATLAS) constraints, and as green 'snowflake' the previous best-fit point. **right**: The $(\tan\beta, m_{1/2})$ plane in the CMSSM. Taken from [26].
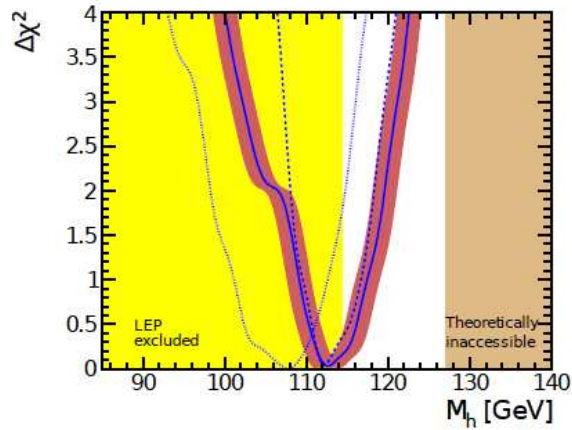
Figure 1.3: The one parameter χ^2 likelihood functions for the lightest MSSM Higgs mass M_h in the CMSSM. The χ^2 functions including the CMS (ATLAS) constraints are shown as dashed (solid) lines, the latter with a red band indicating the estimated theoretical uncertainty in the calculation of M_h of ~ 1.5 GeV, and the pre-LHC χ^2 function is shown as the dotted line. Taken from [26].

15
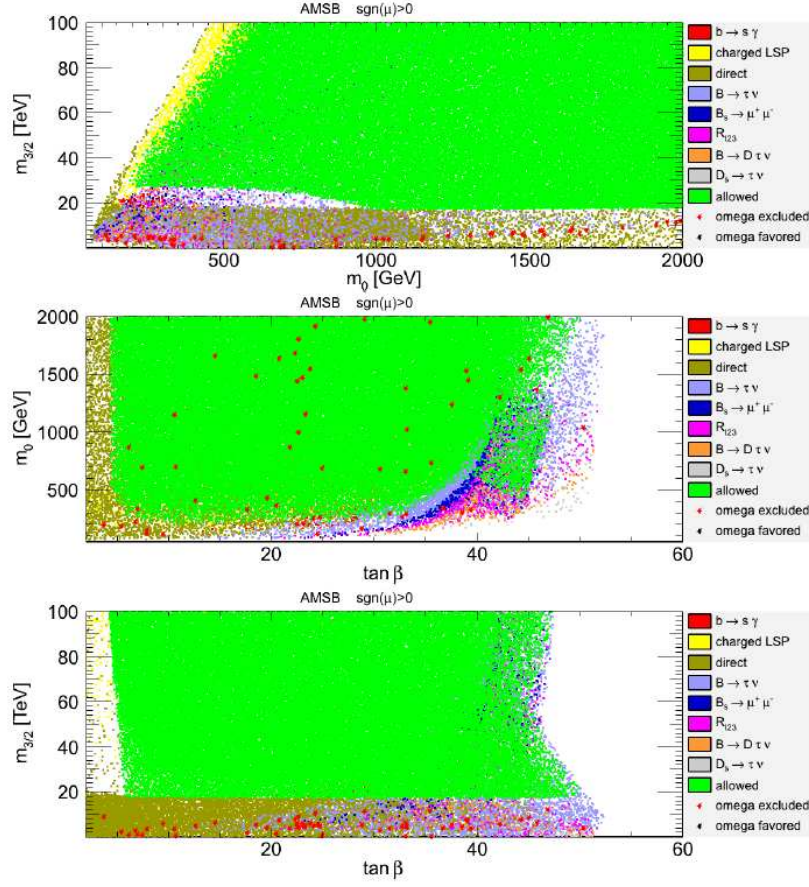
Figure 1.4: Constraints in the minimal AMSB parameter space. The exclusion regions are plotted in the order given in the legend. The red zones are excluded by the inclusive branching ratio of $B \rightarrow X_s \gamma$, the yellow ones correspond to charged LSP, the olive-green areas are excluded by direct collider constraints, the light blue zones are excluded by $\mathrm{BR}(B \rightarrow \tau\nu)$, the dark blue zones by $\mathrm{BR}(B_s \rightarrow \mu^+\mu^-)$, the magenta zones by R_{l23}, the orange zones by $\mathrm{BR}(B \rightarrow D\tau\nu)$ and the grey zones by $\mathrm{BR}(D_s \rightarrow \tau\nu)$. The green are in agreement with all the previously mentioned constraints. The stars are points favoured by the relic density observable, in red if disfavoured by any other constraints and in black if in agreement with all the constraints simultaneously. Taken from [28].

Chapter 2

Renormalization of the MSSM

If SUSY exists it will be tested at the same level as the Standard Model. Experimental accuracies are expected at the per-cent down to the per-mill level [51, 52, 53]. These must be matched from the theoretical side. Furthemore, radiative effects will give insight into the SUSY breaking mechanism. Therefore loop corrections are mandatory (also from the EW sector).

2.1 Regularization

When one wants to calculate processes in quantum field theory at higher order then the tree level one usually encounters divergencies. Then it is inevitable to regularize the divergent parts. After performing the renormalization of the theory the infinite parts cancel out thus leading to a finite result.

There are two types of divergencies. The first one is called infrared divergence (IR). It arises as soon as a massless particle (photon, gluon) appears in the loop. One way how to regularize the infinity is to introduce a small nonzero particle mass λ. After considering photon and/or gluon radiation from the initial and final states one obtains a result independent of the λ and therefore IR convergent.

The second type of divergence is called ultraviolet (UV). It is caused by divergent behaviour of loop integrals as the integration variable approaches infinity. Several regularization procedures have been devised [32, 33]. The final results are finite and independent of this choice.

The most naive prescription is to cut off the large values of the integration variable. This certainly makes any Feynman amplitude finite, but it ruins the Poincaré invariance. Therefore it is used only exceptionally, in heuristic arguments. A variant is a spacetime discretization when the configuration variables x_μ take only discrete values. Here, too, the rotational invariance is lost. Another prescription to render the Feynman integrals finite is to introduce fictitious heavy particles (Pauli-Villars

regularization). The example on regularizing the photon propagator is given in the following equation

$$\frac{1}{(k-p)^2 + i\varepsilon} \to \frac{1}{(k-p)^2 + i\varepsilon} - \frac{1}{(k-p)^2 - \Lambda^2 + i\varepsilon} \qquad (2.1)$$

The integrand is unaffected for small k (since Λ is large), but cuts smoothly when $k \gtrsim \Lambda$. The most popular regularization scheme is Dimensional regularization discussed in the next section.

2.2   Dimensional regularization and reduction

Dimensional regularization (DREG) was introduced by 't Hooft and Veltman [34]. They realized that by lowering the dimension of an initially divergent integral it can be made finite. Everything in DREG is calculated in D-dimensional space where $D = 4 - \varepsilon$ is a complex number. Consequently, the divergent parts arise as poles of the dimensional parameter D at $\varepsilon = 0$. The whole procedure is described in [35, 36, 37].

A general one loop integral can be written as

$$T^N_{\mu_1 \ldots \mu_M}(p_1, \ldots, p_{N-1}, m_0, \ldots, m_{N-1}) = \frac{(2\pi\mu)^{4-D}}{i\pi^2} \int d^D q$$

$$\frac{q_{\mu_1} \ldots q_{\mu_M}}{[q^2 - m_0^2 + i\varepsilon][(q+p_1)^2 - m_1^2 + i\varepsilon] \ldots [(q+p_{N-1})^2 - m_{N-1}^2 + i\varepsilon]} \qquad (2.2)$$

where the convention for the momenta are shown in the following picture. The parameter μ serves for retaining the initial dimensionality of the integral.
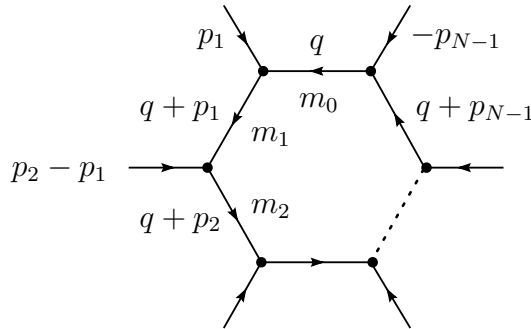
According to the number of particles in the loop we differentiate the integrals of

type A, B, C, D and higher. The first three scalar integrals are denoted as

$$
\begin{align}
T^1 &\equiv A_0(m_0^2) \tag{2.3}\\
T^2 &\equiv B_0(p_1^2, m_0^2, m_1^2) \tag{2.4}\\
T^3 &\equiv C_0(p_1^2, (p_1 - p_2)^2, p_2^2, m_0^2, m_1^2, m_2^2) \tag{2.5}
\end{align}
$$

The other tensor integrals $A^{\mu\nu}, B^\mu, B^{\mu\nu}, C^\mu, C^{\mu\nu}$ etc. can be calculated from the scalar ones through a procedure called tensor reduction

$$
\begin{align}
A^{\mu\nu} &= g^{\mu\nu} A_{00} \tag{2.6}\\
B^\mu &= p_1^\mu B_1 \tag{2.7}\\
B^{\mu\nu} &= g^{\mu\nu} B_{00} + p_1^\mu p_1^\nu B_{11} \tag{2.8}\\
C^\mu &= p_1^\mu C_1 + p_2^\mu C_2 \tag{2.9}\\
C^{\mu\nu} &= g^{\mu\nu} C_{00} + p_1^\mu p_1^\nu C_{11} + (p_1^\mu p_2^\nu + p_2^\mu p_1^\nu) C_{12} + p_2^\mu p_2^\nu C_{22} \tag{2.10}
\end{align}
$$

For more details we refer to [38]. The UV-divergent parts of the loop integrals are listed in Table 2.1. The divergence is contained in the parameter Δ which is defined as

$$
\Delta = \frac{2}{\varepsilon} - \gamma_E + \ln 4\pi \tag{2.11}
$$

with $\gamma_E = \lim_{m\to\infty} \left(\sum_{k-1}^m \frac{1}{k} - \ln m \right) \sim 0.577216$ known as Euler-Mascheroni constant.

Integral		UV divergent part
$A_0(m^2)$	$\rightarrow$	$m^2 \Delta$
$A_1(m^2)$	$\rightarrow$	$-m^2 \Delta$
$A_{00}(m^2)$	$\rightarrow$	$\frac{m^4}{4} \Delta$
B_0	$\rightarrow$	Δ
B_1	$\rightarrow$	$-\frac{1}{2}\Delta$
$B_{00}(p_1^2, m_0^2, m_1^2)$	$\rightarrow$	$-\frac{1}{4}(p_1^2/3 - m_0^2 - m_1^2)\Delta$
B_{11}	$\rightarrow$	$\frac{1}{3}\Delta$
C_{00}	$\rightarrow$	$\frac{1}{4}\Delta$
C_{00i}	$\rightarrow$	$-\frac{1}{12}\Delta$
D_{0000}	$\rightarrow$	$\frac{1}{24}\Delta$

Table 2.1: UV divergent coefficients of the Passarino-Veltman integrals

The IR divergent parts are shown in the Table 2.2. The parameters κ, β_0 are defined

19

as

$$\kappa = \kappa(m_0^2, m_1^2, m_2^2) = \sqrt{\lambda(m_0^2, m_1^2, m_2^2)} \tag{2.12}$$

$$\lambda(x, y, z) = x^2 + y^2 + z^2 - 2xy - 2xz - 2yz \tag{2.13}$$

$$\beta_0 = \frac{m_0^2 - m_1^2 - m_2^2 + \kappa}{2m_1 m_2} \tag{2.14}$$
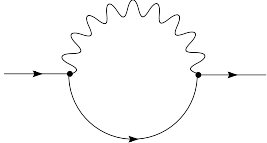
Integral		IR divergent part
$\dot{B}_0(m^2, \lambda^2, m^2) = \dot{B}_0(m^2, m^2, \lambda^2)$	$\rightarrow$	$-\frac{\ln \lambda^2}{2m^2}$
$\dot{B}_1(m^2, m^2, \lambda^2)$	$\rightarrow$	$\frac{\ln \lambda^2}{2m^2}$
$\dot{B}_1(m^2, \lambda^2, m^2)$	$\rightarrow$	0
$\mathrm{Re}[C_0(m_1^2, m_0^2, m_2^2, \lambda^2, m_1^2, m_2^2)]$	$\rightarrow$	$-\frac{\ln \beta_0}{\kappa} \ln \lambda^2$

Table 2.2: IR divergent coefficients of the Passarino-Veltman integrals

A drawback of the Dimensional regularization is that it does not respect super-symmetry. The reason is that the vector fields become D-dimensional and cannot be combined with its fermionic partner to a superfield since the superfield must posses equal number of fermionic and bosonic degrees of freedom. A modified version of dimensional regularization, designed to preserve supersymmetry and gauge invariance, was proposed by Siegel [39] under the name Dimensional reduction (DRED). While the integration momenta are D-dimensional all other tensors and spinors are kept 4-dimensional [40]. For the validity of the field equations and gauge invariance, one must impose the identity

$$g_{\mu\nu}\hat{g}^{\nu\rho} = \hat{g}_\mu{}^\rho \tag{2.15}$$

where $g_{\mu\nu}$ is 4-dimensional metric ($g^\mu{}_\mu = 4$) and $\hat{g}_{\mu\nu}$ the D-dimensional one ($\hat{g}^\mu{}_\mu = D$). At one loop level, DREG differs from DRED by finite terms. A simple example is the electron self-energy in QED

$$\stackrel{DREG}{=} -\frac{e^2}{16\pi^2} \left[4m_e B_0 + 2\not{k} B_1 + \not{k} - 2m_e \right]$$

$$\stackrel{DRED}{=} -\frac{e^2}{16\pi^2} \left[4m_e B_0 + 2\not{k} B_1 \right]$$

where $B_0 = B_0(k^2, m_e^2, 0)$, $B_1 = B_1(k^2, m_e^2, 0)$. Loop integrals as well as dimensional regularization together with constrained differential renormalization (which is at one loop level equivalent to dimensional reduction) are implemented in LoopTools package [40].

20

2.3 Concept of renormalization

A convenient way to perform the renormalization is to introduce renormalized parameters by a suitable reparametrization [41, 42]

$$g_0 = Z_g g \qquad\qquad \psi_0 = Z_\psi^{1/2} \psi \qquad\qquad (2.16)$$

In perturbation theory one writes

$$Z_g = 1 + \delta g \qquad\qquad Z_\psi = 1 + \delta Z_\psi \qquad\qquad (2.17)$$

yielding

$$
\begin{aligned}
\mathcal{L}(\psi_0, g_0) &= \mathcal{L}\left((1 + \delta Z_\psi)^{1/2}\psi, (1 + \delta g)g\right) \\
&= \mathcal{L}(\psi, g) + \mathcal{L}_{\mathrm{ct}}(\psi, g; \delta Z_\psi, \delta g) \qquad\qquad (2.18)
\end{aligned}
$$

The functional dependence of $\mathcal{L}(\psi, g)$ on ψ and g is the same as that of $\mathcal{L}(\psi_0, g_0)$ on ψ_0, g_0, and $\mathcal{L}(\psi, g)$ yields the same Feynman rules for the renormalized field and parameter as $\mathcal{L}(\psi_0, g_0)$ does for the bare ones. Thus the counterterm lagrangian $\mathcal{L}_{\mathrm{ct}}$ summarizes all terms containing the renormalization constants $\delta Z_\psi, \delta g$ and generates the counterterm Feynman rules. These allow to calculate the Green functions and from them the S-matrix elements through the relation (A.21)

$$
\begin{aligned}
S(p_1, \ldots, p_n) &\sim G_R^{tr}(p_1, \ldots, p_n)\,(R_R)^{\frac{n}{2}} \\
&= G_0^{tr}(p_1, \ldots, p_n)\,(R_R)^{\frac{n}{2}}\,Z_\psi^{\frac{n}{2}} \qquad\qquad (2.19)
\end{aligned}
$$

The symbol $\sim$ means that the poles of both sides of the equation are identical. G_R^{tr} stands for the truncated Green function. The renormalized residuum R_R is determined from the renormalized two point function

$$R_R = |\langle M, p\,|\psi_R(x)|0\rangle|^2 = -i(p^2 - M^2)G_R(p, -p)|_{p^2 = M^2} \qquad\qquad (2.20)$$

The requirement that the renormalization constants absorb the divergencies fixes those only up to finite parts. The latter are fixed by renormalization conditions. The choice of the renormalization conditions fixes a renormalization schceme. We will work in the $\overline{\mathrm{DR}}$ scheme which is a modified minimal-substraction scheme based on DRED. Works in which one can find the renormalization of the SM and/or MSSM include [21, 38, 43, 44, 45, 46, 47, 48, 49, 50]. The list is by no means exhaustive or in any way selective.

2.4 Renormalization of scalars

Reparametrization of the fields and of the mass reads

$$\tilde{f}_i \rightarrow \left(\delta_{ij} + \frac{1}{2}\delta Z_{ij}\right)\tilde{f}_j \qquad (2.21)$$

$$m_i^2 \rightarrow m_i^2 + \delta m_i^2 \qquad (2.22)$$

The renormalized self-energy is decomposed as

$$\hat{\Pi}_{ij}(p^2) = \Pi_{ij}(p^2) + \frac{1}{2}\left(p^2 - m_i^2\right)\delta Z_{ij} + \frac{1}{2}\left(p^2 - m_j^2\right)\delta Z_{ji}^* - \delta_{ij}\,\delta m_i^2 \qquad (2.23)$$

The on-shell renormalization conditions for the scalar particles are given by

$$\widetilde{\mathrm{Re}}\,\hat{\Gamma}_{ij}(p^2)\Big|_{p^2=m_j^2} = 0, \qquad \lim_{p^2\to m_i^2}\frac{1}{p^2-m_i^2}\widetilde{\mathrm{Re}}\,\hat{\Gamma}_{ii}(p^2) = 1 \qquad (2.24)$$

They are fullfilled when the counterterms are set to

$$\delta m_i^2 = \widetilde{\mathrm{Re}}\,\Pi_{ii}(m_i^2) \qquad (2.25)$$

$$\delta Z_{ij} = \frac{2}{m_i^2 - m_j^2}\widetilde{\mathrm{Re}}\,\Pi_{ij}(m_j^2) \quad i \neq j \qquad (2.26)$$

$$\delta Z_{ii} = -\widetilde{\mathrm{Re}}\,\dot{\Pi}_{ii}(m_i^2) \qquad (2.27)$$

with $\dot{\Pi}_{ii}(m_i^2) = \left[\frac{\partial}{\partial p^2}\Pi(p^2)\right]_{p^2=m^2}$. In the $\overline{\mathrm{DR}}$ scheme the finite term of the counterterm δm_i^2 is set to zero. However, the finite part becomes important for the calculation of masses in kinematical factors. We also retain the finite parts of the field counterterms as they appear in the S-matrix elements due to LSZ formula (see Appendix A).

$$\mathcal{M} = i\hat{\Gamma}_{ij}$$

$$\hat{\Gamma}_{ij} = \delta_{ij}(p^2 - m_i^2) + \hat{\Pi}_{ij}(p^2)$$
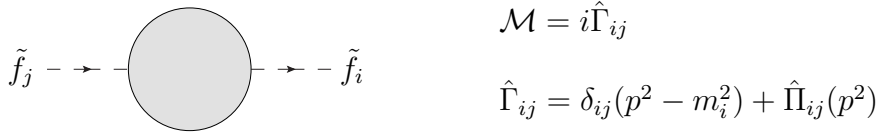
Figure 2.1: Two-point functions for mixing scalars

$$\mathcal{M} = i\bar{u}_i(p)\hat{\Gamma}_{ij}u_j(p)$$

$$\hat{\Gamma}_{ij} = \delta_{ij}(\not{p} - m_i) + \hat{\Pi}_{ij}(p)$$
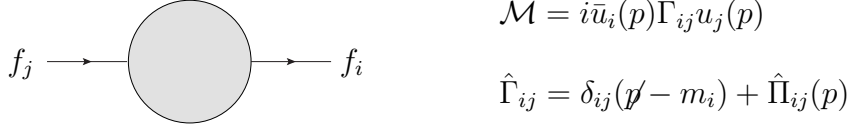
Figure 2.2: Two-point functions for mixing fermions

2.5 Renormalization of fermions

Reparametrization of the fields and of the mass reads

$$f_i \;\rightarrow\; \left(\delta_{ij} + \frac{1}{2}\delta Z^L_{ij}P_L + \frac{1}{2}\delta Z^R_{ij}P_R\right)f_j \tag{2.28}$$

$$m_i \;\rightarrow\; m_i + \delta m_i \tag{2.29}$$

The renormalized self-energy is decomposed as

$$\hat{\Pi}_{ij}(p) = \not{p}P_L\hat{\Pi}^L_{ij}(p) + \not{p}P_R\hat{\Pi}^R_{ij}(p) + P_L\hat{\Pi}^{S,L}_{ij}(p) + P_R\hat{\Pi}^{S,R}_{ij}(p) \tag{2.30}$$

where the left and right parts are

$$\hat{\Pi}^{L/R}_{ij} \;=\; \Pi^{L/R}_{ij} + \frac{1}{2}\left(\delta Z^{L/R}_{ij} + \delta Z^{L/R\dagger}_{ji}\right) \tag{2.31}$$

$$\hat{\Pi}^{S,L/R}_{ij} \;=\; \Pi^{S,L/R}_{ij} - \frac{1}{2}\left(m_i\,\delta Z^{L/R}_{ij} + m_j\,\delta Z^{R/L\dagger}_{ji}\right) - \delta_{ij}\,\delta m_i \tag{2.32}$$

The on-shell renormalization conditions for the fermions are given by

$$\widetilde{\mathrm{Re}}\,\hat{\Gamma}_{ij}(p)u_j(p)\Big|_{p^2=m_j^2} = 0, \qquad \lim_{p^2\to m_i^2}\frac{1}{\not{p}-m_i}\,\widetilde{\mathrm{Re}}\,\hat{\Gamma}_{ii}(p)u_i(p) = u_i(p) \tag{2.33}$$

They are full-filled when the counterterms are set to

$$\delta m_i \;=\; \frac{1}{2}\widetilde{\mathrm{Re}}\left[m_i\Pi^L_{ii}(m_i) + m_i\Pi^R_{ii}(m_i) + \Pi^{S,L}_{ii}(m_i) + \Pi^{S,R}_{ii}(m_i)\right] \tag{2.34}$$

$$\delta Z^{L/R}_{ij} \;=\; \frac{2}{m_i^2 - m_j^2}\widetilde{\mathrm{Re}}\Big[m_j^2\Pi^{L/R}_{ij}(m_j) + m_im_j\Pi^{L/R}_{ij}(m_j)$$

$$+ m_i\Pi^{S,L/R}_{ij}(m_j) + m_j\Pi^{S,R/L}_{ij}(m_j)\Big] \quad i\neq j \tag{2.35}$$

$$\delta Z^{L/R}_{ii} \;=\; -\Pi^{L/R}_{ii}(m_i) + \frac{1}{2m_i}\left[\Pi^{S,L/R}_{ii}(m_i) - \Pi^{S,R/L}_{ii}(m_i)\right]$$

$$- m_i\left[m_i\dot{\Pi}^{L/R}_{ii}(m_i) + m_i\dot{\Pi}^{R/L}_{ii}(m_i) + \dot{\Pi}^{S,L/R}_{ii}(m_i) + \dot{\Pi}^{S,R/L}_{ii}(m_i)\right] \tag{2.36}$$

23

$$\mathcal{M} = -i\varepsilon^\mu(p)\hat{\Gamma}_{\mu\nu}\varepsilon^{*\nu}(p)$$

$$\hat{\Gamma}_{ij} = -g_{\mu\nu}\delta_{VV'}(p^2 - m_V^2) - \hat{\Pi}_{\mu\nu}(p)$$

Figure 2.3: Two-point functions for mixing vector bosons

2.6 Renormalization of gauge bosons

Reparametrization of the fields and of the masses reads

$$W_\mu^\pm \quad \rightarrow \quad (1 + \frac{1}{2}\delta Z_W)W_\mu^\pm \tag{2.37}$$

$$\begin{pmatrix} A_\mu \\ Z_\mu \end{pmatrix} \quad \rightarrow \quad \begin{pmatrix} 1 + \frac{1}{2}\delta Z_{AA} & \frac{1}{2}\delta Z_{AZ} \\ \frac{1}{2}\delta Z_{ZA} & 1 + \frac{1}{2}\delta Z_{ZZ} \end{pmatrix} \begin{pmatrix} A_\mu \\ Z_\mu \end{pmatrix} \tag{2.38}$$

$$m_W^2 \quad \rightarrow \quad m_W^2 + \delta m_W^2 \tag{2.39}$$

$$m_Z^2 \quad \rightarrow \quad m_Z^2 + \delta m_Z^2 \tag{2.40}$$

There is no mass counterterm for the photon. It remains massless after the renormalization. The renormalized selfenergy is decomposed as

$$\hat{\Pi}_{\mu\nu}(p) = \left(g_{\mu\nu} - \frac{p_\mu p_\nu}{p^2}\right)\hat{\Pi}_T(p^2) + \frac{p_\mu p_\nu}{p^2}\hat{\Pi}_L(p^2) \tag{2.41}$$

where

$$\hat{\Pi}_W(p^2) \quad = \quad \Pi_W(p^2) + (p^2 - m_W^2)\delta Z_W - \delta m_W^2 \tag{2.42}$$

$$\hat{\Pi}_{AA}(p^2) \quad = \quad \Pi_{AA}(p^2) + p^2\delta Z_{AA} \tag{2.43}$$

$$\hat{\Pi}_{ZZ}(p^2) \quad = \quad \Pi_{ZZ}(p^2) + (p^2 - m_Z^2)\delta Z_{ZZ} - \delta m_Z^2 \tag{2.44}$$

$$\hat{\Pi}_{AZ}(p^2) \quad = \quad \Pi_{AZ}(p^2) + \frac{1}{2}p^2\delta Z_{AZ} + (p^2 - m_Z^2)\delta Z_{ZA} \tag{2.45}$$

$$\hat{\Pi}_{ZA}(p^2) \quad = \quad \Pi_{ZA}(p^2) + \frac{1}{2}p^2\delta Z_{AZ} + (p^2 - m_Z^2)\delta Z_{ZA} \tag{2.46}$$

valid for both the transverse and the longitudinal parts. The on-shell renormalization conditions for the vector bosons are

$$\widetilde{\text{Re}}\hat{\Gamma}_{\mu\nu}^{VV'}(p)\Big|_{p^2=m_V^2} = 0, \qquad \lim_{p^2 \to m_V^2} \frac{1}{p^2 - m_V^2}\widetilde{\text{Re}}\hat{\Gamma}_{\mu\nu}^{VV'}(p)\varepsilon^\nu(p) = -\varepsilon^\mu(p)$$

$$\text{for } V, V' = A, Z, W \tag{2.47}$$

24

They are fullfilled when the counterterms are set to

$$\delta m_W^2 = \widetilde{\mathrm{Re}}\Pi_T^{WW}(m_W^2), \qquad\qquad \delta m_Z^2 = \widetilde{\mathrm{Re}}\Pi_T^{ZZ}(m_Z^2) \qquad (2.48)$$

$$\delta Z_{VV} = -\widetilde{\mathrm{Re}}\dot\Pi_T^{VV}(m_V^2), \qquad\qquad V = A, Z, W \qquad (2.49)$$

$$\delta Z_{AZ} = -\frac{2\widetilde{\mathrm{Re}}\Pi_T^{AZ}(m_Z^2)}{m_Z^2}, \qquad \delta Z_{ZA} = \frac{2\widetilde{\mathrm{Re}}\Pi_T^{AZ}(0)}{m_Z^2} \qquad (2.50)$$

The weak mixing angle θ_W is a derived quantity and the counterterms are given as

$$\frac{\delta c_W^2}{c_W^2} = \frac{\delta m_W^2}{m_W^2} - \frac{\delta m_Z^2}{m_Z^2}, \qquad \frac{\delta s_W^2}{s_W^2} = -\frac{c_W^2}{s_W^2}\frac{\delta c_W^2}{c_W^2} \qquad (2.51)$$

It is understood that only divergent parts are taken in δc_W^2 and δs_W^2 as well as in the other counter-terms discussed in the following sections.

2.7 Charge renormalization

The reparametrization reads

$$e \to e + \delta e \qquad (2.52)$$

The renormalization condition reads

$$\bar{u}(p)\hat\Gamma_\mu^{eeA}(p,p)u(p)\Big|_{p^2=m_e} = \bar{u}(p)\gamma_\mu u(p) \qquad (2.53)$$

where the renormalized three-point function is

$$\hat\Gamma_\mu^{eeA} = e\gamma_\mu\left(1 + \frac{\delta e}{e} + \frac{1}{2}\delta Z_{AA} - \frac{1}{2}\frac{s_W}{c_W}\delta Z_{ZA} + \delta Z_f\right) + e\Lambda_\mu^{eeA} = e\gamma_\mu \qquad (2.54)$$

Λ_μ^{eeA} is a one loop vertex correction. A Ward identity dictates that it cancels the contribution from the fermion self-energies δZ_f and therefore

$$\frac{\delta e}{e} = -\frac{1}{2}\delta Z_{AA} + \frac{1}{2}\frac{s_W}{c_W}\delta Z_{ZA} \qquad (2.55)$$

2.8 Strong coupling renormalization

Renormalization of the strong coupling can be found in [38]. The reparametrization reads

$$g_s \to g_s + \delta g_s \qquad (2.56)$$

The counter-term δg_s is of the following form

$$\delta g_s = g_s\frac{\alpha}{8\pi}\Delta\left(n_f - 3C_V\right) \qquad (2.57)$$

where Δ is the UV-divergent part, $n_f = 6$ and $C_V = 3$.

2.9 Sfermion sector

Renormalization of the sfermion rotation matrix is done in a similar way to the CKM matrix. The counterterm is set to cancel the anti-hermitian part of the wave function correction

$$\delta R^{\tilde{f}}_{ij} = \sum_{k=1}^{2} \frac{1}{4}(\delta Z^{\tilde{f}}_{ik} - \delta Z^{\tilde{f}*}_{ki})R^{\tilde{f}}_{kj} \tag{2.58}$$

Based on the equation 1.43 the counterterms to the matrix elements are

$$\delta \mathcal{M}^2_{\tilde{f}\ cd} = \sum_{k,l} \left(\delta R^{\tilde{f}\dagger}_{ck}m^2_{\tilde{f}k}\delta_{kl}R^{\tilde{f}}_{ld} + R^{\tilde{f}\dagger}_{ck}\delta m^2_{\tilde{f}k}\delta_{kl}R^{\tilde{f}}_{ld} + R^{\tilde{f}\dagger}_{ck}m^2_{\tilde{f}k}\delta_{kl}\delta R^{\tilde{f}}_{ld} \right) \tag{2.59}$$

The counterterm to parameter A_f may be obtained from the 21-element of the sfermion mass matrix

$$
\begin{aligned}
\delta A_f &= \left[\delta \mathcal{M}^2_{\tilde{f}21} - \left(A_f + \mu \tan \beta^{-2I^{3L}_f} \right) \delta m_f \right] \frac{1}{m_f} \\
&+ \delta \mu \tan \beta^{-2I^{3L}_f} + \mu \delta(\tan \beta^{-2I^{3L}_f})
\end{aligned}
\tag{2.60}
$$

2.10 Neutralino and chargino sector

Also here the counterterm to the rotation matrix is set to cancel the anti-hermitian part of the wave function correction

$$\delta Z_{ij} = \sum_{k=1}^{4} \frac{1}{4}(\delta Z^{\tilde{\chi}^0,L}_{ik} - \delta Z^{\tilde{\chi}^0,L*}_{ki})Z_{kj} \tag{2.61}$$

$$\delta U_{ij} = \sum_{k=1}^{2} \frac{1}{4}(\delta Z^{\tilde{\chi}^-,L}_{ik} - \delta Z^{\tilde{\chi}^-,L*}_{ki})U_{kj} \tag{2.62}$$

$$\delta V_{ij} = \sum_{k=1}^{2} \frac{1}{4}(\delta Z^{\tilde{\chi}^-,R*}_{ik} - \delta Z^{\tilde{\chi}^-,R}_{ki})V_{kj} \tag{2.63}$$

Based on the equation 1.56 the counterms to chargino mass matrix elements are

$$\delta X_{cd} = \sum_{k,l} (\delta U_{kc}m_k\delta_{kl}V_{ld} + U_{kc}\delta m_k\delta_{kl}V_{ld} + U_{kc}m_k\delta_{kl}\delta V_{ld}) \tag{2.64}$$

The counterterm to the parameter μ may be obtained from the 22-element of the chargino mass matrix

$$\delta \mu = \delta X_{22} \tag{2.65}$$

26

2.11   Higgs sector

Let us now first rewrite the Higgs potential to be the function of the mass eigenstates

$$
\begin{aligned}
V &= V_0 + \begin{pmatrix} \phi_1^0 & \phi_2^0 \end{pmatrix} \begin{pmatrix} T_1 \\ T_2 \end{pmatrix} + \frac{1}{2} \begin{pmatrix} \phi_1^0 & \phi_2^0 \end{pmatrix} \mathcal{M}_{\phi^0}^2 \begin{pmatrix} \phi_1^0 \\ \phi_2^0 \end{pmatrix} \\
&\quad + \frac{1}{2} \begin{pmatrix} \chi_1^0 & \chi_2^0 \end{pmatrix} \mathcal{M}_{\chi^0}^2 \begin{pmatrix} \chi_1^0 \\ \chi_2^0 \end{pmatrix} + \begin{pmatrix} \phi_1^- & \phi_2^- \end{pmatrix}^\dagger \mathcal{M}_{\phi^\pm}^2 \begin{pmatrix} \phi_1^- \\ \phi_2^- \end{pmatrix} + \dots \\
&= V_0 + \begin{pmatrix} H^0 & h^0 \end{pmatrix} O(\alpha) \begin{pmatrix} T_1 \\ T_2 \end{pmatrix} \\
&\quad + \frac{1}{2} \begin{pmatrix} H^0 & h^0 \end{pmatrix} \begin{pmatrix} m_{H^0}^2 & 0 \\ 0 & m_{h^0}^2 \end{pmatrix} \begin{pmatrix} H^0 \\ h^0 \end{pmatrix} \\
&\quad + \frac{1}{2} \begin{pmatrix} H^0 & h^0 \end{pmatrix} O(\alpha) \begin{pmatrix} \frac{T_1}{v_1} & 0 \\ 0 & \frac{T_2}{v_2} \end{pmatrix} O(\alpha)^T \begin{pmatrix} H^0 \\ h^0 \end{pmatrix} \\
&\quad + \frac{1}{2} \begin{pmatrix} G^0 & A^0 \end{pmatrix} \begin{pmatrix} 0 & 0 \\ 0 & m_{A^0}^2 \end{pmatrix} \begin{pmatrix} G^0 \\ A^0 \end{pmatrix} \\
&\quad + \frac{1}{2} \begin{pmatrix} G^0 & A^0 \end{pmatrix} O(\beta) \begin{pmatrix} \frac{T_1}{v_1} & 0 \\ 0 & \frac{T_2}{v_2} \end{pmatrix} O(\beta)^T \begin{pmatrix} G^0 \\ A^0 \end{pmatrix} \\
&\quad + \begin{pmatrix} G^- & H^- \end{pmatrix}^\dagger \begin{pmatrix} 0 & 0 \\ 0 & m_{H^\pm}^2 \end{pmatrix} \begin{pmatrix} G^- \\ H^- \end{pmatrix} \\
&\quad + \begin{pmatrix} G^- & H^- \end{pmatrix}^\dagger O(\beta) \begin{pmatrix} \frac{T_1}{v_1} & 0 \\ 0 & \frac{T_2}{v_2} \end{pmatrix} O(\beta)^T \begin{pmatrix} G^- \\ H^- \end{pmatrix} + \dots \quad (2.66)
\end{aligned}
$$

We introduce the following Higgs tadpoles

$$
\begin{pmatrix} T_{H^0} \\ T_{h^0} \end{pmatrix} = O(\alpha) \begin{pmatrix} T_1 \\ T_2 \end{pmatrix} \Rightarrow \begin{pmatrix} T_1 \\ T_2 \end{pmatrix} = \begin{pmatrix} \cos\alpha\, T_{H_0} - \sin\alpha\, T_{h_0} \\ \sin\alpha\, T_{H_0} + \cos\alpha\, T_{h_0} \end{pmatrix} \quad (2.67)
$$

$$
\begin{pmatrix} t_{H^0 H^0} & t_{H^0 h^0} \\ t_{h^0 H^0} & t_{h^0 h^0} \end{pmatrix} = O(\alpha) \begin{pmatrix} \frac{T_1}{v_1} & 0 \\ 0 & \frac{T_2}{v_2} \end{pmatrix} O(\alpha)^T \quad (2.68)
$$

$$
\begin{pmatrix} t_{G^0 G^0} & t_{G^0 A^0} \\ t_{A^0 G^0} & t_{A^0 A^0} \end{pmatrix} = O(\beta) \begin{pmatrix} \frac{T_1}{v_1} & 0 \\ 0 & \frac{T_2}{v_2} \end{pmatrix} O(\beta)^T = \begin{pmatrix} t_{G^\pm G^\pm} & t_{G^\pm H^\pm} \\ t_{H^\pm G^\pm} & t_{H^\pm H^\pm} \end{pmatrix}
$$

The explicit formulas for the tadpoles are

$$
\begin{aligned}
t_{H^0 H^0} &= \frac{e}{2 m_W s_w} \left[T_{h^0} \left(\frac{s_\alpha^2 c_\alpha}{s_\beta} - \frac{c_\alpha^2 s_\alpha}{c_\beta} \right) + T_{H^0} \left(\frac{c_\alpha^3}{c_\beta} + \frac{s_\alpha^3}{s_\beta} \right) \right] \\
t_{H^0 h^0} &= \frac{e}{2 m_W s_w} \left[T_{h^0} \left(\frac{s_\alpha^2 c_\alpha}{c_\beta} + \frac{c_\alpha^2 s_\alpha}{s_\beta} \right) + T_{H^0} \left(-\frac{c_\alpha^2 s_\alpha}{c_\beta} + \frac{s_\alpha^2 c_\alpha}{s_\beta} \right) \right]
\end{aligned}
$$

$$
\begin{aligned}
t_{h^0 h^0} &= \frac{e}{2m_W s_w}\left[T_{h^0}\left(\frac{c_\alpha^3}{s_\beta}-\frac{s_\alpha^3}{c_\beta}\right)+T_{H^0}\left(\frac{s_\alpha^2 c_\alpha}{c_\beta}+\frac{c_\alpha^2 s_\alpha}{s_\beta}\right)\right]\\
t_{A^0 A^0} &= \frac{e}{2m_W s_w}\left[T_{h^0}\left(\frac{-s_\beta^2 s_\alpha}{c_\beta}+\frac{c_\beta^2 c_\alpha}{s_\beta}\right)+T_{H^0}\left(\frac{s_\beta^2 c_\alpha}{c_\beta}+\frac{c_\beta^2 s_\alpha}{s_\beta}\right)\right]\\
t_{G^0 A^0} &= \frac{e}{2m_W s_w}\left[T_{h^0}\left(s_\alpha s_\beta+c_\beta c_\alpha\right)+T_{H^0}\left(-s_\beta c_\alpha+c_\beta s_\alpha\right)\right]\\
t_{G^0 G^0} &= \frac{e}{2m_W s_w}\left[T_{h^0}\left(-s_\alpha c_\beta+s_\beta c_\alpha\right)+T_{H^0}\left(c_\beta c_\alpha+s_\beta s_\alpha\right)\right]
\end{aligned}
\tag{2.69}
$$

Thus we get for the Higgs potential

$$
\begin{aligned}
V &= V_0+H^0 T_{H^0}+h^0 T_{h^0}\\
&+\frac{1}{2}\left(\begin{array}{cc} H^0 & h^0\end{array}\right)\left(\begin{array}{cc} m_{H^0}^2+t_{H^0 H^0} & t_{H^0 h^0}\\ t_{h^0 H^0} & m_{h^0}^2+t_{h^0 h^0}\end{array}\right)\left(\begin{array}{c} H^0\\ h^0\end{array}\right)\\
&+\frac{1}{2}\left(\begin{array}{cc} G^0 & A^0\end{array}\right)\left(\begin{array}{cc} t_{G^0 G^0} & t_{G^0 A^0}\\ t_{A^0 G^0} & m_{A^0}^2+t_{A^0 A^0}\end{array}\right)\left(\begin{array}{c} G^0\\ A^0\end{array}\right)\\
&+\frac{1}{2}\left(\begin{array}{cc} G^- & H^-\end{array}\right)^\dagger\left(\begin{array}{cc} t_{G^- G^-} & t_{G^\pm H^\pm}\\ t_{H^\pm G^\pm} & m_{H^\pm}^2+t_{H^\pm H^\pm}\end{array}\right)\left(\begin{array}{c} G^-\\ H^-\end{array}\right)+\cdots
\end{aligned}
\tag{2.70}
$$

The reparametrization of the Higgs fields and masses reads

$$
\begin{aligned}
H^0 &\to (1+\frac{1}{2}\delta Z_{H^0 H^0})H^0+\frac{1}{2}\delta Z_{H^0 h^0}h^0\\
h^0 &\to (1+\frac{1}{2}\delta Z_{h^0 h^0})h^0+\frac{1}{2}\delta Z_{h^0 H^0}H^0\\
G^0 &\to (1+\frac{1}{2}\delta Z_{G^0 G^0})h^0+\frac{1}{2}\delta Z_{G^0 A^0}A^0\\
A^0 &\to (1+\frac{1}{2}\delta Z_{A^0 A^0})h^0+\frac{1}{2}\delta Z_{A^0 G^0}G^0\\
G^- &\to (1+\frac{1}{2}\delta Z_{G^- G^-})H^-+\frac{1}{2}\delta Z_{G^- H^-}H^-\\
H^- &\to (1+\frac{1}{2}\delta Z_{H^- H^-})H^-+\frac{1}{2}\delta Z_{H^- G^-}G^-\\
m_{H_0}^2 &\to m_{H_0}^2+\delta m_{H_0}^2,\ \ m_{h_0}^2\to m_{h_0}^2+\delta m_{h_0}^2\\
m_{A_0}^2 &\to m_{A_0}^2+\delta m_{A_0}^2,\ \ m_{H_\pm}^2\to m_{H_\pm}^2+\delta m_{H_\pm}^2
\end{aligned}
\tag{2.71}
$$

The counterterms are

$$
\begin{aligned}
\delta Z_{H^0 H^0} &= -\widetilde{\mathrm{Re}}\,\dot{\Pi}_{H^0 H^0}(m_{H^0}^2)\\
\delta Z_{H^0 h^0} &= \frac{2}{m_{H^0}^2-m_{h^0}^2}\widetilde{\mathrm{Re}}\left(\Pi_{H^0 h^0}(m_{h^0}^2)-t_{H^0 h^0}\right)\\
\delta Z_{h^0 H^0} &= \frac{2}{m_{h^0}^2-m_{H^0}^2}\widetilde{\mathrm{Re}}\left(\Pi_{h^0 H^0}(m_{H^0}^2)-t_{H^0 h^0}\right)
\end{aligned}
$$

28

$$\delta Z_{h^0 h^0} = -\widetilde{\mathrm{Re}}\ \dot{\Pi}_{h^0 h^0}(m_{h^0}^2)$$

$$\delta Z_{G^0 G^0} = -\widetilde{\mathrm{Re}}\ \dot{\Pi}_{G^0 G^0}(m_{G^0}^2)$$

$$\delta Z_{G^0 A^0} = \frac{2}{m_{G^0}^2 - m_{A^0}^2}\widetilde{\mathrm{Re}}\ (\Pi_{G^0 A^0}(m_{A^0}^2) - t_{G^0 A^0})$$

$$\delta Z_{A^0 G^0} = \frac{2}{m_{A^0}^2 - m_{G^0}^2}\widetilde{\mathrm{Re}}\ (\Pi_{A^0 G^0}(m_{G^0}^2) - t_{G^0 A^0})$$

$$\delta Z_{A^0 A^0} = -\widetilde{\mathrm{Re}}\ \dot{\Pi}_{A^0 A^0}(m_{A^0}^2)$$

$$\delta Z_{G^\pm G^\pm} = -\widetilde{\mathrm{Re}}\ \dot{\Pi}_{G^\pm G^\pm}(m_{G^\pm}^2)$$

$$\delta Z_{G^\pm H^\pm} = \frac{2}{m_{G^\pm}^2 - m_{H^\pm}^2}\widetilde{\mathrm{Re}}\ (\Pi_{G^\pm H^\pm}(m_{H^\pm}^2) - t_{G^\pm H^\pm})$$

$$\delta Z_{H^\pm G^\pm} = \frac{2}{m_{H^\pm}^2 - m_{G^\pm}^2}\widetilde{\mathrm{Re}}\ (\Pi_{H^\pm G^\pm}(m_{G^\pm}^2) - t_{G^\pm H^\pm})$$

$$\delta Z_{H^\pm H^\pm} = -\widetilde{\mathrm{Re}}\ \dot{\Pi}_{H^\pm H^\pm}(m_{H^\pm}^2)$$

$$\delta m_{H^0}^2 = \widetilde{\mathrm{Re}}\ \Pi_{H^0 H^0}(m_{H^0}^2) - t_{H^0 H^0}$$

$$\delta m_{h^0}^2 = \widetilde{\mathrm{Re}}\ \Pi_{h^0 h^0}(m_{h^0}^2) - t_{h^0 h^0}$$

$$\delta m_{A^0}^2 = \widetilde{\mathrm{Re}}\ \Pi_{A^0 A^0}(m_{A^0}^2) - t_{A^0 A^0}$$

$$\delta m_{H^\pm}^2 = \widetilde{\mathrm{Re}}\ \Pi_{H^\pm H^\pm}(m_{H^\pm}^2) - t_{H^\pm H^\pm} \qquad (2.72)$$

As Pierce and Papadopoulos nicely wrote [49], the terms linear in H^0 and h^0 are to be thought of as counterterms for the tadpoles. To each order in the loop expansion we require that the total tadpole contribution vanishes. At tree level this implies $-iT_{H^0} = 0 = -iT_{h^0}$. This then gives the conventional tree level masses. At one loop $-iT_{H^0}$ must cancel the one loop tadpole diagram $i\tau_{H^0}$ and similarly $-iT_{h^0} + i\tau_{h^0} = 0$. These conditions determine T_{H^0} and T_{h^0} and above equation determine their contribution to the one loop mass matrices (just replace T_{H^0} and T_{h^0} by τ_{H^0} and τ_{h^0} in mass matrices).

The parameter $\tan\beta$ is renormalizad in the following way

$$\tan\beta \rightarrow \tan\beta + \delta\tan\beta$$

$$\delta\tan\beta = \frac{\tan\beta}{m_Z \sin 2\beta}\mathrm{Im}\left(\widetilde{\mathrm{Re}}\Pi_{A^0 Z}(m_{A^0}^2)\right) \qquad (2.73)$$

where the choice that the pseudo-scalar Higgs field A^0 does not mix with the Z boson for on-shell momenta was made.

Chapter 3

Sfermion two-body decays

If the MSSM is realized in nature, LHC will produce supersymmetric particles co-
piously. The best environment for a precise determination of the model parameters
would be a high energy e^+e^- linear collider. Experimental accuracies are expected
at the per-cent down to the per-mill level [51, 52, 53]. These must be matched from
the theoretical side. Therefore loop calculations are mandatory.

3.1 Decay patterns

There are four possibilities of Feynman graphs for a two-body decay of a scalar: the
decay into two scalars, into two fermions, into scalar and a vector particle and into
two vector particles. The fourth possibility is not realized in the decay of a sfermion
in the MSSM. The following sfermion decays are calculated (the first generation is
shown, $i, j, c = 1, 2$; $n = 1, \ldots, 4$):

$\tilde{\nu}_e$	$\to$	$\nu_e \, \tilde{\chi}_n^0$	$\tilde{e}_i$	$\to$	$e \, \tilde{\chi}_n^0$	$\tilde{u}_i$	$\to$	$u \, \tilde{\chi}_n^0$	$\tilde{d}_i$	$\to$	$d \, \tilde{\chi}_n^0$
$\tilde{\nu}_e$	$\to$	$e \, \tilde{\chi}_c^+$	$\tilde{e}_i$	$\to$	$\nu_e \, \tilde{\chi}_c^-$	$\tilde{u}_i$	$\to$	$d \, \tilde{\chi}_c^+$	$\tilde{d}_i$	$\to$	$u \, \tilde{\chi}_c^-$
$\tilde{\nu}_e$	$\to$	$H^+ \tilde{e}_j$	$\tilde{e}_i$	$\to$	$H^- \tilde{\nu}_e$	$\tilde{u}_i$	$\to$	$H^+ \tilde{d}_j$	$\tilde{d}_i$	$\to$	$H^- \tilde{u}_j$
$\tilde{\nu}_e$	$\to$	$W^+ \tilde{e}_j$	$\tilde{e}_i$	$\to$	$h^0 \tilde{e}_j$	$\tilde{u}_i$	$\to$	$h^0 \tilde{u}_j$	$\tilde{d}_i$	$\to$	$h^0 \tilde{d}_j$
			$\tilde{e}_i$	$\to$	$H^0 \tilde{e}_j$	$\tilde{u}_i$	$\to$	$H^0 \tilde{u}_j$	$\tilde{d}_i$	$\to$	$H^0 \tilde{d}_j$
			$\tilde{e}_i$	$\to$	$A^0 \tilde{e}_j$	$\tilde{u}_i$	$\to$	$A^0 \tilde{u}_j$	$\tilde{d}_i$	$\to$	$A^0 \tilde{d}_j$
			$\tilde{e}_i$	$\to$	$\tilde{e}_j \, Z$	$\tilde{u}_i$	$\to$	$\tilde{u}_j \, Z$	$\tilde{d}_i$	$\to$	$\tilde{d}_j \, Z$
			$\tilde{e}_i$	$\to$	$\tilde{\nu}_e \, W^-$	$\tilde{u}_i$	$\to$	$\tilde{d}_j \, W^+$	$\tilde{d}_i$	$\to$	$\tilde{u}_j \, W^-$
						$\tilde{u}_i$	$\to$	$u \, \tilde{g}$	$\tilde{d}_i$	$\to$	$d \, \tilde{g}$

If the squark decay into a gluino is kinematically allowed it will dominate due to the
QCD interaction. The third generation $\tilde{f}_2$ can decay into $\tilde{f}_1$ and a neutral boson

if there is sufficiently large mass splitting. For stops and sbottoms with large mass differences, decays into a charged boson and a sfermion are possible.

3.2   Calculation at full one-loop level

The renormalized one-loop amplitude is the sum of the tree-level amplitude and the one-loop contributions, see Fig. 3.1.
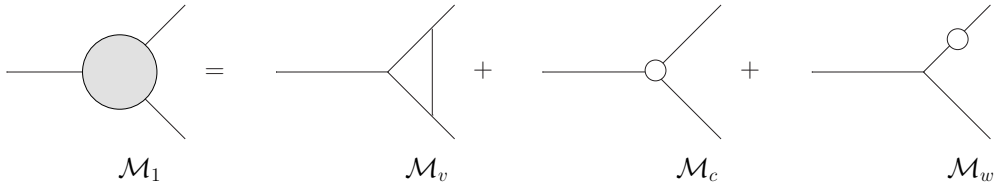
Figure 3.1: One-loop rerormalization procedure for a 1 to 2 process schematically

The tree-level couplings are given at the scale Q, implying that there are coupling counterterms consisting of only divergent parts. In case the renormalized amplitudes are finite it is a proof for RGE invariance of the $\overline{\text{DR}}$ scheme. The vertex corrections and wave function corrections can be directly calculated with FA/FC.

There are many decay channels and it was worthwhile to develop an automatic generator written in Mathematica. First of all, it was necessary to work out all counterterms for the whole MSSM. We did not hard coded all couplings (more than 300) at one-loop level. We instead, worked with the array of all the coupling and the wave function counterterms, we performed the shifts, expanded the amplitude and took terms linear in the counterterms.

The two-body sfermion decay width can be written in one loop approximation as

$$
\begin{aligned}
\Gamma &= N_C \times kin \left(|\mathcal{M}_0|^2 + 2\text{Re}(\mathcal{M}_0^\dagger \mathcal{M}_1) \right) \\
kin &= \frac{\kappa(m_0^2, m_1^2, m_2^2)}{16\pi m_0^3}
\end{aligned}
\tag{3.1}
$$

with the totally symmetric *Källen function* $\kappa(x, y, z) = \sqrt{(x - y - z)^2 - 4yz}$ and the color factor N_C.

The $|\mathcal{M}_0|^2$ for the three configurations are

$$
\begin{aligned}
\text{SSS} \quad &: \quad |g^2| \\
\text{SSV} \quad &: \quad |g^2| \left[m_0^4 - 2(m_1^2 + m - 2^2)m_0^2 + (m_1^2 - m_2^2)^2 \right] \frac{1}{m_2^2} \\
\text{SSF} \quad &: \quad (m_0^2 - m_1^2 - m_2^2)(|g_L|^2 + |g_R|^2) - 2m_1 m_2 (g_L^* g_R + g_L g_R^*)
\end{aligned}
\tag{3.2}
$$

31

$\mathcal{M}_1$ denotes the UV finite one-loop amplitude. The prefactor kin is a function of the on-shell masses of the incoming sfermion and outgoing particles only. Massless particles in loops can cause so-called infrared divergence in Γ. For this purpose, a regulator mass λ for the photon and gluon is introduced. Adding then soft photon (gluon) or real photon (gluon) radiation cancels these divergencies.

3.3 Soft photon radiation

In an observable process in addition to the basic process one includes also radiation of soft photons. This is not only to achieve the IR finiteness of the result, but to have physically a meaningful calculation. Photons are massless and their energies may be arbitrarily small and thus escaping the detector [44].

The soft photon cross section (or decay width) is proportional to the Born cross section

$$\left(\frac{d\sigma}{d\Omega} \right)_s = - \left(\frac{d\sigma}{d\Omega} \right)_0 \frac{e^2}{(2\pi)^3} \int_{|k| \leq \Delta E} \frac{d^3k}{2\omega_k} \sum_{ij} \frac{\pm p_i p_j Q_i Q_j}{p_i k p_j k} \tag{3.3}$$

where $\omega_k = \sqrt{\mathbf{k^2} + \lambda^2}$. ΔE is the cut on the photon energy. The basic integrals

$$I_{ij} = \int_{|k| \leq \Delta E} \frac{d^3k}{2\omega_k} \frac{2p_i p_j}{p_i k p_j k} \tag{3.4}$$

have been worked out by 't Hooft and Veltman [35].

Adding the soft photon cross section to the one loop corrected cross section for the corresponding basic process, the result is free of the parameter λ and the limit $\lambda \to 0$ can be taken.

3.4 Hard photon radiation

Although the inclusion of the real soft photon emission is sufficient to obtain IR-finite results, it is often not adequate for real experiments, because realistic detectors do not provide sufficiently small resolution $\Delta E/E$ necessary for the valididy of the soft photon approximation [44].

3.4.1 Scalar-Scalar-Scalar configuration
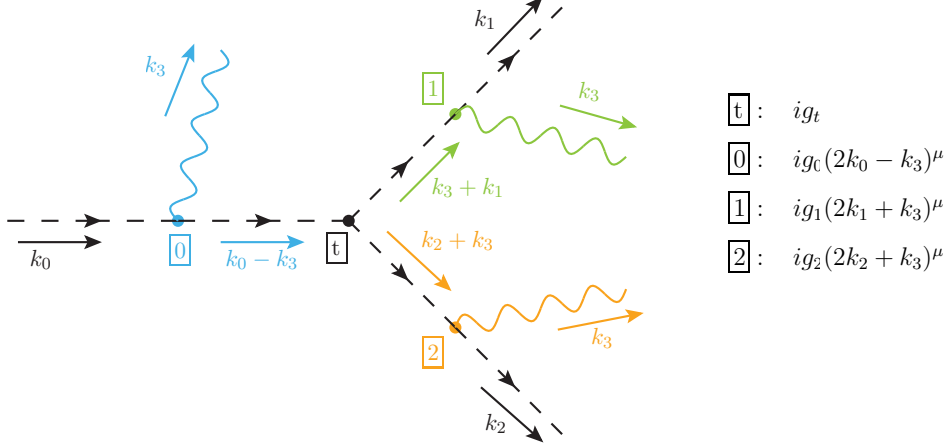
The couplings g_i correspond to QED couplings and therefore are given by $g_i = -eQ_i$ (except for the W boson) where Q is the charge of the considered particle and $e > 0$ in our notation. Charge conservation would mean that $g_0 = g_1 + g_2$. Particular amplitudes are:

$$\mathcal{M}_0 = ig_t \frac{i}{(k_0 - k_3)^2 - m_0^2} ig_0 (2k_0 - k_3)_\mu \varepsilon^{*\mu} \tag{3.5}$$

$$\mathcal{M}_1 = ig_t \frac{i}{(k_1 + k_3)^2 - m_1^2} ig_1 (2k_1 + k_3)_\mu \varepsilon^{*\mu} \tag{3.6}$$

$$\mathcal{M}_2 = ig_t \frac{i}{(k_2 + k_3)^2 - m_2^2} ig_2 (2k_2 + k_3)_\mu \varepsilon^{*\mu} \tag{3.7}$$

The photon polarization vector contracted with its momentum yields zero: $k_{3\mu} \varepsilon_{k_3}^{*\mu} = 0$. By squaring the sum of the amplitudes we obtain the following result (in the unpolarized case)

$$\begin{aligned}
\overline{|\mathcal{M}|^2} = \ |g_t|^2 4 [&-g_0^2 m_0^2 I_{00} - g_0 g_1 (m_0^2 + m_1^2 - m_2^2) I_{10} - g_1^2 m1^2 I_{11} \\
&- g_0 g_2 (m_0^2 - m_1^2 + m_2^2) I_{20} \\
&- g_1 g_2 (m_0^2 - m_1^2 - m_2^2) I_{21} - g_2^2 m_2^2 I_{22} \\
&- g_0 (g_1 + g_2) I_0 - g_1 (g_0 - g_2) I_1 - g_2 (g_0 - g_1) I_2]
\end{aligned} \tag{3.8}$$

where I integrals are so-called bremsstrahlung integrals and their analytic form can be found in [44]. Note that the result is symmetric under the exchange of $1, 2$ indices as it should be.

3.4.2   Scalar-Fermion-Fermion configuration
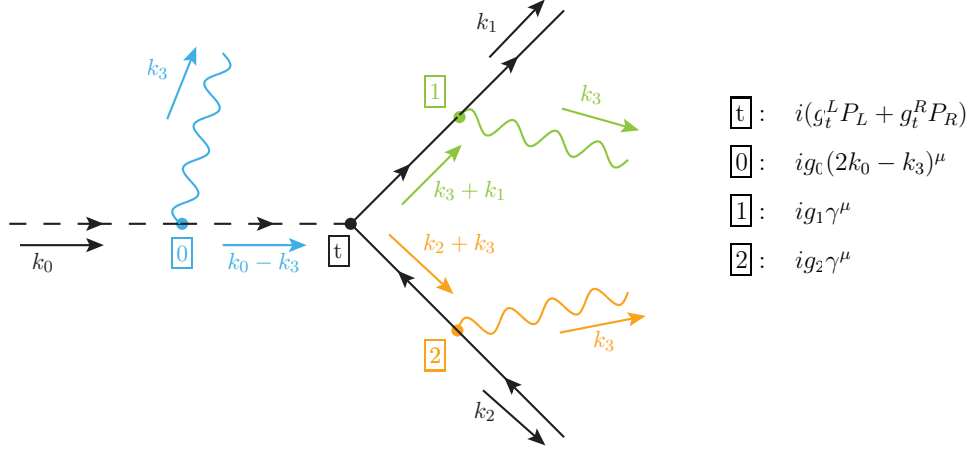
Particular amplitudes are:

$$\mathcal{M}_0 \;=\; \bar{u}(k_1)\,i(g_t^L P_L + g_t^R P_R)\frac{i}{(k_0 - k_3)^2 - m_0^2}\,ig_0\,(2k_0 - k_3)_\mu\,\varepsilon^{*\mu}\,v(k_2) \quad (3.9)$$

$$\mathcal{M}_1 \;=\; \bar{u}(k_1)\,ig_1\gamma_\mu\frac{i(\not{k}_3 + \not{k}_1 + m_1)}{(k_1 + k_3)^2 - m_1^2}\,i(g_t^L P_L + g_t^R P_R)\,\varepsilon^{*\mu}\,v(k_2) \quad (3.10)$$

$$\mathcal{M}_2 \;=\; \bar{u}(k_1)\,i(g_t^L P_L + g_t^R P_R)\frac{i(-\not{k}_2 - \not{k}_3 + m_2)}{(k_2 + k_3)^2 - m_2^2}\,ig_2\gamma_\mu\,\varepsilon^{*\mu}\,v(k_2) \quad (3.11)$$

By squaring the sum of the amplitudes we obtain the following result (in the unpolarized case)

$$
\begin{aligned}
\overline{|\mathcal{M}|^2} \;=\; & 4g_0^2 m_0^2[(|g_t^L|^2 + |g_t^R|^2)(-m_0^2 + m_1^2 + m_2^2) + (g_t^L g_t^{R*} + g_t^{L*} g_t^R)2m_1 m_2]I_{00} \\
+ \; & 4g_0 g_1[(|g_t^L|^2 + |g_t^R|^2)(-m_0^4 + m_1^4 - m_2^4 + 2m_0^2 m_2^2) \\
+ \; & (g_t^L g_t^{R*} + g_t^{L*} g_t^R)2m_1 m_2(m_0^2 + m_1^2 - m_2^2)]I_{10} \\
+ \; & 4g_1^2 m_1^2[(|g_t^L|^2 + |g_t^R|^2)(-m_0^2 + m_1^2 + m_2^2) + (g_t^L g_t^{R*} + g_t^{L*} g_t^R)2m_1 m_2]I_{11} \\
+ \; & 4g_0 g_2[(|g_t^L|^2 + |g_t^R|^2)(m_0^4 + m_1^4 - m_2^4 - 2m_0^2 m_1^2) \\
+ \; & (g_t^L g_t^{R*} + g_t^{L*} g_t^R)2m_1 m_2(-m_0^2 + m_1^2 - m_2^2)]I_{20} \\
+ \; & 4g_1 g_2[(|g_t^L|^2 + |g_t^R|^2)(-m_0^2 + m_1^2 + m_2^2)^2 \\
+ \; & (g_t^L g_t^{R*} + g_t^{L*} g_t^R)2m_1 m_2(-m_0^2 + m_1^2 + m_2^2)]I_{21} \\
+ \; & 4g_2^2 m_2^2[(|g_t^L|^2 + |g_t^R|^2)(-m_0^2 + m_1^2 + m_2^2) + (g_t^L g_t^{R*} + g_t^{L*} g_t^R)2m_1 m_2]I_{22} \\
+ \; & 2g_0[(|g_t^L|^2 + |g_t^R|^2)(g_0(-3m_0^2 + m_1^2 + m_2^2) + (g_1 - g_2)(m_0^2 + m_1^2 + m_2^2)) \\
+ \; & (g_t^L g_t^{R*} + g_t^{L*} g_t^R)2(g_0 + g_1 - g_2)m_1 m_2]I_0 \\
+ \; & 4g_1[(|g_t^L|^2 + |g_t^R|^2)(g_1 m_1^2 + (g_0 + g_2)(m_2^2 - m_0^2)) \\
+ \; & (g_t^L g_t^{R*} + g_t^{L*} g_t^R)(g_0 + g_1 + g_2)m_1 m_2]I_1
\end{aligned}
$$

34

$$
\begin{aligned}
&+\quad 4g_2[(|g_t^L|^2+|g_t^R|^2)(g_2m_2^2+(g_0-g_1)(m_0^2-m_1^2))\\
&+\quad (g_t^L g_t^{R*}+g_t^{L*}g_t^R)(-g_0+g_1+g_2)m_1m_2]I_2\\
&+\quad 2g_1^2(|g_t^L|^2+|g_t^R|^2)I_1^2+2g_2^2(|g_t^L|^2+|g_t^R|^2)I_2^1\\
&+\quad (|g_t^L|^2+|g_t^R|^2)(-g_0^2+g_0g_1-g_0g_2+2g_1g_2)I
\end{aligned}
\tag{3.12}
$$

Note also here that the result after sending the coupling g_2 to $-g_2$ is symmetric under the exchange of indices 1 and 2.

3.4.3 Scalar-Fermion-Fermion configuration (with $m_1 = 0$)

Among all the sfermions decays there is also a decay with a chargino and a neutrino in the final state. The neutrino is considered to be a massless particle in the MSSM theory. Concerning the photon radiation we can freely take the previous general result and set the mass and the coupling of the particle 1 to zero ($m_1 = 0, g_1 = 0$). The result then simplifies to

$$
\begin{aligned}
\overline{|\mathcal{M}|^2} &=\ (|g_t^L|^2+|g_t^R|^2)[4g_0^2m_0^2(-m_0^2+m_2^2)I_{00}+4g_0g_2(m_0^4-m_2^4)I_{20}\\
&+\ 4g_2^2m_2^2(-m_0^2+m_2^2)I_{22}+2g_0(g_0(-3m_0^2+m_2^2)-g_2(m_0^2+m_2^2))I_0\\
&+\ 4g_2(g_2m_2^2+g_0m_0^2)I_2+2g_2^2I_2^1-(g_0^2+g_0g_2)I]
\end{aligned}
\tag{3.13}
$$

However, we cannot now take the analytic expression of the bremsstrahlung integrals as is given in [44]. We have to arrange it little so that at the end we could take the limit $m_1 \to 0$. The necessary integrals with all the auxiliary functions as stated in [44] read

$$
\kappa = \kappa(m_0^2, m_1^2, m_2^2) = \sqrt{m_0^4+m_1^4+m_2^4-2m_0^2m_1^2-2m_1^2m_2^2-2m_0^2m_2^2}
\tag{3.14}
$$

$$
\begin{aligned}
\beta_0 &=\ \frac{m_0^2-m_1^2-m_2^2+\kappa}{2m_1m_2},\\
\beta_1 &=\ \frac{m_0^2-m_1^2+m_2^2-\kappa}{2m_0m_2}, \qquad \beta_2=\frac{m_0^2+m_1^2-m_2^2-\kappa}{2m_0m_1},
\end{aligned}
\tag{3.15}
$$

$$
\begin{aligned}
I_{00} &=\ \frac{1}{4m_0^4}\left[\kappa\log\left(\frac{\kappa^2}{\lambda m_0m_1m_2}\right)-\kappa-(m_1^2-m_2^2)\log\left(\frac{\beta_1}{\beta_2}\right)\right.\\
&\qquad\qquad \left. -m_0^2\log(\beta_0)\right]
\end{aligned}
\tag{3.16}
$$

$$
I_{20} =\ \frac{1}{4m_0^2}\left[-2\log\left(\frac{\lambda m_0m_1m_2}{\kappa^2}\right)\log(\beta_1)+2\log^2(\beta_1)-\log^2(\beta_0)\right.
$$

$$\left. - \log^2(\beta_2) + 2\text{Sp}(1 - \beta_1^2) - \text{Sp}(1 - \beta_0^2) - \text{Sp}(1 - \beta_2^2)\right] \quad (3.17)$$

$$I_{22} = \frac{1}{4m_2^2 m_0^2}\left[\kappa \log\left(\frac{\kappa^2}{\lambda m_0 m_1 m_2}\right) - \kappa - (m_0^2 - m_2^2)\log\left(\frac{\beta_0}{\beta_2}\right)\right.$$

$$\left. - m_2^2 \log(\beta_2)\right] \quad (3.18)$$

$$I = \frac{1}{4m_0^2}\left[\frac{\kappa}{2}(m_0^2 + m_1^2 + m_2^2) + 2m_0^2 m_1^2 \log(\beta_2) + 2m_0^2 m_2^2 \log(\beta_1)\right.$$

$$\left. + 2m_1^2 m_2^2 \log(\beta_0)\right] \quad (3.19)$$

$$I_0 = \frac{1}{4m_0^2}\left[-2m_1^2 \log(\beta_2) - 2m_2^2 \log(\beta_1) - \kappa\right] \quad (3.20)$$

$$I_2 = \frac{1}{4m_0^2}\left[-2m_0^2 \log(\beta_1) - 2m_1^2 \log(\beta_0) - \kappa\right] \quad (3.21)$$

$$I_2^1 = \frac{1}{4m_0^2}\left[m_1^4 \log(\beta_0) - m_0^2(2m_2^2 - 2m_1^2 + m_0^2)\log(\beta_1)\right.$$

$$\left. - \frac{\kappa}{4}(m_2^2 - 3m_1^2 + 5m_0^2)\right] \quad (3.22)$$

Now we are going to explore what happens if the mass m_1 is a small number. The auxiliary functions $\kappa, \beta_0, \beta_1, \beta_2$ after neglecting the higher order terms are as follows

$$\kappa = (m_0^2 - m_2^2)\left[1 - \frac{m_1^2(m_0^2 + m_2^2)}{m_0^2 - m_2^2}\right] + \mathcal{O}(m_1^4) \quad (3.23)$$

$$\beta_0 = \frac{m_0^2 - m_2^2}{m_1 m_2} + \mathcal{O}(m_1), \quad \beta_1 = \frac{m_2}{m_0} + \mathcal{O}(m_1^2) \quad (3.24)$$

$$\beta_2 = \frac{m_1}{2m_0}\left(1 + \frac{m_0^2 + m_2^2}{m_0^2 - m_2^2}\right) + \mathcal{O}(m_1^3) \quad (3.25)$$

Applying the above expansion into the integral I_{00} and neglecting terms which are zero in the limit $m_1 \to 0$ we obtain the following

$$I_{00} = \frac{1}{4m_0^4}\left[(m_0^2 - m_2^2)\log\left(\frac{(m_0^2 - m_2^2)^2}{\lambda m_0 m_1 m_2}\right) - (m_0^2 - m_2^2) + m_2^2 \log\left(\frac{m_2}{m_0}\right)\right.$$

$$\left. - m_2^2 \log\left(\frac{m_1}{2m_0}\left(1 + \frac{m_0^2 + m_2^2}{m_0^2 - m_2^2}\right)\right) - m_0^2 \log\left(\frac{m_0^2 - m_2^2}{m_1 m2}\right)\right]$$

$$+ \mathcal{O}(m_1) \quad (3.26)$$

We see that logarithms of m_1 cancel out and we can perform the limit $m_1 \to 0$. Integral I_{20} is little more tricky. Here also the Spence function is involved. In β_0 the

mass m_1 is in the denominator and we cannot apply directly the Spence function on the expression $(1 - \beta_0^2)$. First, we use the following identity

$$\text{Sp}(1 - x^2) = -2\log^2(x) - \text{Sp}(1 - \frac{1}{x^2}), \qquad x > 0 \qquad (3.27)$$

$$
\begin{aligned}
I_{20} &= \frac{1}{4m_0^2}\left[-2\log\left(\frac{\lambda m_0 m_2 m_1}{(m_0^2 - m_2^2)^2}\right)\log\left(\frac{m_2}{m_0}\right) + 2\log^2\frac{m_2}{m_0} - \log^2\left(\frac{m_0^2 - m_2^2}{m_1 m_2}\right)\right. \\
&\quad - \left. \log^2\left(\frac{m_1}{2m_0}\left(1 + \frac{m_0^2 + m_2^2}{m_0^2 - m_2^2}\right)\right) + 2\text{Sp}\left(1 - \frac{m_2^2}{m_0^2}\right) + 2\log^2\left(\frac{m_0^2 - m_2^2}{m_1 m_2}\right)\right] \\
&\quad + \mathcal{O}(m_1)
\end{aligned}
\qquad (3.28)
$$

Again, one can check that logarithms of m_1 cancel out. Remaining integrals are now easy to calculate. The result is

$$
I_{00} = \frac{1}{4m_0^4}\left[\kappa_0\log\left(\frac{\kappa_0^2}{\lambda m_0 m_2}\right) - \kappa_0 + m_2^2\log\left(\frac{m_2\kappa_0}{m_0^2}\right) - m_0^2\log\left(\frac{\kappa_0}{m_2}\right)\right] \qquad (3.29)
$$

$$
\begin{aligned}
I_{20} &= \frac{1}{4m_0^2}\left[-2\log\left(\frac{\lambda m_0 m_2}{\kappa_0^2}\right)\log\left(\frac{m_2}{m_0}\right) + 2\log^2\left(\frac{m_2}{m_0}\right) + \log^2\left(\frac{\kappa_0}{m_2}\right)\right. \\
&\quad \left. - \log^2\left(\frac{m_0}{\kappa_0}\right) + 2\text{Sp}\left(\frac{\kappa_0}{m_0^2}\right)\right]
\end{aligned}
\qquad (3.30)
$$

$$
\begin{aligned}
I_{22} &= \frac{1}{4m_2^2 m_0^2}\left[\kappa_0\log\left(\frac{\kappa_0^2}{\lambda m_0 m_2}\right) - \kappa_0 + m_0^2\log\left(\frac{m_2^2}{\kappa_0 m_0}\right)\right. \\
&\quad \left. - m_2^2\log\left(\frac{m_0}{\kappa_0}\right)\right]
\end{aligned}
\qquad (3.31)
$$

$$
I = \frac{1}{4m_0^2}\left[\frac{\kappa_0}{2}(m_0^2 + m_2^2) + 2m_0^2 m_2^2\log\left(\frac{m_2}{m_0}\right)\right] \qquad (3.32)
$$

$$
I_0 = \frac{1}{4m_0^2}\left[-2m_2^2\log\left(\frac{m_2}{m_0}\right) - \kappa_0\right] \qquad (3.33)
$$

$$
I_2 = \frac{1}{4m_0^2}\left[-2m_0^2\log\left(\frac{m_2}{m_0}\right) - \kappa_0\right] \qquad (3.34)
$$

$$
I_2^1 = \frac{1}{4m_0^2}\left[-m_0^2(2m_2^2 + m_0^2)\log\left(\frac{m_2}{m_0}\right) - \frac{\kappa_0}{4}(m_2^2 + 5m_0^2)\right] \qquad (3.35)
$$

where $\kappa_0 = m_0^2 - m_2^2$.

3.4.4 Scalar-Fermion-Fermion configuration (with clashing)

The orientation in the following diagram is assumed to go from down to up [54].
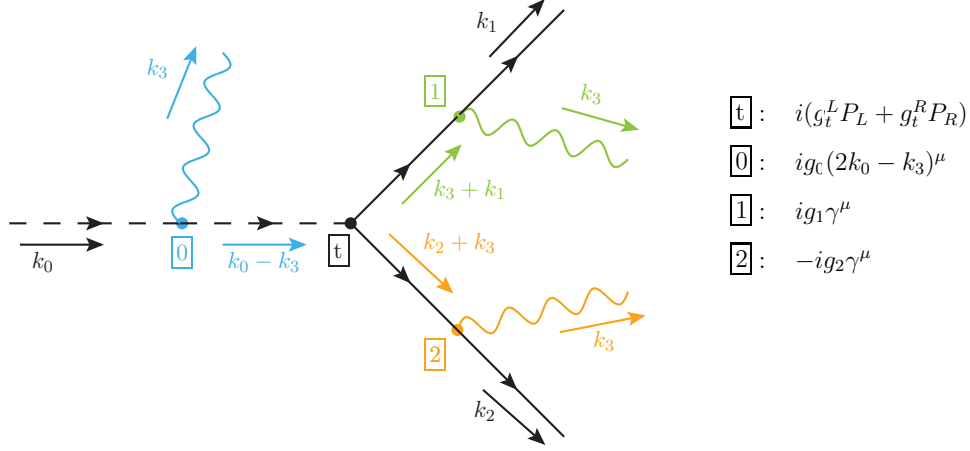
Particular amplitudes are:

$$\mathcal{M}_0 = \bar{u}(k_1)\,i(g_t^L P_L + g_t^R P_R)\frac{i}{(k_0 - k_3)^2 - m_0^2}\,ig_0\,(2k_0 - k_3)_\mu\,\varepsilon^{*\mu}\,v(k_2) \quad (3.36)$$

$$\mathcal{M}_1 = \bar{u}(k_1)\,ig_1\gamma_\mu\frac{i(\slashed{k}_3 + \slashed{k}_1 + m_1)}{(k_1 + k_3)^2 - m_1^2}\,i(g_t^L P_L + g_t^R P_R)\,\varepsilon^{*\mu}\,v(k_2) \quad (3.37)$$

$$\mathcal{M}_2 = \bar{u}(k_1)\,i(g_t^L P_L + g_t^R P_R)\frac{i(-\slashed{k}_2 - \slashed{k}_3 + m_2)}{(k_2 + k_3)^2 - m_2^2}\,(-ig_2\gamma_\mu)\,\varepsilon^{*\mu}\,v(k_2) \quad (3.38)$$

If we compare the amplitudes with the amplitudes in the non-clashing scenario they are exactly the same up to the minus sign in the $\mathcal{M}_2$ element. Thus we can use the previous result from non-clashing scenario and send the coupling g_2 to $-g_2$.

3.4.5 Scalar-Scalar-Vector configuration
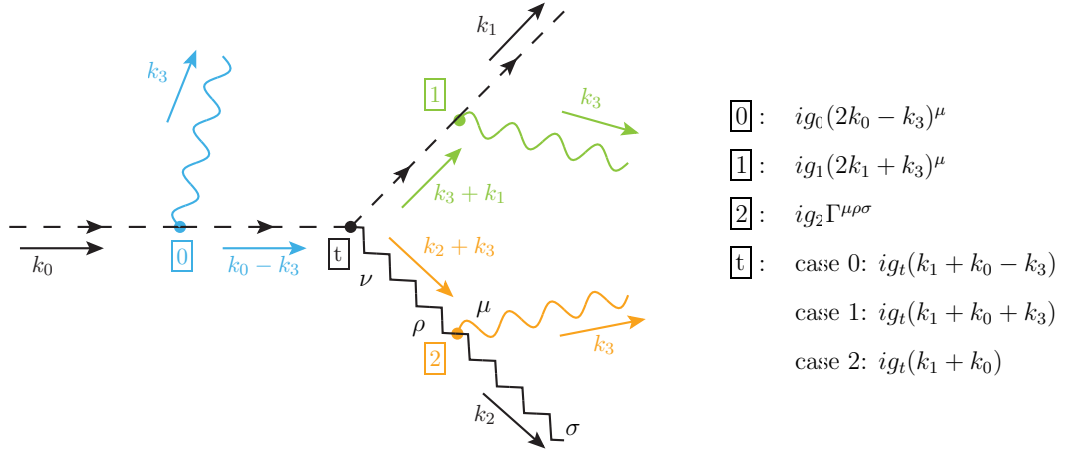
There is one more possibility in the SSV configuration. Photon can be radiated from the vertex too as in the MSSM model also the SSVV vertex exists.
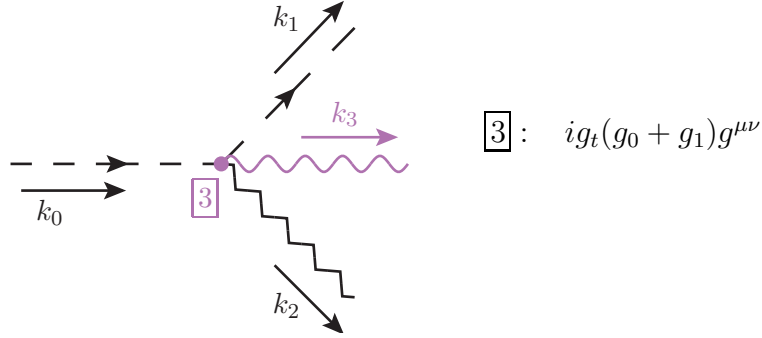
$$\boxed{3}: \quad ig_t(g_0 + g_1)g^{\mu\nu}$$

Particular amplitudes (in unitary gauge) are:

$$\mathcal{M}_0 = ig_t(k_0 + k_1 - k_3)_\nu \frac{i}{(k_0 - k_3)^2 - m_0^2} ig_0(2k_0 - k_3)_\mu \varepsilon_{k_2}^{*\nu}\varepsilon_{k_3}^{*\mu} \qquad (3.39)$$

$$\mathcal{M}_1 = ig_t(k_0 + k_1 + k_3)_\nu \frac{i}{(k_1 + k_3)^2 - m_1^2} ig_1(2k_1 + k_3)_\mu \varepsilon_{k_2}^{*\nu}\varepsilon_{k_3}^{*\mu} \qquad (3.40)$$

$$\mathcal{M}_2 = ig_t(k_0 + k_1)_\nu \frac{-i(g^{\nu\rho} - \frac{(k_2+k_3)^\nu (k_2+k_3)^\rho}{m_2^2})}{(k_2 + k_3)^2 - m_2^2} ig_2\Gamma_{\mu\rho\sigma}\,\varepsilon_{k_2}^{*\sigma}\varepsilon_{k_3}^{*\mu} \qquad (3.41)$$

$$\mathcal{M}_3 = ig_t(g_0 + g_1)g_{\mu\nu}\varepsilon_{k_2}^{*\nu}\varepsilon_{k_3}^{*\mu} \qquad (3.42)$$

where $\Gamma_{\mu\rho\sigma} = (-2k_2 - k_3)_\mu g_{\rho\sigma} + (2k_3 + k_2)_\sigma g_{\mu\rho} + (k_2 - k_3)_\rho g_{\sigma\mu}$

At this point we want to stress again that $k_{3\mu}\varepsilon_{k_3}^{*\mu} = 0$. Such a contraction of the photon polarization vector with its momentum can arise for instance in the amplitude $\mathcal{M}_2$ when the momentum k_3^ρ in the weak boson propagator meets the metric tensor $g_{\mu\rho}$ in the coupling $\Gamma_{\mu\rho\sigma}$ and this is then contracted with the photon polarization vector. Squaring the sum of the amplitudes we get (in unpolarized case). Another possibility is to keep the momentum k_3 in the amplitudes. Final result should be independent. The main point is that if one wants to apply the condition $k_{3\mu}\varepsilon_{k_3}^{*\mu} = 0$ one should apply it everywhere, in every amplitude. This is not that easy in the SFF configuration. Therefore if one wants to be at the safe side it is better to keep the photon momentum k_3 in all the matrix elements.

$$\overline{|\mathcal{M}|^2} = |g_t|^2[4g_0^2 m_0^2(2m_0^2 + 2m_1^2 - m_2^2 - \frac{(m_0^2 - m_1^2)^2}{m_2^2})I_{00}$$

$$+ \quad 4g_0 g_1(3m_0^4 + 2m_0^2 m_1^2 + 3m_1^4 - 3m_0^2 m_2^2 - 3m_1^2 m_2^2 + m_2^4$$

$$- \quad \frac{(m_0^2 - m_1^2)^2(m_0^2 + m_1^2)}{m_2^2})I_{10}$$

$$+ \quad 4g_1^2 m_1^2(2m_0^2 + 2m_1^2 - m_2^2 - \frac{(m_0^2 - m_1^2)^2}{m2^2})I_{11}$$

39

$$+ \quad 4g_0g_2(m_0^4 + 2m_0^2m_1^2 - 3m_1^4 + m_0^2m_2^2 + 3m_1^2m_2^2 - m_2^4 - \frac{(m_0^2 - m_1^2)^3}{m_2^2})I_{20}$$

$$+ \quad 4g_1g_2(3m_0^4 - 2m_0^2m_1^2 - m_1^4 - 3m_0^2m_2^2 - m_1^2m_2^2 + m_2^4 - \frac{(m_0^2 - m_1^2)^3}{m_2^2})I_{21}$$

$$+ \quad 4g_2m_2^2(2m_0^2 + 2m_1^2 - m_2^2 - \frac{(m_0^2 - m_1^2)^2}{m_2^2})I_{22}$$

$$+ \quad (2g_0^2 + 2g_0g_1 + 2g_1^2 - g_0g_2 + g_1g_2 + g_2^2$$

$$+ \quad \frac{1}{m_2^2}(m_0^2(2g_0g_1 + g_0g_2 - g_1^2 - 3g_1g_2 - 2g_2^2)$$

$$+ \quad m_1^2(g_0^2 + 2g_0g_1 + 3g_0g_2 - g_1g_2 - 2g_2^2)))I$$

$$+ \quad 2g_0((g_1 + g_2)(2m_0^2 + 6m_1^2 - 3m_2^2) + g_0(2m_0^2 - 2m_1^2 + m_2^2)$$

$$- \quad \frac{1}{m_2^2}(m_0^2 - m_1^2)(g_0(3m_0^2 + m_1^2) - (g_1 + g_2)(m_0^2 + 3m_1^2)))I_0$$

$$+ \quad 2g_1(g_0(6m_0^2 + 2m_1^2 - 3m_2^2) + g_1(-2m_0^2 + 2m_1^2 + m_2^2)$$

$$+ \quad g_2(-6m_0^2 - 2m_1^2 + 3m_2^2)$$

$$- \quad \frac{1}{m_2^2}((m_0^2 - m_1^2)(g_0(3m_0^2 + m_1^2) - g_2(3m_0^2 + m_1^2) - g_1(m_0^2 + 3m_1^2)))I_1$$

$$+ \quad 4g_2(2g_0(m_0^2 + m_1^2) - 2g_1(m_0^2 + m_1^2) - g_2m_2^2$$

$$- \quad \frac{(2g_0 - 2g_1 - g_2)(m_0^2 - m_1^2)^2)}{m_2^2})I_2$$

$$+ \quad g_0(-g_0 + 3g_2 + \frac{1}{m_2^2}(m_0^2(-g_0 - 4g_1 - 3g_2) + m_1^2(3g_0 + 2g_1 - g_2)))I_0^1$$

$$+ \quad g_0(g_0 - 2g_1 + g_2 + \frac{1}{m_2^2}(m_0^2(g_0 - 6g_1 - 5g_2) + m_1^2(g_0 + 4g_1 + g_2)))I_0^2$$

$$+ \quad g_1(-g_1 - 3g_2 + \frac{1}{m_2^2}(m_0^2(2g_0 + 3g_1 + g_2) + m_1^2(-4g_0 - g_1 + 3g_2)))I_1^0$$

$$+ \quad (-2g_0g_1 + g_1^2 - g_1g_2 + \frac{1}{m_2^2}(m_0^2(4g_0g_1 + g_1^2 - g_1g_2)$$

$$+ \quad m_1^2(-6g_0g_1 + g_1^2 + 5g_1g_2)))I_1^2$$

$$+ \quad 2(g_0g_2 + 3g_1g_2 + \frac{1}{m_2^2}(m_0^2(2g_1g_2 + g_2^2) + m_1^2(-2g_1g_2 - g_2^2)))I_2^0$$

$$+ \quad 2g_2(-3g_0 - g_1 + \frac{1}{m_2^2}(m_0^2(2g_0 - g_2) + m_1^2(-2g_0 + g_2)))I_2^1$$

$$- \quad \frac{g_0^2m_0^2}{m_2^2}(I_{00}^{11} + 2I_{00}^{21} + I_{00}^{22}) - \frac{g_1^2m_1^2}{m_2^2}(I_{11}^{00} + 2I_{11}^{20} + I_{11}^{22}) + 2g_2^2(I_{22}^{00} - 2I_{22}^{10} + I_{22}^{11})$$

$$- \quad \frac{2}{m_2^2}(g_0 + g_1)(g_0 - g_1 - g_2)I^1 - \frac{1}{m_2^2}(g_0 - g_1 - g_2)(2g_1 + g_2)I^2$$

$$+ \quad \frac{2g_2}{m_2^2}(g_0 - g_1 - g_2)I_2^{11}] \tag{3.43}$$

The coefficients which go with integrals I^1, I^2 and I_2^{11} are zero after invoking the charge conservation.

3.5 Gauge used

The gauge fixing lagrangian in the general linear R_ξ gauge is given by

$$\mathcal{L}^{GF} = -\frac{1}{\xi_W}F^+F^- - \frac{1}{\xi_A}|F^A|^2, \qquad A = Z, \gamma, g \tag{3.44}$$

with $F^+ = \partial_\mu W^{\mu+} + i\xi_W m_W G^+$, $F^Z = \partial_\mu Z^\mu + \xi_Z m_Z G^0$, $F^\gamma = \gamma_\mu A^\mu$ and $F^g = \gamma_\mu G^{a\mu}$. The Higgs-ghost propagators are $i/(q^2 - \xi_V m_V^2)$ and the vector-boson propagator reads

$$D_V^{\mu\nu} = \frac{-i\left(g^{\mu\nu} - (1-\xi_V)\frac{q^\mu q^\nu}{q^2 - \xi_V m_V^2}\right)}{q^2 - m_V^2} \tag{3.45}$$

The ξ-dependent part is a product of two propagators leading to a (n+1)-point loop integral. Performing a decomposition into partial fractions, it can be split into a form with single propagators only

$$D_V^{\mu\nu} = \frac{-ig^{\mu\nu}}{q^2 - m_V^2} + \frac{i}{m_V^2}\left(\frac{q^\mu q^\nu}{q^2 - m_V^2} - \frac{q^\mu q^\nu}{q^2 - \xi_V m_V^2}\right) \tag{3.46}$$

We have implemented this second form into FA for the W and Z bosons.

3.6 Input parameters

At the start, our program reads the file in SLHA format (e.g. SPheno.spc), where the Yukawa couplings, the gauge couplings g_1, g_2, g_3, gaugino masses, the soft breaking terms, the VEV, $m_{A^0}, \tan\beta, \mu$ are taken as input parameters at the scale Q. These parameters may be further changed. In that case, the program recalculates on-shell masses of Susy particles and does not take them from the input file.

3.7 Resummation

Part of a vertex correction proportional to $\tan\beta$ can be resummed (in the effective potential approach) by replacing the Yukawa coupling with [55]

$$y_b \to \frac{y_b}{1 + \Delta_b}, \qquad y_\tau \to \frac{y_\tau}{1 + \Delta_\tau} \tag{3.47}$$

Leading terms proportional to $\tan\beta$ come from gluino-sbottom, chargino-stop, chargino-sneutrino and neutralino-stau loops (see Appendix C)

$$
\begin{aligned}
\Delta_b \;=\; & -\frac{2\alpha_s}{3\pi} m_{\tilde{g}}\mu\tan\beta\, I(m_{\tilde{b}_1}^2, m_{\tilde{b}_2}^2, m_{\tilde{g}}^2) \\
& + \frac{y_t^2}{16\pi^2}\mu A_t \tan\beta\, I(m_{\tilde{t}_1}^2, m_{\tilde{t}_2}^2, \mu^2) \\
& - \frac{e^2}{16\pi^2 s_W^2}\mu M_2 \tan\beta\left[\cos\theta_t^2 I(m_{\tilde{t}_1}^2, M_2^2, \mu^2) + \sin\theta_t^2 I(m_{\tilde{t}_2}^2, M_2^2, \mu^2)\right] \;(3.48)
\end{aligned}
$$

$$
\begin{aligned}
\Delta_\tau \;=\; & \frac{e^2}{16\pi^2 c_W^2}\mu M_1 \tan\beta\left(\frac{1}{2}I(M_1^2, \mu^2, m_{\tilde{\tau}_1}^2 - I(M_1^2, \mu^2, m_{\tilde{\tau}_2}^2)\right. \\
& \left. \qquad\qquad\qquad\qquad +I(m_{\tilde{\tau}_1}^2, m_{\tilde{\tau}_2}^2, M_1^2)\right) \\
& - \frac{e^2}{16\pi^2 s_W^2}\mu M_2 \tan\beta\left(\frac{1}{2}I(M_2^2, \mu^2, m_{\tilde{\tau}_1}^2) + I(M_2^2, \mu^2, m_{\tilde{\nu}_\tau}^2)\right) \qquad (3.49)
\end{aligned}
$$

with

$$
I(a,b,c) = \frac{ab\log\frac{a}{b} + bc\log\frac{b}{c} + ca\log\frac{c}{a}}{(a-b)(b-c)(a-c)} \qquad (3.50)
$$

Chapter 4

Numerical results

There are a few program packages available for the automatic computation of amplitudes at full one-loop level in the MSSM: FeynArts/FormCalc [56], SloopS [57, 58] and GRACE/SUSY-loop [59]. SloopS and GRACE/SUSY-loop also perform renormalization at one-loop level. However, so far there is no publicly available code for the two-body sfermion decays at full one-loop level within the MSSM. Therefore, we have developed the Fortran code SFOLD [60] (and HFOLD [61, 62]). Like HFOLD, it adopts the renormalization prescription of the SUSY Parameter Analysis project (SPA) [63] and supports the SUSY Les Houches Accord (SLHA) input and output format [64]. The package SFOLD (Sfermion Full One-Loop Decays) computes all two-body decay widths and the corresponding branching ratios of all sfermions at full one-loop level.

Full one-loop radiative corrections to decays of sfermions into charginos and neutralinos are discussed in [65] for all sfermion flavours and generations. Yukawa corrections to sbottom decays into a lighter stop and a charged Higgs boson are given in [66]. SUSY-QCD corrections to top and bottom squark decays into all Higgs bosons are calculated in [67]. SUSY-QCD corrections to stop and sbottom decays into weak bosons can be found in [68]. Finally, SUSY-QCD corrections to squark decays to gluinos are given in [69]. Up to now, the electroweak corrections to sfermion decays into Higgs and gauge bosons have not been fully addressed. It turns out that also these corrections cannot be neglected in a significant part of the parameter space.

We also analyze corrections for the GMSB and the AMSB model. We show plenty of plots where the electroweak corrections in bosonic decays cannot be neglected. We focus on the decays of $\tilde{b}_2, \tilde{b}_1, \tilde{t}_2, \tilde{t}_1, \tilde{\tau}_2, \tilde{\tau}_1$ as these have the most interesting decay patterns.

For every analyzed particle we show four plots: first one in the CMSSM model, the second one in the GMSB model, the third one in the AMSB model, and the last one in the MSSM model. In first two plots the solid lines correspond to the full

one-loop result, dashed line to the SUSY-QCD result, dotted line to the tree level result. In last two plots, the solid lines correspond to the tree level result and the dotted to the full one-loop result.

In the CMSSM model, the partial widths are functions of the mSugra parameter m_0. Other parameters are: $m_{\frac{1}{2}} = am_0^2 + bm_0 + c$, $\tan\beta = 3$, $\text{sign}(\mu) = 1$, $A_0 = -300$, where a, b, c are chosen such that the whole parabola lies just above the excluded region given by ATLAS in Figure 1.1. The parabola goes through the points $[m_0, m_{1/2}]$ = [40, 330], [450, 300] and [740, 120]; $a = -0.00078217$, $b = 0.310093$, $c = 318.848$.

In the GMSB model, the partial widths are functions of the scale Λ. Other parameters are: $M_s = 10^7\Lambda$, $\tan\beta = 15$, $N_5 = 3$, $\text{sign}(\mu) > 0$.

In the AMSB model, the partial widths are functions of the parameter $m_{3/2}$. Other parameters are: $m_0 = 0.0075m_{3/2}$, $\tan\beta = 10$, $\text{sign}(\mu) > 0$.

In the MSSM model, the partial widths are functions of the parameter μ. Other parameters are: $M' = 100$ GeV, $M = 200$ GeV, $m_{\tilde{g}} = 600$ GeV, $A_e = A_\mu = A_\tau = -400$, $A_t = -600$, $A_b = -900$, $M_{A_0} = 140$ GeV, $\tan\beta = 10$, $M_L^2 = 200$ GeV, $M_{\tilde{E}}^2 = 100$ GeV, $M_{\tilde{Q}}^2 = M_{\tilde{U}}^2 = M_{\tilde{D}}^2 = 500$ GeV.

The masses of the supersymmetric particles in the CMSSM model are depicted on Figures 4.1 and 4.2.
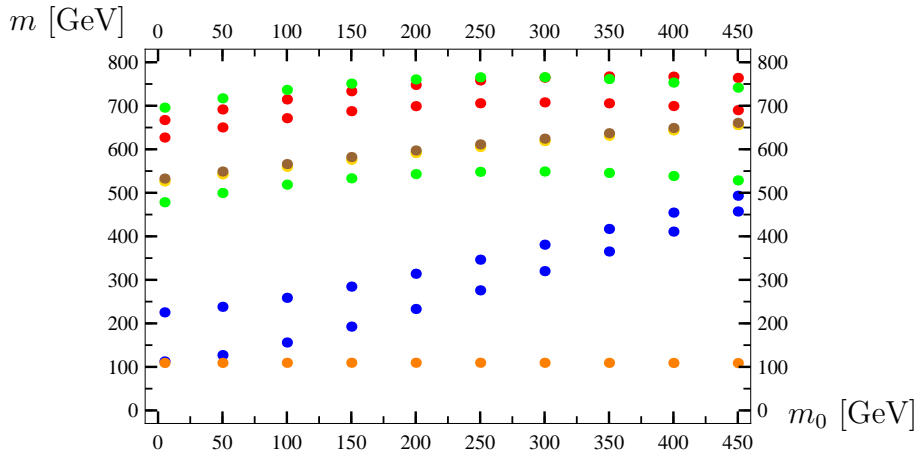
Figure 4.1: Masses of the supersymmetric particles. red: bottom squarks, green: top squarks, blue: tau sleptons, orange: h_0, gold: H^0, A^0, brown: $h^\pm$.

4.1 sbottom 2

CMSSM: The dominant decay is the decay into $\tilde{t}_1$ and W^- if $m_0 \lesssim 200$ GeV. It is clearly seen that the electroweak corrections can reach about 20%.
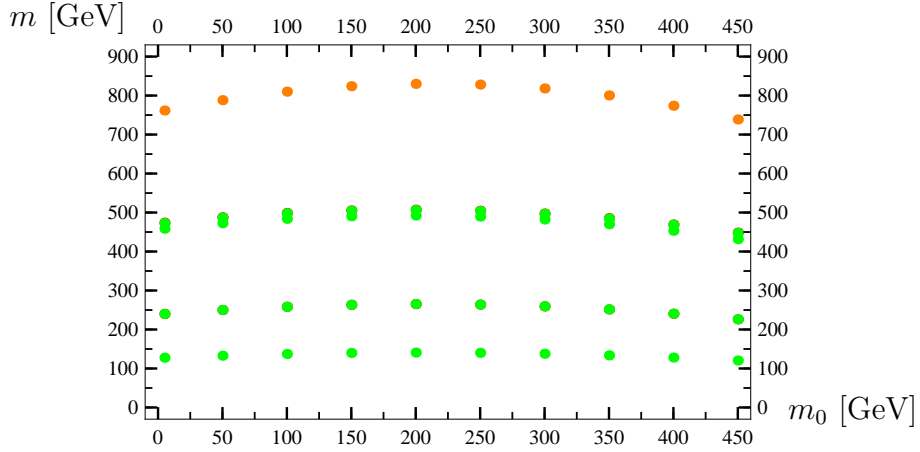
Figure 4.2: Masses of the supersymmetric particles. red: charginos, green: neutralinos, orange: gluino. Here $\tilde{\chi}_1^\pm \sim \tilde{\chi}_1^0$, $\tilde{\chi}_2^\pm \sim \tilde{\chi}_2^0$.

GMSB: $\tilde{b}_2$ decays mostly into charginos and neutralinos. The EW corrections are non-negligible.
AMSB: Dominant is the decay into the second chargino and bottom quark. The EW corrections are small.
MSSM: $\tilde{b}_2$ decays mostly into charginos. In these decays the EW corrections are rather large.

Figure 4.3: $\tilde{b}_2$ decays; CMSSM model. red: $t\,\tilde{\chi}_1^-$, green: $t\,\tilde{\chi}_2^-$, blue: $b\,\tilde{\chi}_1^0$, gold: $b\,\tilde{\chi}_2^0$, violet: $b\,\tilde{\chi}_3^0$, cyan: $b\,\tilde{\chi}_4^0$, orange: $b\,\tilde{g}$, purple: $\tilde{t}_1\,W^-$.

45

Figure 4.4: $\tilde{b}_2$ decays; GMSB model. red: $t\,\tilde{\chi}_1^-$, green: $t\,\tilde{\chi}_2^-$, blue: $b\,\tilde{\chi}_1^0$, gold: $b\,\tilde{\chi}_2^0$, violet: $b\,\tilde{\chi}_3^0$, cyan: $b\,\tilde{\chi}_4^0$, orange: $\tilde{t}_1\,W^-$.
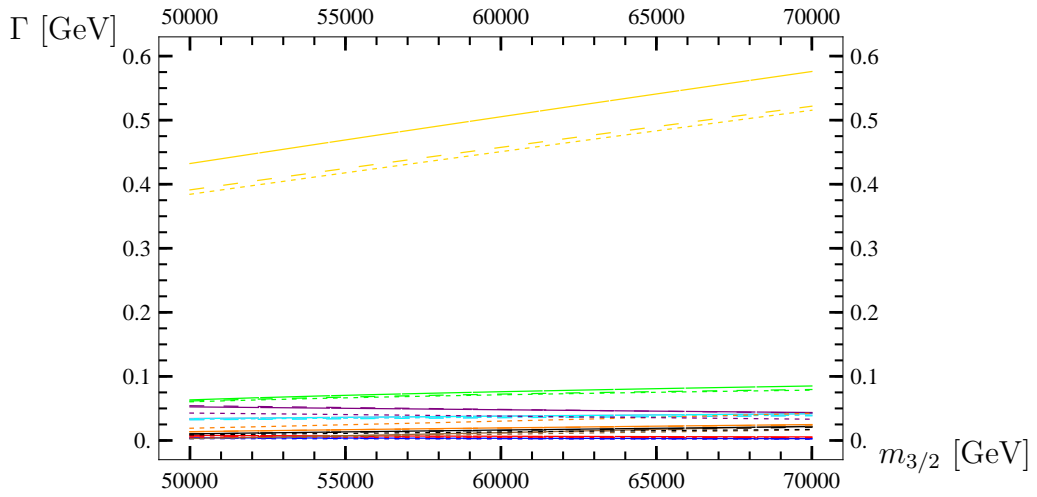
Figure 4.5: $\tilde{b}_2$ decays; AMSB model. red: $t\,\tilde{\chi}_1^-$, green: $t\,\tilde{\chi}_2^-$, blue: $b\,\tilde{\chi}_1^0$, gold: $b\,\tilde{\chi}_2^0$, violet: $b\,\tilde{\chi}_3^0$, cyan: $b\,\tilde{\chi}_4^0$, orange: $h_0\,\tilde{b}_1$, purple: $\tilde{t}_1\,W^-$, brown: $\tilde{t}_2\,W^-$, black: $\tilde{b}_1\,Z$.
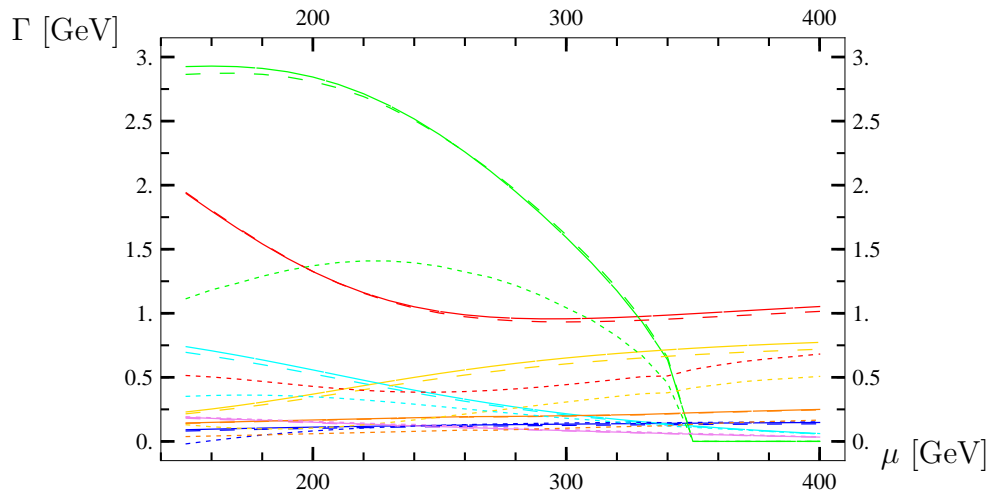
Figure 4.6: $\tilde{b}_2$ decays; MSSM model. red: $t\,\tilde{\chi}_1^-$, green: $t\,\tilde{\chi}_2^-$, blue: $b\,\tilde{\chi}_1^0$, gold: $b\,\tilde{\chi}_2^0$, violet: $b\,\tilde{\chi}_3^0$, cyan: $b\,\tilde{\chi}_4^0$, orange: $\tilde{t}_1\,W^-$.

4.2 sbottom 1

CMSSM: Also for sbottom 1, the decay into the W boson cannot be neglected. The electroweak corrections are of the same size as the SUSY-QCD corrections but of opposite sign. Therefore the full result is very close to the tree level result.

GMSB: Dominant are decays into charginos and neutralinos. The electroweak corrections grow with the increasing scale Λ.

AMSB: Branching ratio for the decay into stop 1 and the W boson is approximately one fifth of the total decay width and the electroweak corrections are 10%.

MSSM: Bosonic decays are very suppressed. The electroweak corrections in the decays into charginos and neutralinos are very large.

47

Figure 4.7: $\tilde{b}_1$ decays; CMSSM model. red: $t\,\tilde{\chi}_1^-$, green: $t\,\tilde{\chi}_2^-$, blue: $b\,\tilde{\chi}_1^0$, gold: $b\,\tilde{\chi}_2^0$, violet: $b\,\tilde{\chi}_3^0$, cyan: $b\,\tilde{\chi}_4^0$, orange: $\tilde{t}_1\,W^-$.
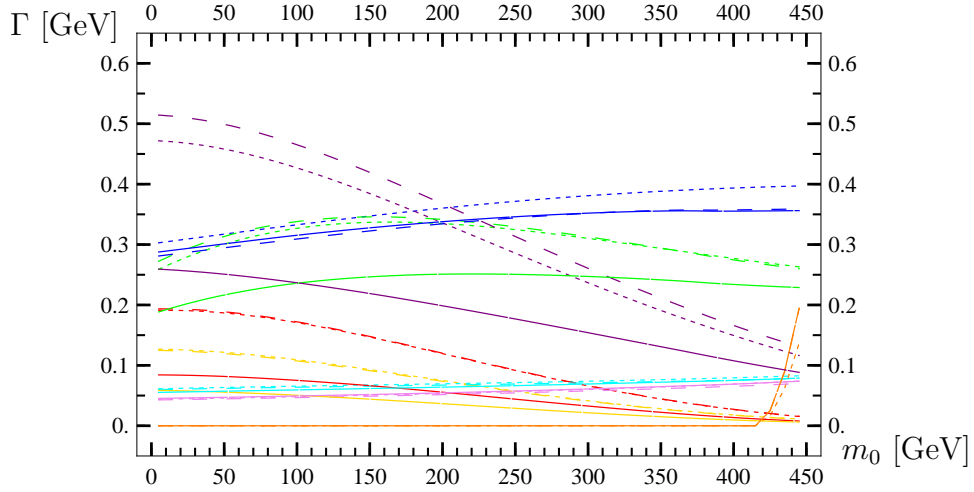

Figure 4.8: $\tilde{b}_1$ decays; GMSB model. red: $t\,\tilde{\chi}_1^-$, green: $t\,\tilde{\chi}_2^-$, blue: $b\,\tilde{\chi}_1^0$, gold: $b\,\tilde{\chi}_2^0$, violet: $b\,\tilde{\chi}_3^0$, cyan: $b\,\tilde{\chi}_4^0$, orange: $\tilde{t}_1\,W^-$.

Figure 4.9: $\tilde{b}_1$ decays; AMSB model. red: $t\,\tilde{\chi}_1^-$, green: $b\,\tilde{\chi}_1^0$, blue: $b\,\tilde{\chi}_2^0$, gold: $b\,\tilde{\chi}_3^0$, violet: $b\,\tilde{\chi}_4^0$, cyan: $\tilde{t}_1\,W^-$.
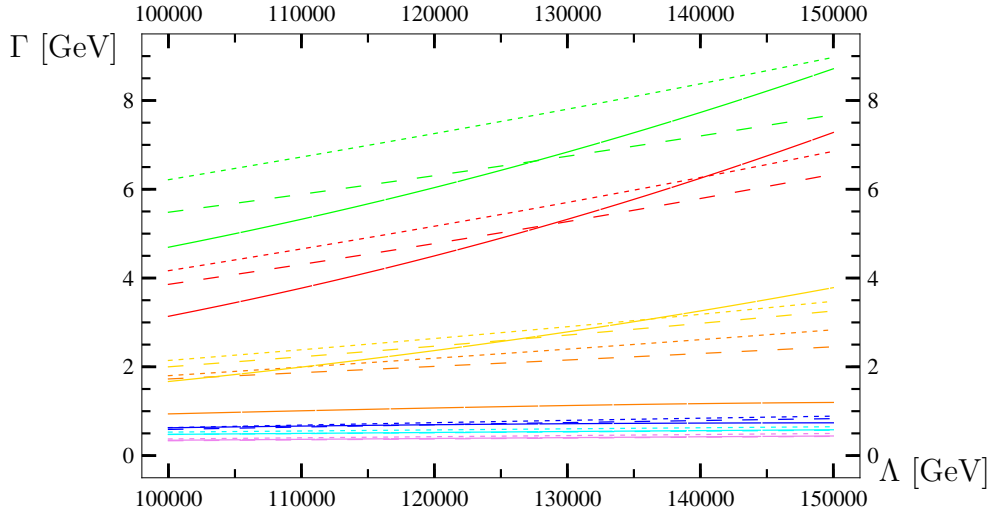

Figure 4.10: $\tilde{b}_1$ decays; MSSM model. red: $t\,\tilde{\chi}_1^-$, green: $t\,\tilde{\chi}_2^-$, blue: $b\,\tilde{\chi}_1^0$, gold: $b\,\tilde{\chi}_2^0$, violet: $b\,\tilde{\chi}_3^0$, cyan: $b\,\tilde{\chi}_4^0$, orange: $\tilde{t}_1\,W^-$.

4.3   stop 2

CMSSM: For $m_0 \lesssim 100$ GeV the decay into the Z boson and stop 1 dominates. The electroweak corrections in this decay channel are two times bigger and of the opposite sign as the SUSY-QCD corrections. Another bosonic decay which cannot be neglected is the decay into the neutral Higgs boson h_0 and stop 1. The electroweak correction in this process are at 25% level.

GMSB: Stop 2 decays dominantly into charginos and neutralinos.

AMSB: The branching ratios for the bosonic decays are below 10%. The electroweak corrections are rather small.

MSSM: The EW corrections in the bosonic decay $\tilde{t}_2 \to \tilde{t}_1 Z$ are small.

4.4   stop 1

CMSSM: Stop 1 decays into charginos and neutralinos. The electroweak corrections are small.

GMSB: Also here stop 1 decays into charginos and neutralinos. The electroweak corrections may reach around 7%.

AMSB: Stop 1 decays only into charginos and neutralinos. The EW corrections are about 7%.

MSSM: Stop1 decays only into charginos and neutralinos. The EW corrections are small.
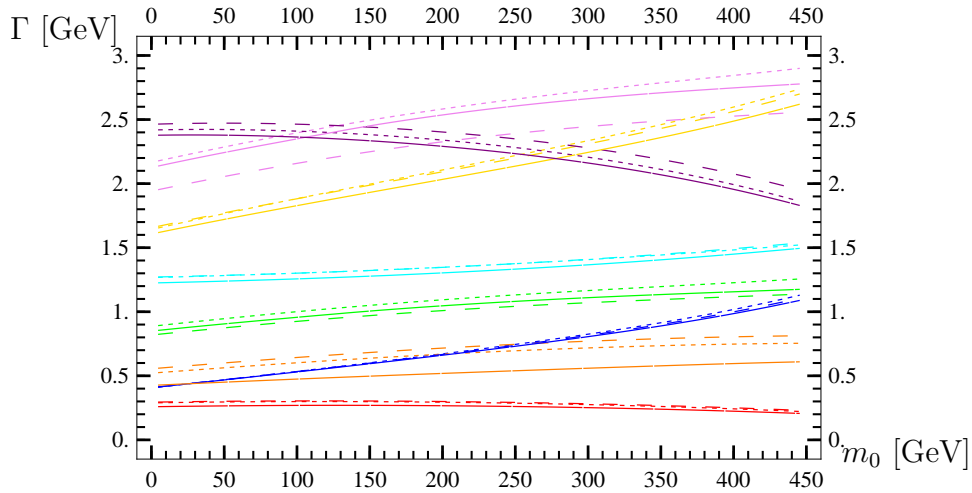
Figure 4.11: $\tilde{t}_2$ decays; CMSSM model. red: $t \tilde{\chi}_1^0$, green: $t \tilde{\chi}_2^0$, blue: $t \tilde{\chi}_3^0$, gold: $t \tilde{\chi}_4^0$, violet: $b \tilde{\chi}_1^+$, cyan: $b \tilde{\chi}_2^+$, orange: $h_0 \tilde{t}_1$, purple: $\tilde{t}_1 Z$.
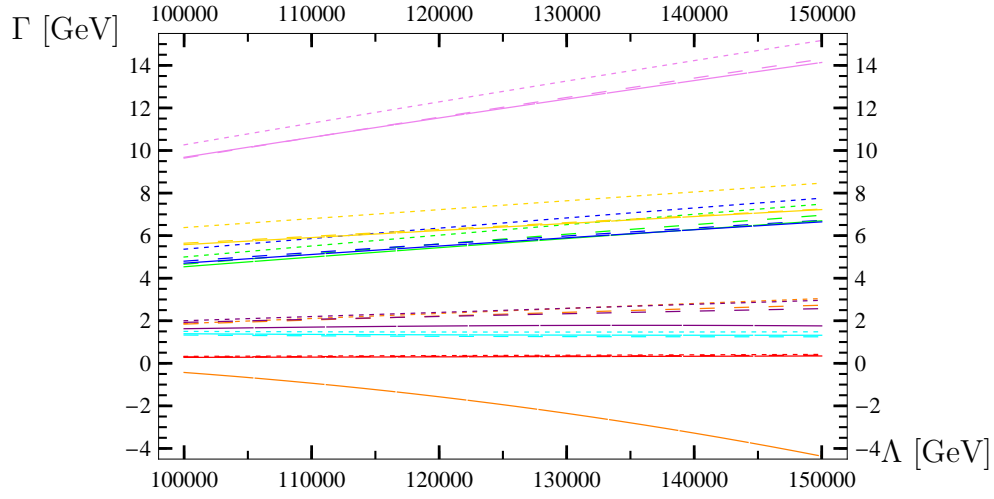
Figure 4.12: $\tilde{t}_2$ decays; GMSB model. red: $t\,\tilde{\chi}_1^0$, green: $t\,\tilde{\chi}_2^0$, blue: $t\,\tilde{\chi}_3^0$, gold: $t\,\tilde{\chi}_4^0$, violet: $b\,\tilde{\chi}_1^+$, cyan: $b\,\tilde{\chi}_2^+$, orange: $h_0\,\tilde{t}_1$, purple: $\tilde{t}_1\,Z$.
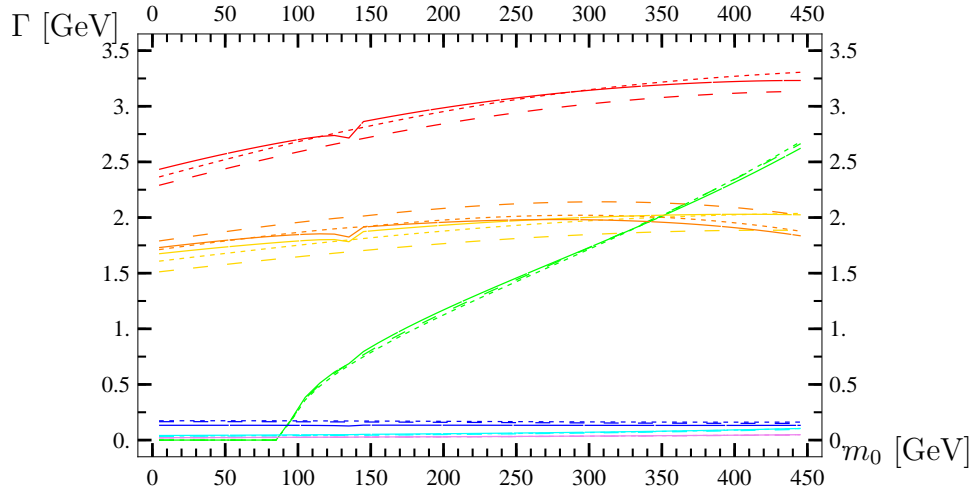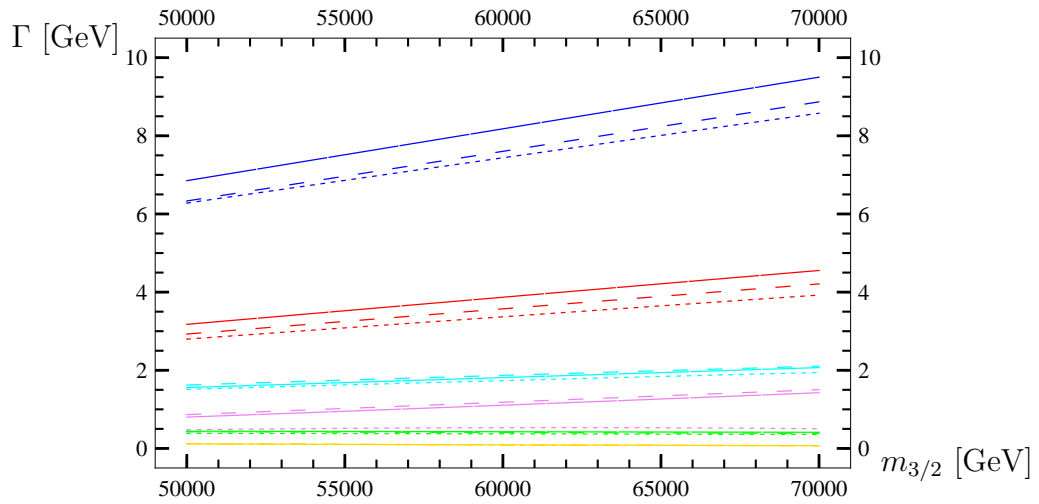

Figure 4.13: $\tilde{t}_2$ decays; AMSB model. red: $t\,\tilde{\chi}_1^0$, green: $t\,\tilde{\chi}_2^0$, blue: $t\,\tilde{\chi}_3^0$, gold: $t\,\tilde{\chi}_4^0$, violet: $h_0\,\tilde{t}_1$, cyan: $\tilde{t}_1\,Z$.
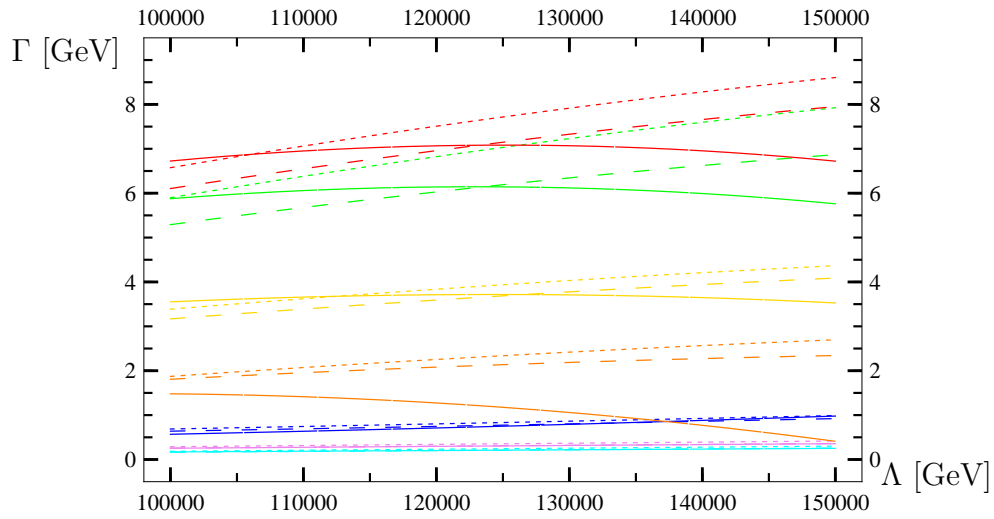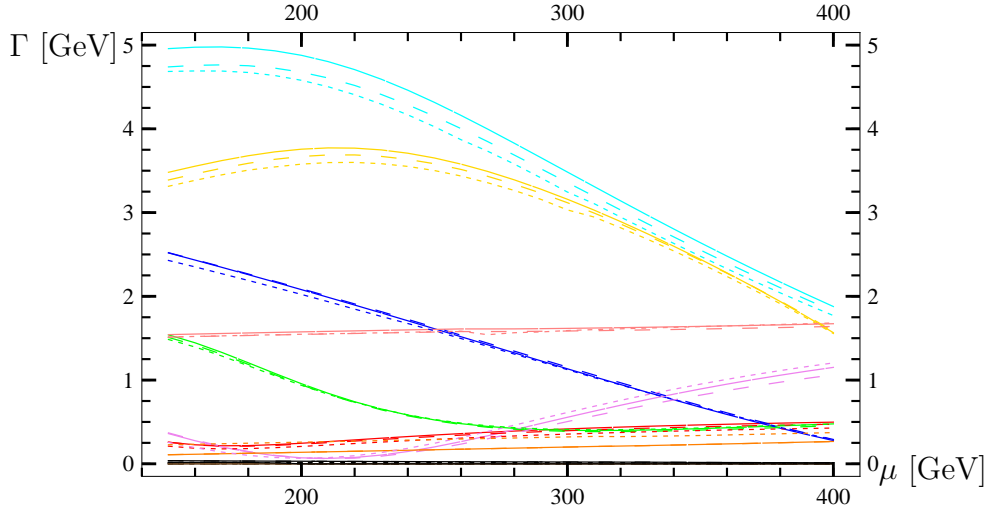
Figure 4.14: $\tilde{t}_2$ decays; MSSM model. red: $t\,\tilde{\chi}_1^0$, green: $t\,\tilde{\chi}_2^0$, blue: $t\,\tilde{\chi}_3^0$, gold: $t\,\tilde{\chi}_4^0$, violet: $b\,\tilde{\chi}_1^+$, cyan: $b\,\tilde{\chi}_2^+$, pink: $\tilde{t}_1\,Z$, orange: $\tilde{b}_1\,W^+$.
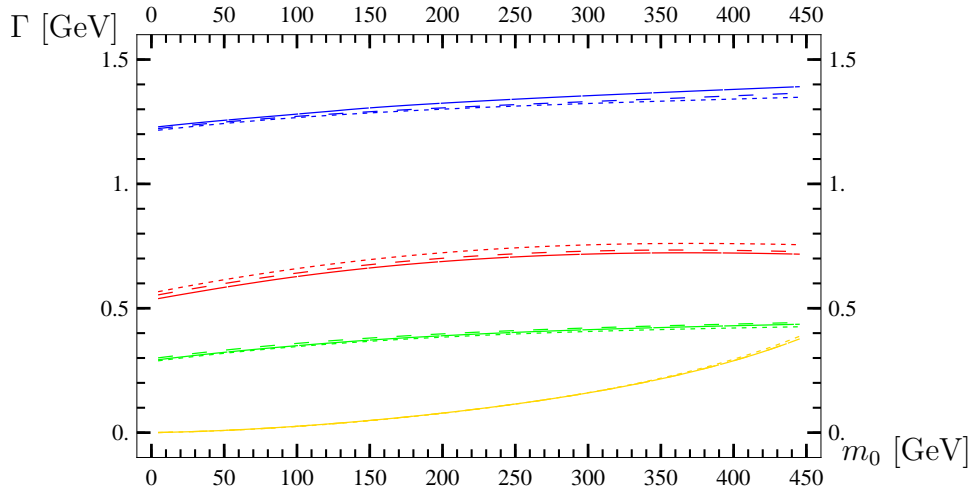
Figure 4.15: $\tilde{t}_1$ decays; CMSSM model. red: $t\,\tilde{\chi}_1^0$, green: $t\,\tilde{\chi}_2^0$, blue: $b\,\tilde{\chi}_1^+$, gold: $b\,\tilde{\chi}_2^+$.
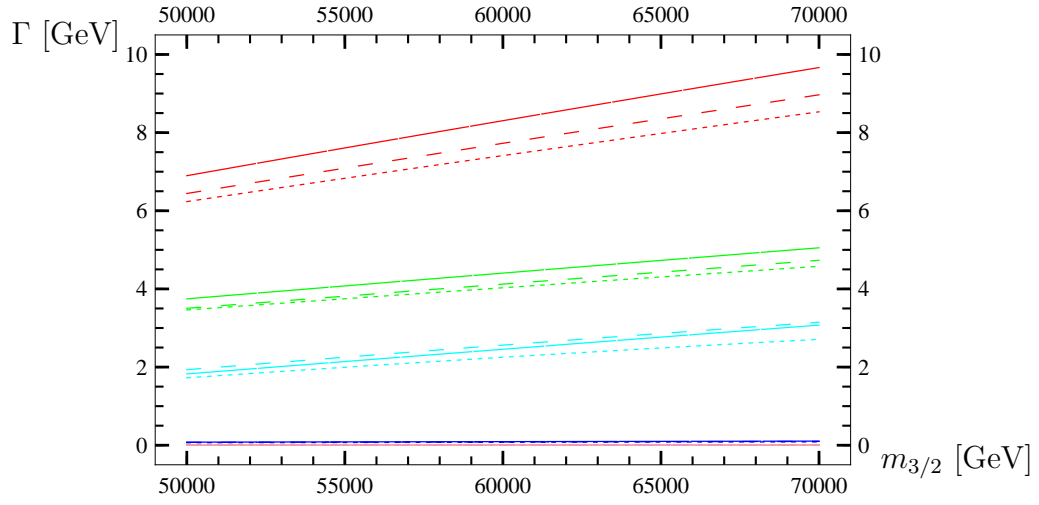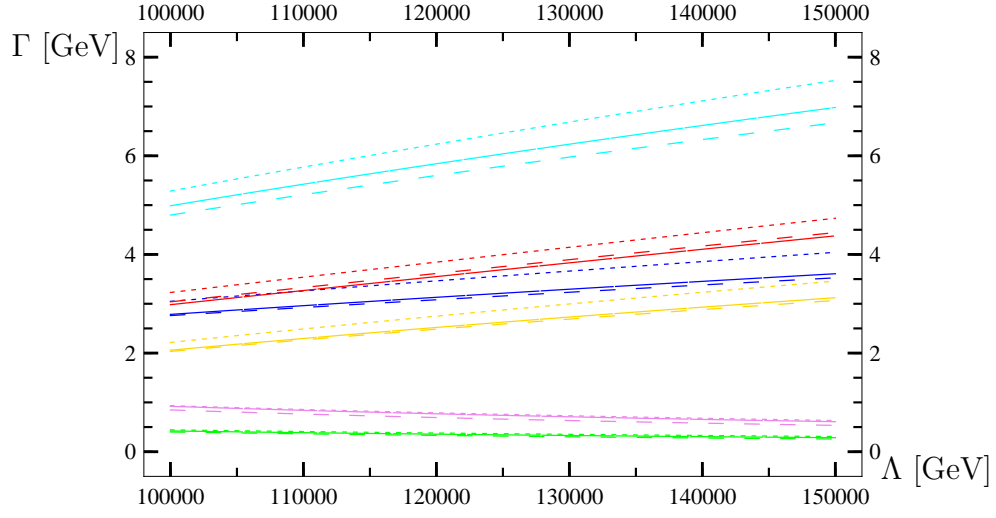
Figure 4.16: $\tilde{t}_1$ decays; GMSB model. red: $t\,\tilde{\chi}_1^0$, green: $t\,\tilde{\chi}_2^0$, blue: $t\,\tilde{\chi}_3^0$, gold: $t\,\tilde{\chi}_4^0$, violet: $b\,\tilde{\chi}_1^+$, cyan: $b\,\tilde{\chi}_2^+$.
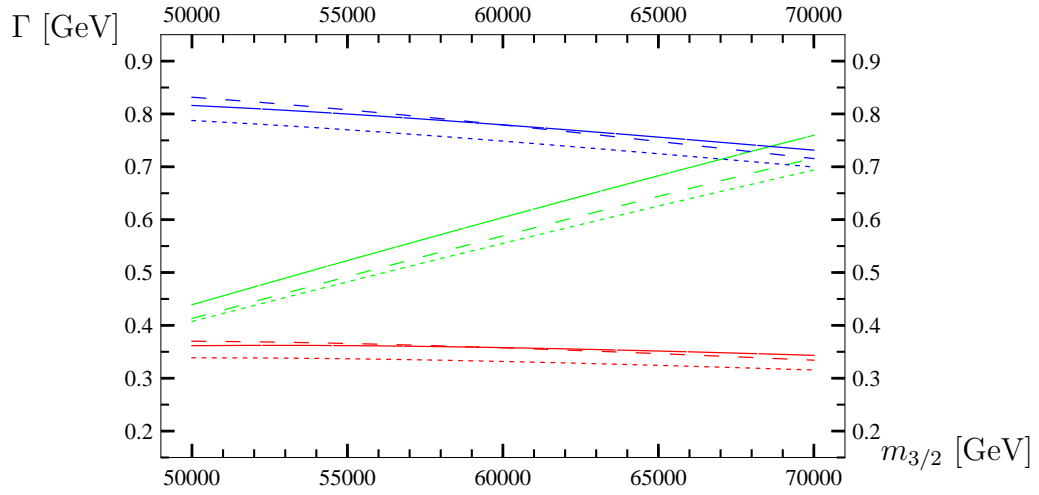
Figure 4.17: $\tilde{t}_1$ decays; AMSB model. red: $t\,\tilde{\chi}_1^0$, green: $t\,\tilde{\chi}_2^0$, blue: $b\,\tilde{\chi}_1^+$.
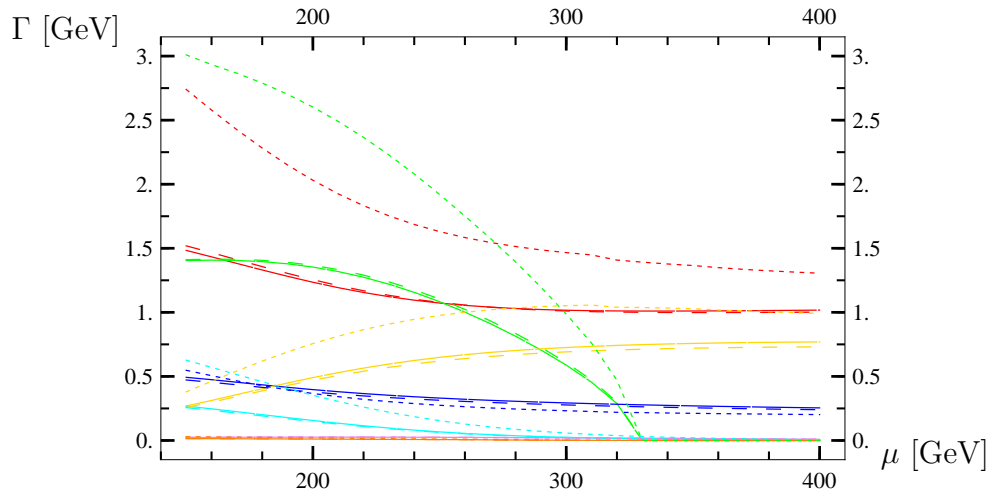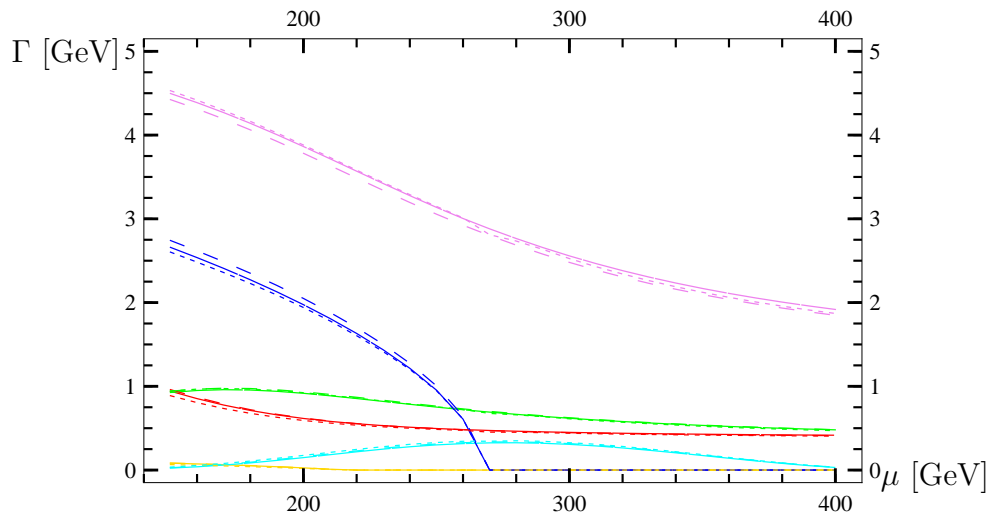
Figure 4.18: $\tilde{t}_1$ decays; MSSM model. red: $t\,\tilde{\chi}_1^0$, green: $t\,\tilde{\chi}_2^0$, blue: $t\,\tilde{\chi}_3^0$, gold: $t\,\tilde{\chi}_4^0$, violet: $b\,\tilde{\chi}_1^+$, cyan: $b\,\tilde{\chi}_2^+$.

4.5   stau 2

It is interesting to look at the plot in the GMSB model where the two bosonic decays $\tilde{\tau}_2 \to h_0\tilde{\tau}_1$, $\tilde{\tau}_2 \to Z\tilde{\tau}_1$ have second (third) largest branching ratio. The electroweak corrections are small. This applies to also other models.

4.6   stau 1

Stau 1 decays into charginos and neutralinos. We note that the EW corections in the AMSB model reach 16%.
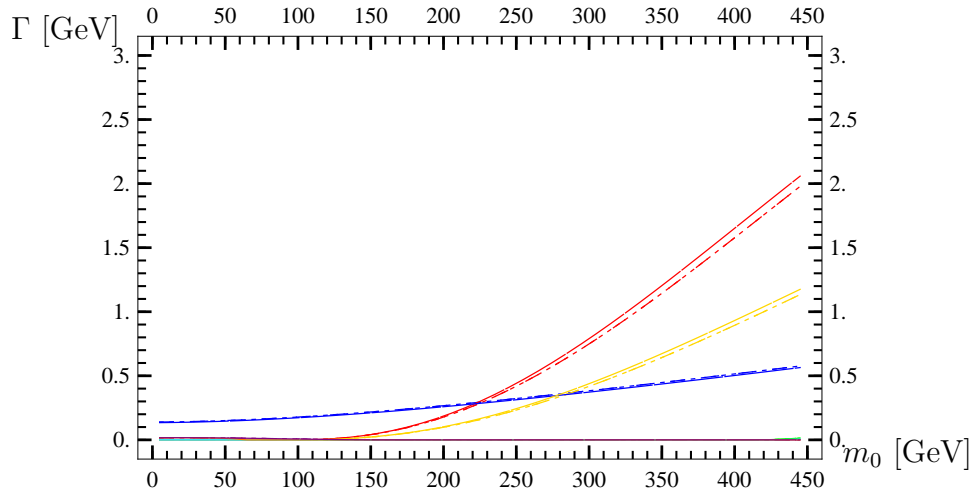
Figure 4.19: $\tilde{\tau}_2$ decays; CMSSM model. red: $\nu_\tau \chi_1^-$, green: $\nu_\tau \chi_2^-$, blue: $\tau\chi_1^0$, gold: $\tau\chi_2^0$.
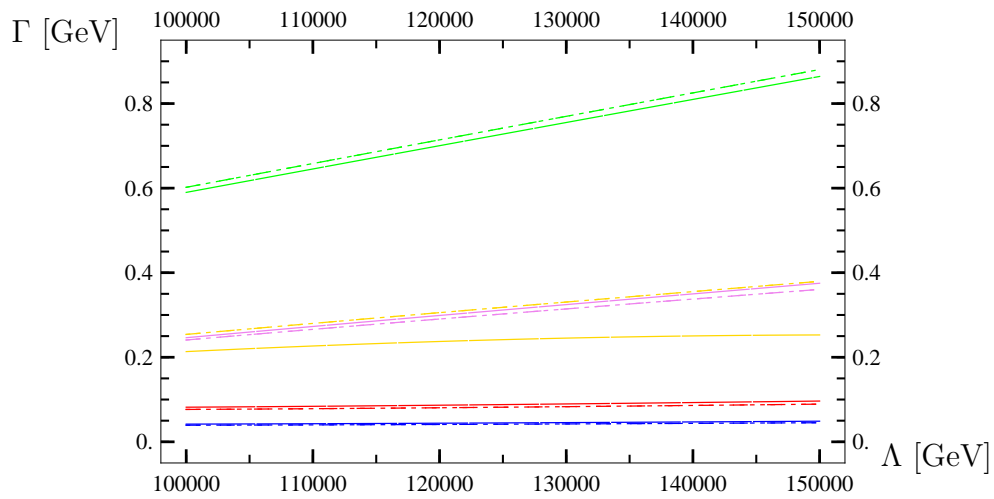
Figure 4.20: $\tilde{\tau}_2$ decays; GMSB model. red: $\nu_\tau \tilde{\chi}_1^-$, green: $\tau \tilde{\chi}_1^0$, blue: $\tau \tilde{\chi}_2^0$, gold: $h_0 \tilde{\tau}_1$, violet: $\tilde{\tau}_1 Z$.
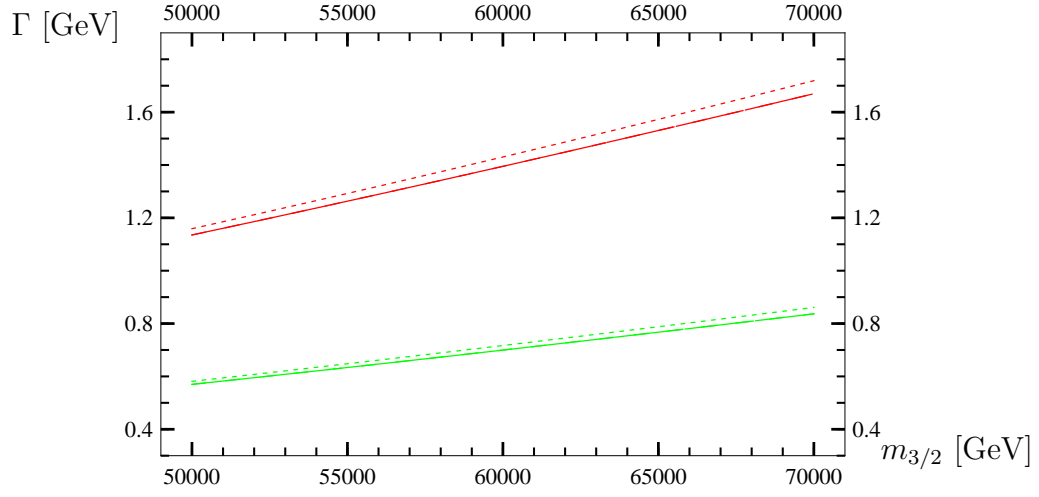
Figure 4.21: $\tilde{\tau}_2$ decays; AMSB model. red: $\nu_\tau\,\chi_1^-$, green: $\tau\chi_1^0$.
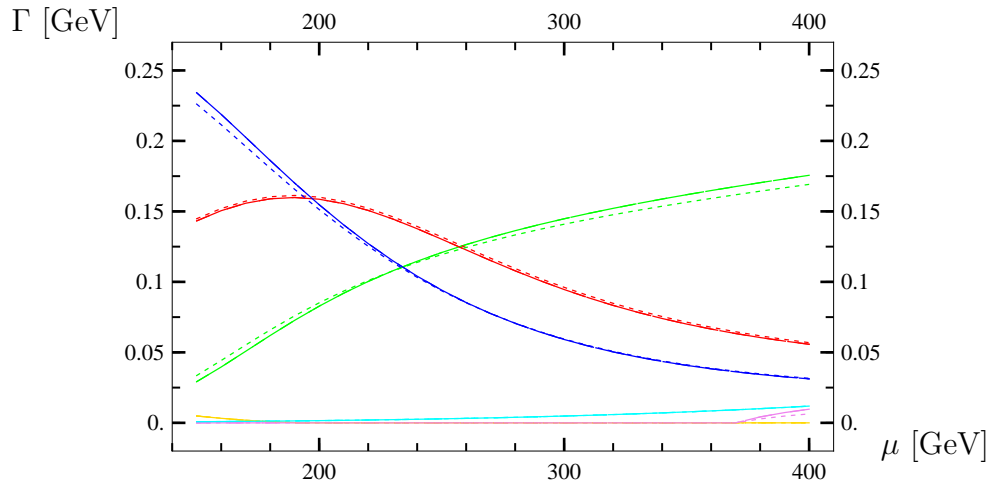
Figure 4.22: $\tilde{\tau}_2$ decays; MSSM model. red: $\nu_\tau\,\chi_1^-$, green: $\tau\chi_1^0$, blue: $\tau\chi_2^0$, gold: $\tau\chi_3^0$, violet: $h_0\,\tilde{\tau}_1$, cyan: $\tilde{\tau}_1\,Z$.
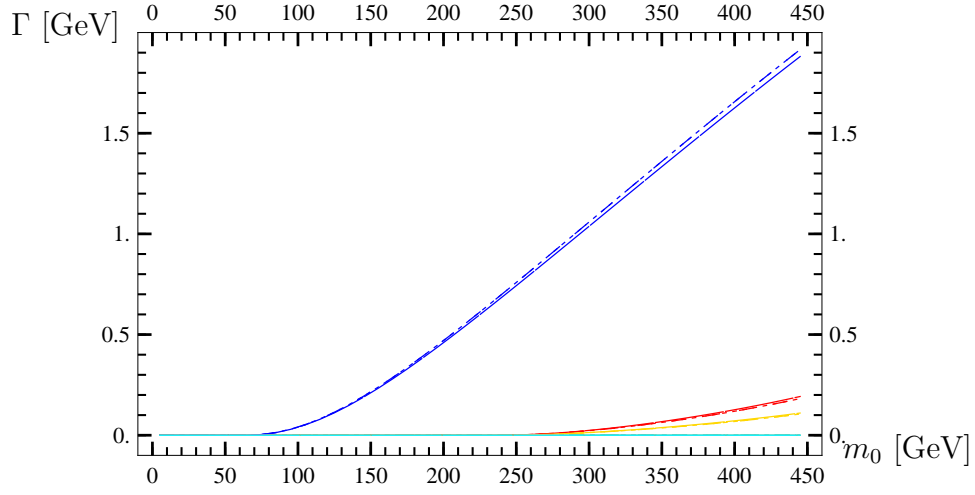
Figure 4.23: $\tilde{\tau}_1$ decays; CMSSM model. red: $\nu_\tau \chi_1^-$, green: $\nu_\tau \chi_2^-$, blue: $\tau\chi_1^0$, gold: $\tau\chi_2^0$. violet: $\tau\chi_3^0$, cyan: $\tau\chi_4^0$.
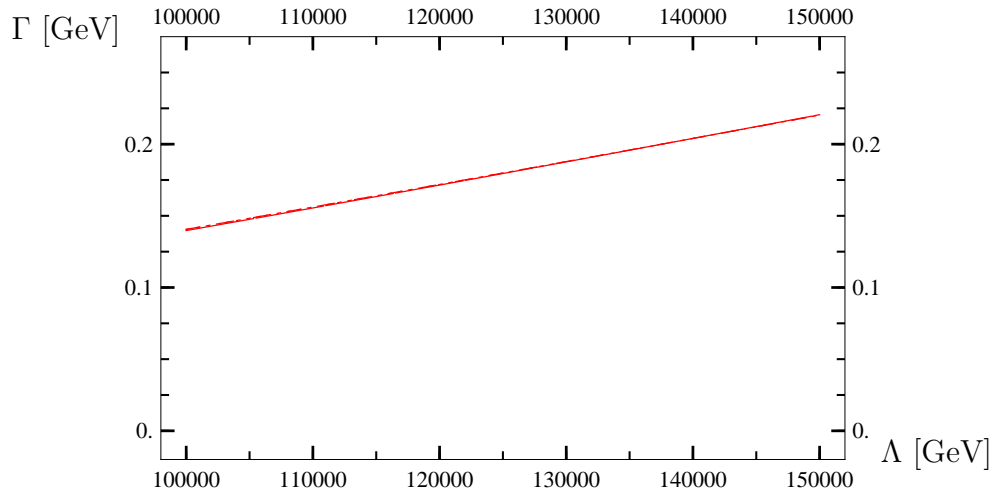
Figure 4.24: $\tilde{\tau}_1$ decays; GMSB model. red: $\tau\,\tilde{\chi}_1^0$.

57
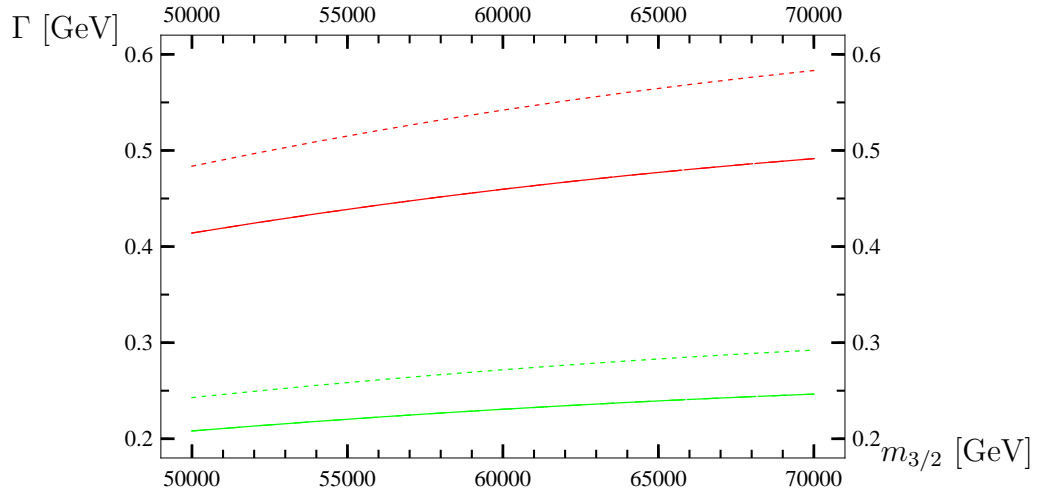
Figure 4.25: $\tilde{\tau}_1$ decays; AMSB model. red: $\nu_\tau \chi_1^-$, green: $\tau\chi_1^0$.
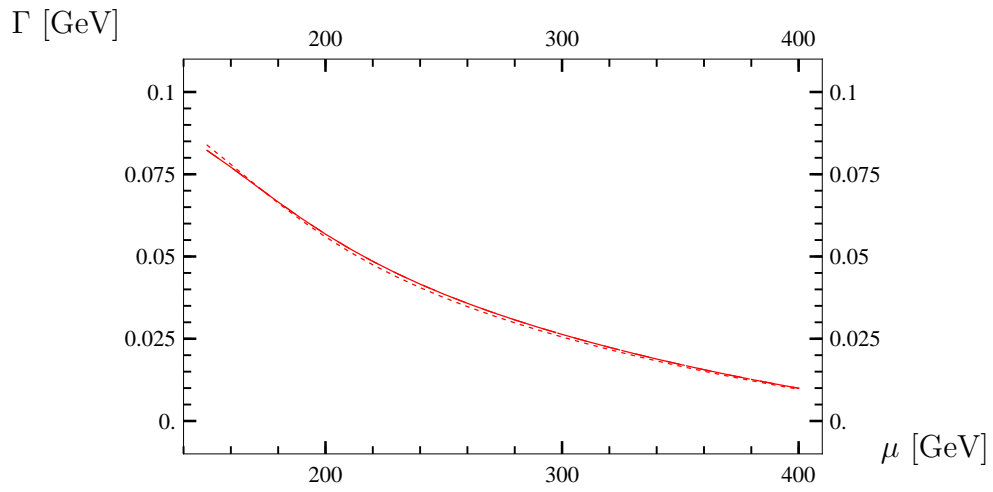
Figure 4.26: $\tilde{\tau}_1$ decays; MSSM model. red: $\tau\chi_1^0$.

58

4.7   BRs for sbottom 2 in the GMSB model

At the end of this chapter we give an example on the electroweak corrections to the branching ratios for the decay of the sbottom 2 particle. The program output for the GMSB model where the parameter $\Lambda = 10^5$ GeV is given below. We see that whereas the EW corrections for the partial widths for the four dominant channels are from 14% to 45% (decay into W boson) the EW corrections to the branching ratios are from 1% to 33%.

```
tree
    ~b_2 -> t chi_1-         :   0.416531E+001 / BR : 0.2627
    ~b_2 -> t chi_2-         :   0.621542E+001 / BR : 0.3920
    ~b_2 -> b chi_10         :   0.629803E+000 / BR : 0.0397
    ~b_2 -> b chi_20         :   0.214240E+001 / BR : 0.1351
    ~b_2 -> b chi_30         :   0.374585E+000 / BR : 0.0236
    ~b_2 -> b chi_40         :   0.528818E+000 / BR : 0.0336
    ~b_2 -> ~t_1 W-          :   0.179996E+001 / BR : 0.1135
    ----------------------------------------------------------
                 Total width = 0.158563E+002
sqcd
    ~b_2 -> t chi_1-         :   0.385721E+001 / BR : 0.2667
    ~b_2 -> t chi_2-         :   0.548204E+001 / BR : 0.3790
    ~b_2 -> b chi_10         :   0.589113E+000 / BR : 0.0407
    ~b_2 -> b chi_20         :   0.199935E+001 / BR : 0.1382
    ~b_2 -> b chi_30         :   0.333661E+000 / BR : 0.0231
    ~b_2 -> b chi_40         :   0.475512E+000 / BR : 0.0329
    ~b_2 -> ~t_1 W-          :   0.172601E+001 / BR : 0.1193
    ----------------------------------------------------------
                 Total width = 0.144629E+002
full
    ~b_2 -> t chi_1-         :   0.313758E+001 / BR : 0.2639
    ~b_2 -> t chi_2-         :   0.469375E+001 / BR : 0.3949
    ~b_2 -> b chi_10         :   0.625958E+000 / BR : 0.0527
    ~b_2 -> b chi_20         :   0.166853E+001 / BR : 0.1404
    ~b_2 -> b chi_30         :   0.345159E+000 / BR : 0.0290
    ~b_2 -> b chi_40         :   0.477370E+000 / BR : 0.0402
    ~b_2 -> ~t_1 W-          :   0.938806E+000 / BR : 0.0790
    ----------------------------------------------------------
                 Total width = 0.118871E+002
```

Appendix A

The LSZ formula and the $\overline{\text{DR}}$ scheme

We start our analysis by writing down the LSZ reduction formula for bosonic non-mixing particles which gives the relation between the Fourier transform of the n-point Green function and the S matrix element. First, it was formulated and proved (for stable particles) in 1955 by Lehmann, Symanzik and Zimmermann [70] and can be found in any of the today standard textbooks [33, 41, 71]. The formula reads

$$
\int d^4 x e^{ip_j x} \ldots \int d^4 y e^{-ip_i y} \left\langle \Omega | T\{\phi_j(x) \ldots \phi_i(y)^\dagger\} | \Omega \right\rangle
$$
$$
\sim \quad \frac{i \left\langle \Omega | \phi_j(0) | p_j \right\rangle}{p_j^2 - M_j^2 + i\varepsilon} \ldots \frac{i \left\langle p_i | \phi_i^\dagger(0) | \Omega \right\rangle}{p_i^2 - M_i^2 + i\varepsilon} \ \left\langle p_j \ldots | S | \ldots p_i \right\rangle \tag{A.1}
$$

where Ω is the vacuum in the interaction theory, T is the time-ordering product, ϕ_i, ϕ_j are the fields in the Heisenberg picture, M_i, M_j are on-shell masses and p_i and p_j are momenta of the incoming and outgoing particles. The symbol $\sim$ means that the poles of both sides of the equation are identical.
In the following we denote the factors

$$
\left\langle \Omega | \phi_i(0) | p_i \right\rangle = R_i^{\frac{1}{2}}, \qquad \left\langle p_i | \phi_i^\dagger(0) | \Omega \right\rangle = \bar{R}_i^{\frac{1}{2}}, \qquad \text{where } R^{\frac{1}{2}} = \bar{R}^{\frac{1}{2}\dagger} \tag{A.2}
$$

They are called *wave-function renormalization constants (WFR) (or LSZ factors, field strength renormalization factors)*. In the case of unstable particles, the hermitian conjugation relationship is broken by the imaginary part of the particle's self-energy [72]. The WFR factors can be determined from the propagation of a particle in the interaction vacuum

$$
G(p, -p) = \int d^4 x \ e^{ip(x-y)} \left\langle \Omega | T\phi(x)\phi^\dagger(y) | \Omega \right\rangle \sim \frac{iR^{\frac{1}{2}} \bar{R}^{\frac{1}{2}}}{p^2 - M^2 + i\varepsilon} \tag{A.3}
$$

Let us now recall how one computes the n-point Green function

$$G(x_1, \ldots, x_n) = \langle \Omega | T[\phi(x_1) \ldots \phi(x_n)] | \Omega \rangle$$

$$= \lim_{T \to \infty(1-i\varepsilon)} \frac{\langle 0| T \left\{ \phi_I(x_1) \ldots \phi_I(x_n) \exp\left[-i \int_{-T}^{T} dt \; H_I(t)\right] \right\} |0\rangle}{\langle 0| T \left\{ \exp\left[-i \int_{-T}^{T} dt \; H_I(t)\right] \right\} |0\rangle}$$

$$= \begin{pmatrix} \text{sum of all connected diagrams} \\ \text{with n external points} \end{pmatrix} \tag{A.4}$$

The propagation amplitude for a bosonic particle can be written as a geometric series which can be resummed to

$$
\begin{aligned}
G(p, -p) &= \frac{i}{p^2 - m^2} + \frac{i}{p^2 - m^2} \, i\Pi(p^2) \frac{i}{p^2 - m^2} \\
&+ \frac{i}{p^2 - m^2} \, i\Pi(p^2) \frac{i}{p^2 - m^2} \, i\Pi(p^2) \frac{i}{p^2 - m^2} + \ldots \\
&= \frac{i}{p^2 - m^2 + \Pi(p^2)}
\end{aligned}
\tag{A.5}
$$

where the self-energy $i\Pi(p^2)$ is defined to be

$$i\Pi(p^2) = \;\text{(1PI)}$$

If we could calculate the self-energy to infinity-loop level (obtaining thus the full propagator), we would recover the structure (A.3) with the residuum $R^{\frac{1}{2}} \bar{R}^{\frac{1}{2}}$ being UV finite. (Actually, the value would be somewhere between 0 and 1). This also must hold for the n-point Green function $G(p_1, \ldots, p_n)$ since it can be related to the S-matrix element according to (A.1). However, in the real world, we are not able to deal with infinitely many loops. We can only calculate the Green functions up to a definite loop order which leads to UV divergent results. To obtain finite results at a definite loop order we must reparametrize the theory - express the original (bare) parameters in the original lagrangian in terms of new (renormalized) parameters and thus render the results finite order by order.

On-shell renormalization scheme

Let us consider the following lagrangian (only the kinetic and the quadratic part) for bosons which do not mix

$$\mathcal{L}_0 = \partial_\mu \phi^{0*} \partial^\mu \phi^0 - (m^0)^2 \phi^{0*} \phi^0 \tag{A.6}$$

We reparametrize the masses and the fields as follows

$$\phi^0 = Z^{\frac{1}{2}}\phi^R = (1 + \frac{1}{2}\delta Z)\phi^R + \text{h.o.t} \tag{A.7}$$

$$(m^0)^2 = m^2 + \delta m^2 \tag{A.8}$$

After the reparametrization the lagrangian gets the form

$$\mathcal{L}_0 = \partial_\mu \phi^{R*}\partial^\mu \phi^R - m^2\phi^{R*}\phi^R + \frac{1}{2}(\delta Z + \delta Z^*)\partial_\mu \phi^{R*}\partial^\mu \phi^R$$
$$- \frac{1}{2}m^2(\delta Z + \delta Z^*)\phi_i^{R*}\phi_j^R - \delta m^2\phi^{R*}\phi^R + \text{h.o.t} \tag{A.9}$$

To fix the counterterms δm and δZ one can choose the following on-shell renormalization conditions, where the mass m is the pole of the renormalized propagator, and the residuum by $p^2 = m^2$ is 1

$$\hat{\Pi}(p^2)|_{p^2=m^2} = 0, \qquad \lim_{p^2 \to m^2} \frac{\hat{\Pi}(p^2)}{p^2 - m^2} = 0 \tag{A.10}$$

In the above equations the renormalized self-energy reads

$$\hat{\Pi}(p^2) = \Pi(p^2) + \frac{1}{2}(p^2 - m^2)(\delta Z + \delta Z^*) - \delta m^2 \tag{A.11}$$

Solving the on-shell renormalization conditions we get

$$\delta m^2 = \Pi(m^2) \tag{A.12}$$

$$\frac{1}{2}(\delta Z + \delta Z^*) = -\dot{\Pi}(m^2) \tag{A.13}$$

The equation (A.13) cannot be fullfilled for unstable particles, as the self-energy also develops an imaginary part in the general case. The way around is to use $\widetilde{\text{Re}}\ \Pi(p^2)$ instead of $\Pi(p^2)$ in the renormalization conditions (A.10) or to work in the complex mass scheme (CMS) [73]. Let us now check that the renormalized propagator is of the desired form (the pole is the physical mass and the residuum equals one). Recall that before the renormalization

$$G_0(p, -p) = \frac{i}{p^2 - m_0^2 + \Pi(p^2)} \tag{A.14}$$

After the renormalization

$$G_R(p, -p) = \int d^4x\ e^{ip(x-y)}\langle\Omega|T\phi_R(x)\phi_R^\dagger(y)|\Omega\rangle$$
$$= \frac{1}{(Z\bar{Z})^{\frac{1}{2}}}\int d^4x\ e^{ip(x-y)}\langle\Omega|T\phi_0(x)\phi_0^\dagger(y)|\Omega\rangle \tag{A.15}$$
$$= \frac{1}{(Z\bar{Z})^{\frac{1}{2}}}G_0(p, -p) = \frac{1}{(Z\bar{Z})^{\frac{1}{2}}}\frac{i}{p^2 - m^2 - \delta m^2 + \Pi(p^2)}$$

62

Substituting for the mass counterterm δm and for the $Z\bar{Z}$ we get

$$
\begin{aligned}
G_R(p, -p) &= \frac{1}{(Z\bar{Z})^{\frac{1}{2}}} \frac{i}{p^2 - m^2 - \Pi(m^2) + \Pi(p^2)} \\
&= \frac{1}{(Z\bar{Z})^{\frac{1}{2}}} \frac{i}{(p^2 - m^2)\left[1 + \dot{\Pi}(m^2) + \mathcal{O}(p^2 - m^2)\right]} \\
&\sim \frac{i}{p^2 - m^2}
\end{aligned}
\tag{A.16}
$$

Thus we have seen that the renormalized propagator has the structure

$$
G_R(p, -p) \sim \frac{R_0}{(Z\bar{Z})^{\frac{1}{2}}} \frac{i}{p^2 - m^2} = R_R \frac{i}{p^2 - m^2}
\tag{A.17}
$$
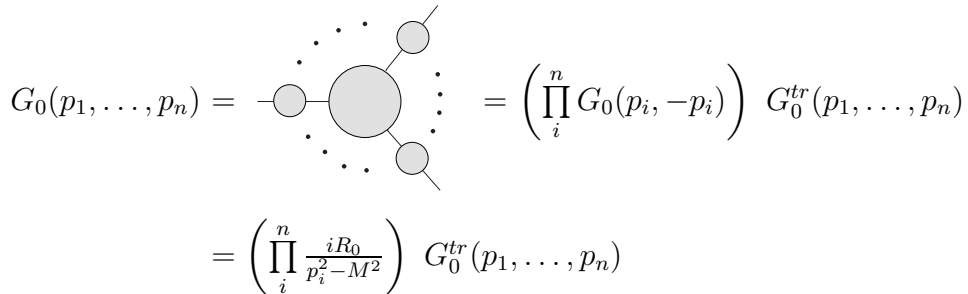
with R_0 being the residuum before the field renormalization $R_0 = (1 + \dot{\Pi}(m^2))^{-1}$, Z being the field renormalization constant and R_R we name to be the renormalized residuum (after the field renormalization). In the on-shell scheme $R_R = 1$.

LSZ formula for renormalized fields

Suppose now that we want to calculate a process in which p particles interact and $n - p$ particles come out as a result. The LSZ formula (A.1) tells us how to calculate the S-matrix element. One first calculates the Fourier transform of the n-point Green function $G_0(p_1, \ldots, p_n)$ using the equation (A.4) and not forgetting also the radiative corrections on external lines. The S-matrix element is then given by the n-point Green function through the following relation

$$
G_0(p_1, \ldots, p_n) \sim \prod_i^n \left(\frac{i R_0^{\frac{1}{2}}}{p_i^2 - M^2} \right) S(p_1, \ldots, p_n)
\tag{A.18}
$$

Or one can calculate the truncated n-point Green function G_0^{tr}

$$
G_0(p_1, \ldots, p_n) = \quad \text{} \quad = \left(\prod_i^n G_0(p_i, -p_i) \right) G_0^{tr}(p_1, \ldots, p_n)
$$

$$
= \left(\prod_i^n \frac{i R_0}{p_i^2 - M^2} \right) G_0^{tr}(p_1, \ldots, p_n)
$$

where we assumed the residuum to be real. The S-matrix element is then given by

$$
G_0^{tr}(p_1, \ldots, p_n) R_0^{\frac{n}{2}} \sim S(p_1, \ldots, p_n)
\tag{A.19}
$$

The S-matrix element is generally not finite at one loop level. To obtain UV-finite results we have to renormalize our couplings and masses. Afterwards, the Green function is still not finite, however, the S-matrix element already is. If we want also the n-point Green function to be finite, we have to perform the renormalization of the fields as well. Let us have a look how this will effect the relation between the renormalized n-point Green function and the S-matrix element.

After rescaling the fields (equation (A.7), the renormalized Green functions are

$$
\begin{aligned}
G_R(p, -p) &= Z^{-1} G_0(p, -p) \\
G_R(p_1, \ldots, p_n) &= Z^{-\frac{n}{2}} G_0(p_1, \ldots, p_n) \\
G_R^{tr}(p_1, \ldots, p_n) &= Z^{\frac{n}{2}} G_0^{tr}(p_1, \ldots, p_n)
\end{aligned}
\tag{A.20}
$$

where we assumed the field renormalization constant Z to be real. Substituting for the G_0^{tr} in the equation (A.19) we finally obtain

$$
\begin{aligned}
S(p_1, \ldots, p_n) &\sim G_R^{tr}(p_1, \ldots, p_n) \, (R_R)^{\frac{n}{2}} \\
&= G_0^{tr}(p_1, \ldots, p_n) \, (R_R)^{\frac{n}{2}} \, Z^{\frac{n}{2}}
\end{aligned}
\tag{A.21}
$$

with $R_R = \frac{R_0}{Z}$. In the on-shell scheme, R_R equals one. It is because the propagation amplitude of a renormalized field resembles that of a free field. In- and -out states of the S-matrix element are asymptotic states in the far future or far past, in which interaction is switched off (switching on and off must be done adiabatically). So, it follows that in the on-shell scheme the renormalized field has already properties of in- and -out state and therefore the S-matrix element is given only by the renormalized truncated Green function. But generally, the time limit of a renormalized field (after arbitrary field renormalization - arbitrary factor Z) does not lead to a field which propagates as a free field, and therefore, there must be some factor in the LSZ reduction formula which takes into account this fact.

Let us now recapitulate how to calculate a process at one loop level. First, we renormalize the parameters in the lagrangian (masses, couplings, fields). We then calculate the renormalized truncated n-point Green function G_R^{tr} according to

$$
\begin{aligned}
G_R^{tr}(x_1, \ldots, x_n) &= \langle \Omega | T[\phi_R(x_1) \ldots \phi_R(x_n)] | \Omega \rangle \\
&= \lim_{T \to \infty(1-i\varepsilon)} \frac{\langle 0 | T \left\{ \phi_{RI}(x_1) \ldots \phi_{RI}(x_n) \exp\left[-i \int_{-T}^{T} dt \, H_I(t) \right] \right\} | 0 \rangle}{\langle 0 | T \left\{ \exp\left[-i \int_{-T}^{T} dt \, H_I(t) \right] \right\} | 0 \rangle} \\
&= \begin{pmatrix} \text{sum of all connected diagrams} \\ \text{with n external points} \\ \text{with extended Feynman rules} \end{pmatrix}
\end{aligned}
\tag{A.22}
$$

64

with no corrections on the external lines. Feynman rules are extended to include those for counter-term vertices (with $\delta m, \delta Z, \delta g$). The renormalized residuum R_R is obtained from the renormalized propagator $G_R(p, -p)$. The S-matrix element is given by equation (A.21).

$\overline{\text{DR}}$ renormalization scheme

The $\overline{\text{DR}}$ renormalization conditions read (compare with (A.10))

$$\hat{\Pi}^\Delta(p^2)|_{p^2=m^2} = 0, \qquad \lim_{p^2 \to m^2} \frac{\hat{\Pi}^\Delta(p^2)}{p^2 - m^2} = 0 \qquad (A.23)$$

where Δ denotes the UV-divergent part. Thus the counterterms $\delta m, \delta Z$ are given by

$$\delta m^2 = \Pi^\Delta(m^2) \qquad (A.24)$$
$$\delta Z = -\dot{\Pi}^\Delta(m^2) \qquad (A.25)$$

From the LSZ reduction formula (A.21) it directly follows that the product $R_R Z$, the unrenormalized LSZ factor, is independent of the renormalization scheme. Taking advantage of this result one finds that

$$R_R = 1 - \dot{\Pi}^{\text{fin}}(m^2) \qquad (A.26)$$

in the $\overline{\text{DR}}$ scheme at one loop level.

Appendix B

Mathematica files

B.1   CTs.m

We worked with FA version 5.3 and FC version 3.3.

```
DivHeader = UVDivergentPart  (* DRbar scheme *)

(* see arXiv:hep-ph/0212259 p.18 *)
rulePaVeRxi = Derivative[0, 1, 0, 0][B0i][bb001, p2_, m12_, m22_] ->
  1/8*(2*m12*DB1[p2, m12, m22] + (p2 - m22 + m12)*DB11[p2, m12, m22]
  + B11[p2, m12, m22] + 1/6)


RenConst[ dAlfa21 ] := 2*Alfa*dAlfa1
RenConst[ dAlfa1  ] := EL/(2*\[Pi])*dEL1
RenConst[ dEL1  ] := DivHeader[EL*RenConst[dZe1]];
RenConst[ dZe1  ] := -1/2 (RenConst[dZAA1]
                    - $HKSign SW/CW RenConst[dZZA1])
RenConst[ dZAA1 ] := FieldRC[V[1]]
RenConst[ dZZA1 ] := FieldRC[V[2], V[1]]


RenConst[ dZZZ1 ] := FieldRC[V[2]]/. rulePaVeRxi
RenConst[ dZWW1 ] := FieldRC[V[3]]/. rulePaVeRxi


RenConst[ dMZ21 ] := DivHeader[MassRC[V[2]]]
RenConst[ dMW21 ] := DivHeader[MassRC[V[3]]]


RenConst[ dMW1 ] := dMW21/(2*MW)
RenConst[ dMZ1 ] := dMZ21/(2*MZ)
```

```
RenConst[ dSW1  ] := $HKSign CW^2/SW/2 (dMZ21/MZ^2 - dMW21/MW^2)
RenConst[ dCW1  ] := - (SW/CW)*dSW1
RenConst[ dSW21 ] := 2*dSW1*SW

(* Fermion sector ************************************************)

RenConst[ dME1  ] := dMf1[2,1]
RenConst[ dMU1  ] := dMf1[3,1]
RenConst[ dMD1  ] := dMf1[4,1]

RenConst[ dMM1  ] := dMf1[2,2]
RenConst[ dMC1  ] := dMf1[3,2]
RenConst[ dMS1  ] := dMf1[4,2]

RenConst[ dML1  ] := dMf1[2,3]
RenConst[ dMT1  ] := dMf1[3,3]
RenConst[ dMB1  ] := dMf1[4,3]

RenConst[ dME21 ] := 2*ME*dME1
RenConst[ dMU21 ] := 2*MU*dMU1
RenConst[ dMD21 ] := 2*MD*dMD1

RenConst[ dMM21 ] := 2*MM*dMM1
RenConst[ dMC21 ] := 2*MC*dMC1
RenConst[ dMS21 ] := 2*MS*dMS1

RenConst[ dML21 ] := 2*ML*dML1
RenConst[ dMT21 ] := 2*MT*dMT1
RenConst[ dMB21 ] := 2*MB*dMB1

RenConst[ dMf1[type_, j1_] ] := DivHeader[MassRC[F[type, {j1}]]]

RenConst[ dMLE1[gen_] ] := dMf1[2, gen];
RenConst[ dMQU1[gen_] ] := dMf1[3, gen];
RenConst[ dMQD1[gen_] ] := dMf1[4, gen];

RenConst[ dZfL1[type_, j1_, j1_] ] :=
                      FieldRC[F[type, {j1}], F[type,{j1}]][[1]]
RenConst[ dZfL1[type_, j1_, j2_] ] :=
                      FieldRC[F[type, {j1}], F[type, {j2}]][[1]]
RenConst[ dZfR1[type_, j1_, j1_] ] :=
```

```
                              FieldRC[F[type, {j1}], F[type, {j1}]][[2]]
RenConst[ dZfR1[type_, j1_, j2_] ] :=
                              FieldRC[F[type, {j1}], F[type, {j2}]][[2]]


(* Strong sector ************************************************)

RenConst[ dGS1 ] := Divergence*GS*Alfas/(8*\[Pi])*
                        (ctbV5*(2/3*6 - 11/3*3) + ctbF15*(1/3*6 + 2/3*3))

RenConst[ PiglSL ] := Block[{m = MGl}, ReTilde[LScalarCoeff[
                                   SelfEnergy[F[15] -> F[15], m]]]];
RenConst[ PiglSR ] := Block[{m = MGl}, ReTilde[RScalarCoeff[
                                   SelfEnergy[F[15] -> F[15], m]]]];
RenConst[ dZglL1 ] := Block[{m = MGl}, FieldRC[F[15]][[1]]
                                   + (1/(2*m))*(PiglSL - PiglSR)];
RenConst[ dZglR1 ] := Block[{m = MGl}, FieldRC[F[15]][[2]]
                                   + (1/(2*m))*(PiglSR - PiglSL)];


(* Sfermion sector ************************************************)

RenConst[ dMSf21[1, 1, j1_] ] := DivHeader[MassRC[S[11, {j1}]]];
RenConst[ dMSf21[2, 1, j1_] ] := 0;

RenConst[ dMSf21[c1_, ftype_, j1_] ] :=
                         DivHeader[MassRC[S[10 + ftype, {c1, j1}]]];

RenConst[ dZSf1[1, 1, 1, j1_] ] := FieldRC[S[11, {j1}]];
RenConst[ dZSf1[1, 2, 1, j1_] ] := 0;
RenConst[ dZSf1[2, 1, 1, j1_] ] := 0;
RenConst[ dZSf1[2, 2, 1, j1_] ] := 0;

RenConst[ dZSf1[c1_, c1_, ftype_, j1_] ] :=
                                 FieldRC[S[10 + ftype, {c1, j1}]];
RenConst[ dZSf1[c1_, c2_, ftype_, j1_] ] :=
          FieldRC[S[10 + ftype, {c1, j1}], S[10 + ftype, {c2, j1}]];

RenConst[ dZSfC1[j__] ] := Conjugate[dZSf1[j]];

RenConst[ dUSf1[c1_, c2_, ftype_, j1_]] :=
           DivHeader[1/4*Sum[(RenConst[dZSf1[c1, isf, ftype, j1]]
            - Conjugate[RenConst[dZSf1[isf, c1, ftype, j1]]])
```

68

```
                 *USf[isf, c2, ftype, j1] , {isf, 2}]];
RenConst[ dUSfC1[j__]] := Conjugate[dUSf1[j]];

(* RenConst[dMSfmat1[1, 1, 1, j1_]] := dMSf21[1, 1, j1]; *)
RenConst[ dMSfmat1[c1_, c2_, t_, j1_] ] :=
     Sum[dUSfC1[k,c1,t,j1]*(MSf[k,t,j1]^2)
     * IndexDelta[k,l]*USf[l,c2,t,j1]
     + Conjugate[USf[k,c1,t,j1]]*dMSf21[k,t,j1]
     * IndexDelta[k,l]*USf[l,c2,t,j1]
     + Conjugate[USf[k,c1,t,j1]]*(MSf[k,t,j1]^2)
     * IndexDelta[k,l]*dUSf1[l,c2,t,j1],{k,2},{l,2}];

RenConst[ dAf1[2,j1_, j1_] ] := ((dMSfmat1[2, 1, 2, j1]
                  -(Af[2,j1]-Conjugate[MUE]*TB)*dMf1[2,j1])/MLE[j1]
                  +(dMUEC1*TB+dTB1*Conjugate[MUE]));
RenConst[ dAf1[3,j1_, j1_] ] := ((dMSfmat1[2, 1, 3, j1]
                  -(Af[3,j1]-Conjugate[MUE]/TB)*dMf1[3,j1])/MQU[j1]
                  +(dMUEC1/TB-Conjugate[MUE]*dTB1/(TB*TB)));
RenConst[ dAf1[4,j1_, j1_] ] := ((dMSfmat1[2, 1, 4, j1]
                  -(Af[4,j1]-Conjugate[MUE]*TB)*dMf1[4,j1])/MQD[j1]
                  +(dMUEC1*TB+dTB1*Conjugate[MUE]));
RenConst[ dAfC1[j1__]] := Conjugate[dAf1[j1]];


(* Neutralino sector ******************************************)

RenConst[ PiNeuSL[j1_, j2_] ] :=
                    Block[{m2 = MNeu[j2]}, ReTilde[LScalarCoeff[
                    SelfEnergy[F[11, {j2}] -> F[11, {j1}], m2]]]];
RenConst[ PiNeuSR[j1_, j2_] ] :=
                    Block[{m2 = MNeu[j2]}, ReTilde[RScalarCoeff[
                    SelfEnergy[F[11, {j2}] -> F[11, {j1}], m2]]]];

RenConst[ dZNeuL1[j1_, j1_] ] :=
                  Block[{m1 = MNeu[j1]}, FieldRC[F[11, {j1}]][[1]]
                  + (1/(2*m1))*(PiNeuSL[j1, j1] - PiNeuSR[j1,j1])];
RenConst[ dZNeuR1[j1_, j1_] ] :=
                  Block[{m1 = MNeu[j1]}, FieldRC[F[11, {j1}]][[2]]
                  + (1/(2*m1))*(PiNeuSR[j1, j1] - PiNeuSL[j1,j1])];
RenConst[ dZNeuL1[j1_, j2_] ] :=
                        FieldRC[F[11, {j1}], F[11, {j2}]][[1]];
RenConst[ dZNeuR1[j1_, j2_] ] :=
```

69

```
                                FieldRC[F[11, {j1}], F[11, {j2}]][[2]];

RenConst[ PiNeuSLuv[j1_, j2_] ] :=
          Block[{m2 = MNeu[j2]}, ReTilde[LScalarCoeff[
          DivHeader[SelfEnergy[F[11, {j2}] -> F[11, {j1}], m2]]]]];
RenConst[ PiNeuSRuv[j1_, j2_] ] :=
          Block[{m2 = MNeu[j2]}, ReTilde[RScalarCoeff[
          DivHeader[SelfEnergy[F[11, {j2}] -> F[11, {j1}], m2]]]]];


RenConst[ dZNeuL1uv[j1_, j1_] ] :=
        Block[{m1 = MNeu[j1]}, DivHeader[FieldRC[F[11, {j1}]][[1]]]
        + (1/(2*m1))*(PiNeuSLuv[j1, j1] - PiNeuSRuv[j1,j1])];
RenConst[ dZNeuR1uv[j1_, j1_] ] :=
        Block[{m1 = MNeu[j1]}, DivHeader[FieldRC[F[11, {j1}]][[2]]]
        + (1/(2*m1))*(PiNeuSRuv[j1, j1] - PiNeuSLuv[j1,j1])];
RenConst[ dZNeuL1uv[j1_, j2_] ] :=
                DivHeader[FieldRC[F[11, {j1}], F[11, {j2}]][[1]]];
RenConst[ dZNeuR1uv[j1_, j2_] ] :=
                DivHeader[FieldRC[F[11, {j1}], F[11, {j2}]][[2]]];


RenConst[ dZNeuRM1[j1_, j2_] ] := Sum[(1/4)*(dZNeuL1uv[j1, Neu1]
        - Conjugate[dZNeuL1uv[Neu1, j1]])*ZNeu[Neu1, j2], {Neu1, 4}];
RenConst[ dZNeuRMC1[j__] ] := Conjugate[RenConst[dZNeuRM1[j]]];


(* Chargino Sector **********************************************)

RenConst[ PiChaSR[j1_, j2_] ] := Block[{m2 = MCha[j2]}, ReTilde[
        RScalarCoeff[SelfEnergy[F[12, {j2}] -> F[12, {j1}], m2]]]];
RenConst[ PiChaSL[j1_, j2_] ] := Block[{m2 = MCha[j2]}, ReTilde[
        LScalarCoeff[SelfEnergy[F[12, {j2}] -> F[12, {j1}], m2]]]];


RenConst[ dZChaL1[j1_, j1_] ] := Block[{m1 = MCha[j1]},
        FieldRC[F[12, {j1}]][[1]] + (1/(2*m1))
        *(RenConst[PiChaSL[j1, j1]] - RenConst[PiChaSR[j1, j1]])];
RenConst[ dZChaR1[j1_, j1_] ] := Block[{m1 = MCha[j1]},
        FieldRC[F[12, {j1}]][[2]] + (1/(2*m1))
        *(RenConst[PiChaSR[j1, j1]] - RenConst[PiChaSL[j1, j1]])];
RenConst[ dZChaL1[j1_, j2_] ] :=
                        FieldRC[F[12, {j1}], F[12, {j2}]][[1]];
RenConst[ dZChaR1[j1_, j2_] ] :=
                        FieldRC[F[12, {j1}], F[12, {j2}]][[2]];
```

70

```
RenConst[ dUCha1[j1_, j2_] ] := DivHeader[(1/4)*Sum[
  (RenConst[dZChaL1[j1, ii]] - Conjugate[RenConst[dZChaL1[ii, j1]]])
  *UCha[ii, j2],{ii,2}]];
RenConst[ dVCha1[j1_, j2_] ] := DivHeader[(1/4)*Sum[(
  Conjugate[RenConst[dZChaR1[j1, ii]]] - RenConst[dZChaR1[ii, j1]])
  *VCha[ii, j2],{ii,2}]];
RenConst[ dUChaC1[j__] ] := Conjugate[RenConst[dUCha1[j]]];
RenConst[ dVChaC1[j__] ] := Conjugate[RenConst[dVCha1[j]]];


RenConst[ dmCha[j1_] ] := DivHeader[MassRC[F[12, {j1}]]];


RenConst[ dXCha[j1_, j2_] ] :=
          Sum[ dUCha1[k,j1]*MCha[k]*IndexDelta[k,l]*VCha[l,j2]
          + UCha[k,j1]*dmCha[k]*IndexDelta[k,l]*VCha[l,j2]
          + UCha[k,j1]*MCha[k]*IndexDelta[k,l]*dVCha1[l,j2],
          {k,2},{l,2}];


RenConst[ dMUE1 ] := dXCha[2,2];
RenConst[ dMUEC1 ] := Conjugate[dMUE1];


(* h0 - H0 system ***********************************************)

RenConst[ htadh0 ] := SelfEnergy[S[1] -> {}, Mh0];
RenConst[ htadHH ] := SelfEnergy[S[2] -> {}, MHH];
RenConst[ htadHHHH ] := EL/(2 SW MW)*((CA SA^2/SB - CA^2 SA/CB)*htadh0
                                     + (CA^3/CB + SA^3/SB)*htadHH);
RenConst[ htadh0h0 ] := EL/(2 SW MW)*((CA^3/SB - SA^3/CB)*htadh0
                                     + (SA CA^2/SB + SA^2 CA/CB)*htadHH);
RenConst[ htadh0HH ] := EL/(2 SW MW)*((SA CA^2/SB + SA^2 CA/CB)
    *RenConst[htadh0] + (CA SA^2/SB - CA^2 SA/CB)*RenConst[htadHH]);


RenConst[ dZH1[1, 1] ] := FieldRC[S[1]];
RenConst[ dZH1[2, 2] ] := FieldRC[S[2]];
RenConst[ dZH1[1, 2] ] := FieldRC[S[1], S[2]]
                                - RenConst[htadh0HH] 2/(Mh0^2 - MHH^2);
RenConst[ dZH1[2, 1] ] := FieldRC[S[2], S[1]]
                                - RenConst[htadh0HH] 2/(MHH^2 - Mh0^2);


RenConst[ dCA1 ] :=  DivHeader[-SA*(RenConst[dZH1[2, 1]]
                                    - RenConst[dZH1[1, 2]])/4];
```

71

```
RenConst[ dSA1 ] :=  DivHeader[ CA*(RenConst[dZH1[2, 1]]
                                        - RenConst[dZH1[1, 2]])/4];


(* A0 - G0 system ************************************************)

RenConst[ htadA0G0 ] := (EL*((CA*CB + SA*SB)*htadh0
                               + (CB*SA - CA*SB)*htadHH))/(2*MW*SW);

RenConst[ dZH1[3, 3] ] := FieldRC[S[3]];
RenConst[ dZH1[4, 4] ] := FieldRC[S[4]] /.(GaugeRules/.
                                       Options[CreateFeynAmp]);
RenConst[ dZH1[3, 4] ] := (SelfEnergy[S[4] -> S[3], MG0]
                  *2/(MA0^2-MG0^2) - htadA0G0*(2/(MA0^2 - MG0^2)))
                  /.(GaugeRules/.Options[CreateFeynAmp]);
RenConst[ dZH1[4, 3] ] := (SelfEnergy[S[3] -> S[4], MA0]
                  *2/(MG0^2-MA0^2) - htadA0G0*(2/(MG0^2 - MA0^2)))
                  /.(GaugeRules/.Options[CreateFeynAmp]);


RenConst[ dTB1 ] := DivHeader[-TB*(1/(2*MZ*SB*CB))
                  *ReTilde[(-I)*(SelfEnergy[S[3] -> V[2], MA0])]];

RenConst[ dSB1 ] := SB*CB^2*(dTB1/TB);
RenConst[ dCB1 ] := (-CB)*SB^2*(dTB1/TB);
RenConst[ dSB21 ] := 2*SB*dSB1;
RenConst[ dCB21 ] := 2*CB*dCB1;

RenConst[ dSAB1 ] := dSA1*CB + SA*dCB1 + dCA1*SB + CA*dSB1;
RenConst[ dCAB1 ] := dCA1*CB + CA*dCB1 - dSA1*SB - SA*dSB1;

RenConst[ dSBA1 ] := dSB1*CA + SB*dCA1 - dCB1*SA - CB*dSA1;
RenConst[ dCBA1 ] := dCB1*CA + CB*dCA1 + dSB1*SA + SB*dSA1;

RenConst[ dS2B1 ] := 2*C2B*dTB1*CB2;
RenConst[ dTB21 ] := 2*TB*dTB1;



(* H- - G- system ************************************************)

RenConst[ dZHp1[1, 1] ] := FieldRC[S[5]];
RenConst[ dZHp1[2, 2] ] := FieldRC[S[6]]
                          /. (GaugeRules /. Options[CreateFeynAmp]);
```

72

```
RenConst[ dZHp1[1, 2] ] := (SelfEnergy[S[6] -> S[5], MGp]
                *2/(MHp^2-MGp^2) - htadA0G0*(2/(MHp^2 - MGp^2)))
                /.(GaugeRules/.Options[CreateFeynAmp]);
RenConst[ dZHp1[2, 1] ] := (SelfEnergy[S[5] -> S[6], MHp]
                *2/(MGp^2-MHp^2) - htadA0G0*(2/(MGp^2 - MHp^2)))
                /.(GaugeRules/.Options[CreateFeynAmp]);
```

B.2   MassRC.m

The following is needed for calculation of on-shell masses.

```
RenConst[ htadh0os ] := SelfEnergy[S[1] -> {}, Mh0];
RenConst[ htadHHos ] := SelfEnergy[S[2] -> {}, MHH];
RenConst[ htadHHHHos ] := EL/(2 SW MW)*((CA SA^2/SB - CA^2 SA/CB)
                            *htadh0os + (CA^3/CB + SA^3/SB)*htadHHos);
RenConst[ htadh0h0os ] := EL/(2 SW MW)*((CA^3/SB - SA^3/CB)
                    *htadh0os + (SA CA^2/SB + SA^2 CA/CB)*htadHHos);
RenConst[ htadA0A0os ] := (EL*((-SB^2*SA/CB + CB^2*CA/SB)
        *htadh0os + (SB^2*CA/CB + CB^2*SA/SB)*htadHHos))/(2*MW*SW);

RenConst[ dMT1os ] := MassRC[F[3,{3}]]


RenConst[ dMGlos ] := MassRC[F[15]]
RenConst[ dMSf21os[1, 1, j1_] ] := MassRC[S[11, {j1}]];
RenConst[ dMSf21os[2, 1, j1_] ] := 0;
RenConst[ dMSf21os[c1_, ftype_, j1_] ] :=
                                  MassRC[S[10 + ftype, {c1, j1}]];
RenConst[ dmNeuos[j1_] ] := MassRC[F[11, {j1}]];
RenConst[ dmChaos[j1_] ] := MassRC[F[12, {j1}]];


RenConst[ dMh021os ] := MassRC[S[1]] - htadh0h0os;
RenConst[ dMHH21os ] := MassRC[S[2]] - htadHHHHos;
RenConst[ dMA021os ] := MassRC[S[3]] - htadA0A0os;
RenConst[ dMHp21os ] := MassRC[S[5]] - htadA0A0os;
```

Appendix C

$\triangle_b$

We will discuss the case with real parameters. The relation between the bare mass m_b^0 and the renormalized mass m_b^R is given by

$$m_b^0 = m_b^R + \delta m_b^R \qquad (C.1)$$

C.1 gluino - sbottom loop

$$
\begin{aligned}
\delta m_b^{(\tilde{g},\tilde{b})} &= -\frac{\alpha_s}{3\pi} m_{\tilde{g}} \Bigg[\sum_{s=1}^{2} B_0(m_b^2, m_{\tilde{g}}^2, m_{\tilde{b}_s}^2) R_{s2}^{\tilde{b}} R_{s1}^{\tilde{b}*} \; \mathrm{SqrtEgl}^2 \\
&\quad + \sum_{s=1}^{2} B_0(m_b^2, m_{\tilde{g}}^2, m_{\tilde{b}_s}^2) R_{s1}^{\tilde{b}} R_{s2}^{\tilde{b}*} \; \mathrm{SqrtEglC}^2 \Bigg] + \ldots \qquad (C.2)
\end{aligned}
$$

with

$$R^{\tilde{b}} = \begin{pmatrix} \cos\theta_b & \sin\theta_b \\ -\sin\theta_b & \cos\theta_b \end{pmatrix} \qquad (C.3)$$

$$\delta m_b^{(\tilde{g},\tilde{b})} = -\frac{\alpha_s}{3\pi} m_{\tilde{g}} \sin(2\theta_b) \left[B_0(m_b^2, m_{\tilde{g}}^2, m_{\tilde{b}_1}^2) - B_0(m_b^2, m_{\tilde{g}}^2, m_{\tilde{b}_2}^2) \right] \mathrm{SqrtEgl}^2 + .. \;(C.4)$$

$$
\begin{aligned}
M_b^2 &= \begin{pmatrix} m_{bL}^2 & a_b m_b \\ a_b m_b & m_{bR}^2 \end{pmatrix} = R^{\tilde{b}\dagger} \begin{pmatrix} m_{\tilde{b}1}^2 & 0 \\ 0 & m_{\tilde{b}2}^2 \end{pmatrix} R^{\tilde{b}} \\
&\Rightarrow \quad \sin(2\theta_b) = \frac{2 m_b A_b - \mu \tan\beta}{m_{\tilde{b}1}^2 - m_{\tilde{b}2}^2} \qquad (C.5)
\end{aligned}
$$

$$\delta m_b^{(\tilde{g},\tilde{b})} = \frac{\alpha_s}{3\pi} m_{\tilde{g}} \frac{2 m_b \mu \tan\beta}{m_{\tilde{b}1}^2 - m_{\tilde{b}2}^2} \left[B_0(m_b^2, m_{\tilde{g}}^2, m_{\tilde{b}_1}^2) - B_0(m_b^2, m_{\tilde{g}}^2, m_{\tilde{b}_2}^2) \right] \mathrm{SqrtEgl}^2 + ..(C.6)$$

with

$$\frac{1}{m_{\tilde{b}1}^2 - m_{\tilde{b}2}^2} \left[B_0(0, m_{\tilde{g}}^2, m_{\tilde{b}_1}^2) - B_0(0, m_{\tilde{g}}^2, m_{\tilde{b}_2}^2) \right] = I(m_{\tilde{b}_1}^2, m_{\tilde{b}_2}^2, m_{\tilde{g}}^2) \tag{C.7}$$

where

$$I(a^2, b^2, c^2) = \frac{1}{(a^2 - b^2)(b^2 - c^2)(a^2 - c^2)} \left(a^2 b^2 \log \frac{a^2}{b^2} + b^2 c^2 \log \frac{b^2}{c^2} + c^2 a^2 \log \frac{c^2}{a^2} \right) \tag{C.8}$$

$$\delta m_b^{(\tilde{g}, \tilde{b})} = -\frac{2\alpha_s}{3\pi} m_{\tilde{g}} m_b \mu \tan \beta I(m_{\tilde{b}_1}^2, m_{\tilde{b}_2}^2, m_{\tilde{g}}^2) \mathrm{SqrtEgl}^2 + \dots \tag{C.9}$$

C.2 chargino - stop loop

For sizeable values of the trilinear soft SUSY- breaking parameter A_t, the supersymmetric electroweak corrections are dominated by the charged higgsino-stop contribution. The wino-sbottom contributions are generally smaller [55].

part 1

$$\delta m_b^{(\tilde{\chi}^+, \tilde{t})} = \frac{h_t h_b}{32\pi^2} \sum_{c=1}^{2} \sum_{s=1}^{2} m_{\tilde{\chi}_c^+} B_0(m_b^2, m_{\tilde{\chi}_c^+}^2, m_{\tilde{t}_s}^2)$$
$$\left[U_{c2} V_{c2} R_{s1}^{\tilde{t}} R_{s2}^{\tilde{t}*} + U_{c2}^* V_{c2}^* R_{s2}^{\tilde{t}} R_{s1}^{\tilde{t}*} \right] + \dots \tag{C.10}$$

We simplify the expression by setting the chargino masses to M_2 and μ. This simplification is a good approximation [55]. The unitary matrices U and V (orthonormal matrices in real case) can be written in the following form

$$V = \begin{pmatrix} \cos \theta_V & \sin \theta_V \\ -\sin \theta_V & \cos \theta_V \end{pmatrix}, \qquad U = \begin{pmatrix} \cos \theta_U & \sin \theta_U \\ -\sin \theta_U & \cos \theta_U \end{pmatrix} \tag{C.11}$$

By solving the matrix equation

$$\begin{pmatrix} M_2 & \sqrt{2} m_W \sin \beta \\ \sqrt{2} m_W \cos \beta & \mu \end{pmatrix} = X = U^\top \begin{pmatrix} M_2 & 0 \\ 0 & \mu \end{pmatrix} V \tag{C.12}$$

we obtain

$$\cos \theta_U \sin \theta_V = \frac{\sqrt{2} m_W (M_2 \sin \beta + \mu \cos \beta)}{M_2^2 - \mu^2}$$

$$\cos \theta_V \sin \theta_U = \frac{\sqrt{2} m_W (\mu \sin \beta + M_2 \cos \beta)}{M_2^2 - \mu^2}$$

$$\cos \theta_V \cos \theta_U = 1$$

$$\sin \theta_V \sin \theta_U = 0 \tag{C.13}$$

Since $U_{12}V_{12} = 0$ we get

$$\delta m_b^{(\tilde{\chi}^+,\tilde{t})} = \frac{h_t h_b}{32\pi^2}\mu\sin(2\theta_t)\left[B_0(m_b^2,\mu^2,m_{\tilde{t}_1}^2) - B_0(m_b^2,\mu^2,m_{\tilde{t}_2}^2)\right] + \dots \quad \text{(C.14)}$$

using relations

$$h_t h_b = h_t^2 \tan\beta \frac{m_b}{m_t} \quad \text{(C.15)}$$

$$\sin(2\theta_t) = \frac{2m_t(A_t - \mu\cot\beta)}{m_{\tilde{t}_1}^2 - m_{\tilde{t}_2}^2} \quad \text{(C.16)}$$

we finally obtain

$$\delta m_b^{(\tilde{\chi}^+,\tilde{t})} = -\frac{h_t^2}{16\pi^2}\mu m_b \frac{(A_t\tan\beta - \mu)}{m_{\tilde{t}_1}^2 - m_{\tilde{t}_2}^2} I(m_{\tilde{t}_1}^2, m_{\tilde{t}_2}^2, \mu^2) + \dots \quad \text{(C.17)}$$

part 2

$$\delta m_b^{(\tilde{\chi}^+,\tilde{t})} = -\frac{e h_b}{32\pi^2 s_w}\sum_{c=1}^{2}\sum_{s=1}^{2} m_{\tilde{\chi}_c^+} B_0(m_b^2, m_{\tilde{\chi}_c^+}^2, m_{\tilde{t}_s}^2)$$

$$\left[U_{c2}V_{c1}R_{s1}^{\tilde{t}}R_{s1}^{\tilde{t}*} + U_{c2}^*V_{c1}^*R_{s1}^{\tilde{t}}R_{s1}^{\tilde{t}*}\right] + \dots \quad \text{(C.18)}$$

using the identity

$$\frac{e}{s_w}h_b\sqrt{2}m_W = m_b\frac{g_2^2}{\cos\beta} \quad \text{(C.19)}$$

we obtain

$$\delta m_b^{(\tilde{\chi}^+,\tilde{t})} = \frac{m_b g_2^2 \cos\theta_t^2}{16\pi^2(\mu^2 - M_2^2)}\left[M_2(\mu\tan\beta + M_2)B_0(m_b^2, M_2^2, m_{\tilde{t}_1}^2)\right.$$

$$\left. -\mu(M_2\tan\beta + \mu)B_0(m_b^2, \mu^2, m_{\tilde{t}_1}^2)\right]$$

$$+ \frac{m_b g_2^2 \sin\theta_t^2}{16\pi^2(\mu^2 - M_2^2)}\left[M_2(\mu\tan\beta + M_2)B_0(m_b^2, M_2^2, m_{\tilde{t}_2}^2)\right.$$

$$\left. -\mu(M_2\tan\beta + \mu)B_0(m_b^2, \mu^2, m_{\tilde{t}_2}^2)\right]$$

$$+ \dots \quad \text{(C.20)}$$

collecting only the terms proportional to $\tan\beta$ and neglecting the bottom mass in the Passarino-Veltman integral B_0, the final form reads

$$\delta m_b^{(\tilde{\chi}^+,\tilde{t})} = \frac{m_b g_2^2}{16\pi^2}\mu M_2 \tan\beta\left[\cos\theta_t^2 I(m_{\tilde{t}_1}^2, M_2^2, \mu^2) + \sin\theta_t^2 I(m_{\tilde{t}_2}^2, M_2^2, \mu^2)\right] + \dots$$

$$\text{(C.21)}$$

Bibliography

[1] Y. A. Gol'fand, E. P. Likhtman, JETP Lett. 13 (1971) 323.

[2] D. V. Volkov, V. P. Akulov, JETP Lett. 16 (1972) 438.

[3] J. Wess, B. Zumino, Nucl. Phys. B 70 (1974) 39.

[4] S. R. Coleman, J. Mandula, Phys. Rev. 159 (1967) 1251.

[5] R. Haag, J. T. Lopuszanski, M. Sohnius, Nucl. Phys. B 88 (1975) 257.

[6] J. Wess, J. Bagger: *Supersymmetry and Supergravity*, Princeton University Press, 1992

[7] H. J. W. Müller-Kirsten, A. Wiedemann: *Supersymmetry: An Introduction with Conceptual and Calculational Details*, World Scientific, Singapore, 1987

[8] D. Bailin, A. Love: *Supersymmetric Gauge Field Theory and String Theory*, IOP Publishing Ltd, 1994

[9] G. Kane, Physics Today 63 (2010) 39.

[10] D. J. H. Chung, L. L. Everett, G. L. Kane, S. F. King, J. Lykken, Lian-Tao Wang, Phys. Rept. 407 (2005) 1 [arXiv:hep-ph/0312378v1]; M. C. Rodriguez, 2009, [arXiv:hep-ph/0911.5338v1]

[11] P. Nath, R. Arnowitt, Phys. Lett. B 56 (1975) 177; D. Z. Freedman, P. van Nieuwenhuizen, S. Ferrara, Phys. Rev. D 13 (1976) 3214; S. Deser, B. Zumino, Phys. Lett. B 62 (1976) 335.

[12] U. Amaldi, W. de Boer, H. Fürstenau, Phys. Lett. B 260 (1991) 447.

[13] K. Inoue, A. Komatsu, S. Takeshita, Prog. Theor. Phys. 68 (1982) 927; Prog. Theor. Phys. 70 (1983) 330.

[14] V. Barger, M. S. Berger, P. Ohmann, Phys. Rev. D 47 (1993) 1093; W. de Boer, R. Ehret, D. Kazakov, Z. Phys. C 67, (1995) 647; W. de Boer et al., Z. Phys. C 71 (1996) 415.

[15] H. Pagels, J. R. Primack, Phys. Rev. Lett. 48 (1982) 223; H. Goldberg, Phys. Rev. Lett. 50 (1983) 1419.

[16] L. E. Ibañez, G. G. Ross, Phys. Lett. B 131 (1983) 335; B. Pendleton, G. G. Ross, Phys. Lett. B 98 (1981) 291.

[17] S. Dimopoulos, S. Raby, F. Wilczek, Phys. Rev. D 24 (1981) 1681; S. Dimopoulos, H. Georgi, Nucl. Phys. B 193 (1981) 150; L. E. Ibañez, G. G. Ross, Phys. Lett. B 105 (1981) 439; M. B. Einhorn, D. R. T. Jones, Nucl. Phys. B 196 (1982) 475.

[18] G. L. Kane, C. Kolda, J. Wells, Phys. Rev. Lett. 70 (1993) 2686 [arXiv:hep-ph/9210242]; J. R. Espinosa, M. Quiros, Phys. Lett. B 302 (1993) 51 [arXiv:hep-ph/9212305].

[19] H. E. Haber and G. L. Kane, Phys. Rep. 117 (1985) 75.

[20] H. Hluchá, *QCD corrections to the neutralino decay to an antisbottom and a bottom quark within MSSM*, Master thesis, 2007.

[21] K. Kovařík, *Precise Predictions for Sfermion Pair Production at a Linear Collider*, PhD thesis, 2005; W. Öller, *Precise Predictions for Neutralino and Chargino Pair Production in Supersymmetry*, PhD thesis, 2005; Ch. Weber, *Electroweak Corrections to Higgs Boson Decays into Sfermions in the Minimal Supersymmetric Standard Model*, PhD thesis, 2005, [URL:http://wwwhephy.oeaw.ac.at/susy/englversthesesanddis.htm].

[22] S. P. Martin, 2008 [arXiv:hep-ph/9709356v5].

[23] The CMS Collaboration, submitted to Phys. Lett. B (2011) [arXiv:hep-ex/1101.1628v1].

[24] The ATLAS Collaboration, submitted to Phys. Rev. Lett. (2011) [arXiv:hep-ex/1102.2357v2].

[25] K. Nakamura et al. (Particle Data Group), JPG 37 (2010) 075021 [URL:http://pdg.lbl.gov].

[26] O. Buchmueller et al., DESY-10-249, CERN-PH-TH-2010-321, KCL-PH-TH-2011-04, 2011 [arXiv:hep-ph/1102.4585].

[27] S.-S. Yu (for the CDF and D0 collaboration), Presented at HCP2008 [arXiv:hep-ex/0905.2285v1].

[28] A. Arbey, A. Deandrea, A. Tarhini, CERN-PH-TH-2011-052, LYCEN-2011-01, 2011 [arXiv:hep-ph/1103.3244v1].

[29] ATLAS Technical Design Report, CERN/LHCC/99-15, ATLAS TDR 15 (1999); CMS Technical Proposal, CERN/LHCC/94-38 (1994).

[30] J.A. Aguilar-Saavedra *et al.*, TESLA Technical Design Report, DESY 01-011, [arXiv:hep-ph/0106315]; T. Abe *et al.* [American LC WG], in *Proceedings of the APS/DPF/DPB Summer Study on the Future of Particle Physics (Snowmass 2001)* , SLAC-R-570, [arXiv:hep-ex/0106055-58]; T. Abe *et al.* [Asian LC WG], KEK-Report–2001-011, [arXiv:hep-ph/0109166].

[31] LHC/LC Study Group, G. Weiglein *et al.*, *LHC+LC Report*, Phys. Rept. 426 (2006) 47 [arXiv:hep-ph/0410364].

[32] C. Itzykson, J.-B. Zuber, *Quantum Field Theory*, Dover Publications, 2006.

[33] M. E. Peskin, D. V. Schroeder: *An Introduction to Quantum Field Theory*, Addison-Wesley Publishing Company, 1995.

[34] G 't Hooft, M. J. G. Veltman, Nucl. Phys. B 44 (1972) 189.

[35] G 't Hooft, M. J. G. Veltman, Nucl. Phys. B 153 (1979) 365.

[36] G. Passarino, M. J. G. Veltman, Nucl. Phys. B 160 (1979) 151.

[37] J. Collins, *Renormalization*, Cambridge Univ. Press, 1984.

[38] H. Eberl, *Strahlungskorrekturen im minimalen supersymmetrischen Standardmodell*, PhD thesis, 1998
[URL:http://wwwhephy.oeaw.ac.at/helmut].

[39] W. Siegel, Phys. Lett. B 84(1979) 193.

[40] T. Hahn, M. Perez-Victoria, Comp. Phys. Comm. 118 (1999) 153 [arXiv:hep-ph/9807565v1].

[41] M. Böhm, A. Denner, H. Joos, *Gauge Theories of the Strong and Electroweak Interaction*, Teubner Verlag, 2001.

[42] M. Steinhauser: *Übungen zu Strahlungskorrekturen in Eichtheorien*, Herbstschule für Hochenenergiephysik, Maria Laach 2003.

[43] A. Kraft, *Produktion geladener Higgs-Bosonen in Erweiterungen des Stan-dardmodells*, PhD thesis (in german), 1999; T. Blank, *Strahlungskorrekturen zur Chargino- und Neutralinoproduktion in e+e- und Hadronkollisionen*, PhD thesis (in german), 2000, [URL:http://www-itp.particle.uni-karlsruhe.de/phd.de.shtml]; T. Fritzsche, *Berechnung von Observablen zur supersymmetrischen Teilchenerzeugung an Hochenergie-Collidern unter Einschluss höherer Ordnungen*, PhD thesis (in german), 2005.

[44] A. Denner, Fortschr. Phys. 41 (1993) 307 [arXiv:hep-ph/0709.1075v1].

[45] M. Bohm, H. Spiesberger, W. Hollik, Fortsch. Phys. 34 (1986) 687; W. Hollik, Fortsch. Phys. 38 (1990) 165; .

[46] F. Jegerlehner, *Renormalizing the standard model*, In the Proceedings of Testing the Standard Model - TASI-90, 1990.

[47] P. H. Chankowski, S. Pokorski, J. Rosiek, Nucl. Phys. B 423 (1994) 437 [arXiv:hep-ph/9303309].

[48] A. Dabelstein, Z. Phys. C 67 (1995) 495 [arXiv:hep-ph/9409375]; A. Dabelstein, Nucl. Phys. B 456 (1995) 25 [arXiv:hep-ph/9503443].

[49] D. Pierce, A. Papadopoulos, Phys. Rev. D 47 (1993) 222 [arXiv:hep-ph/9206257].

[50] N. Baro, F. Boudjema, A. Semenov, Phys. Rev. D 78 (2008) 115003 [arXiv:hep-ph/0807.4668]; N. Baro, F. Boudjema, Phys. Rev. D 80 (2009) 076010 [arXiv:hep-ph/0906.1665].

[51] ATLAS Technical Design Report, CERN/LHCC/99-15, ATLAS TDR 15 (1999); CMS Technical Proposal, CERN/LHCC/94-38 (1994).

[52] J.A. Aguilar-Saavedra *et al.*, TESLA Technical Design Report, DESY 01-011, [arXiv:hep-ph/0106315]; T. Abe *et al.* [American LC WG], in *Proceedings of the APS/DPF/DPB Summer Study on the Future of Particle Physics (Snowmass 2001)* , SLAC-R-570, [arXiv:hep-ex/0106055-58]; T. Abe *et al.* [Asian LC WG], KEK-Report–2001-011, [arXiv:hep-ph/0109166].

[53] LHC/LC Study Group, G. Weiglein *et al.*, *LHC+LC Report*, Phys. Rept. 426 (2006) 47 [arXiv:hep-ph/0410364].

[54] A. Denner, H. Eck, O. Hahn, J. Kublbeck, Nucl. Phys. B 387 (1992) 467.

[55] M. Carena, D. Garcia, U. Nierste, C.E.M. Wagner, Nucl. Phys. B (2000) 577 [arXiv:hep-ph/9912516]; D. M. Pierce, J. A. Bagger, K. T. Matchev, R.-J. Zhang, Nucl. Phys. B 491 (1997) 3 [arXiv:hep-ph/9606211]; J. Girrbach, S. Mertens, U. Nierste, S. Wiesenfeldt, JHEP 1005 (2010) 026 [arXiv:hep-ph/0910.2663].

[56] T. Hahn, Comp. Phys. Comm. 140 (2001) 418 [arXiv:hep-ph/0012260]; T. Hahn, C. Schappacher, Comp. Phys. Comm. 143 (2002) 54 [arXiv:hep-ph/0105349].

[57] N. Baro, F. Boudjema, A. Semenov, Phys. Rev. D78 (2008) 115003 [arXiv:hep-ph/0807.4668v2].

[58] N. Baro, F. Boudjema, Phys. Rev. D80 (2009) 076010 [arXiv:hep-ph/0906.1665v2].

[59] J. Fujimoto, T. Ishikawa, M. Jimbo, T. Kaneko, T. Kon, Y. Kurihara, M. Kuroda and Y. Shimizu, Nucl. Phys. Proc. Suppl. (2006) 157.

[60] H. Hlucha, H. Eberl, W. Frisch, submitted to Comp. Phys. Comm. [arXiv:hep-ph/1104.2151v2]. The tool SFOLD can be downloaded from http:/www.hephy.at/tools.

[61] H. Eberl, W. Frisch, H. Hlucha, Nucl. Phys. Proc. Suppl. (2010) 277.

[62] W. Frisch, H. Eberl, H. Hlucha, Comp. Phys. Comm. 182 (2011) 2219 [arXiv:hep-ph/1012.5025v1].

[63] J. A. Aguilar-Saavedra *et al.*, Eur. Phys. J C46 (2006) 43; J. Kalinowski, Acta Phys. Polon. B37 (2006) 1215 [arXiv:hep-ph/0511344].

[64] P. Skands et al., JHEP 0407 (2004) 36.

[65] J. Guasch, W. Hollik, J. Sola, JHEP (2002) 0210:040 [arXiv:hep-ph/0207364].

[66] L. G. Jin, Ch. S. Li, Phys. Rev. D65 (2002) 035007 [arXiv:hep-ph/0106253].

[67] A. Bartl, H. Eberl, K. Hidaka, S. Kraml, W. Majerotto, W. Porod, Y. Yamada, Phys. Rev. D59 (1999) 115007 [arXiv:hep-ph/9806299].

[68] A. Bartl, H. Eberl, K. Hidaka, S. Kraml, W. Majerotto, W. Porod, Y. Yamada, Phys. Lett. B419 (1998) 243 [arXiv:hep-ph/9710286].

[69] W. Beenakker, R. Hopker, P.M. Zerwas, Phys. Lett. B378 (1996) 159 [arXiv:hep-ph/9602378].

[70] H. Lehmann, K. Symanzik and W. Zimmermann, Nuovo Cimento 1 (1955) 1425.

[71] S. Weinberg, *The Quantum Theory of Fields*, Cambridge University Press, 1995.

[72] Y. Zhou, Mod. Phys. Lett. A 21 (2006) 2763, [arXiv:hep-ph/0502186v7].

[73] A. Denner, S. Dittmaier, Nucl. Phys. Proc. Suppl. 160 (2006) 22 [arXiv:hep-ph/0605312v1].

Lebenslauf

Personalien

Name:	Hana Hluchá
Geburtsdatum:	21. Februar 1984
Geburtsort	Trnava, Slowakei
Eltern	Ján Hluchý, Olga Hluchá

Bildungsgang

1997 - 2002 Gymnasium in Trnava

2002 - 2007 Magister studium - Comenius University in Bratislava

2007 - 2009 Early stage researcher, HEPTOOLS - EU projekt MRTN-CT-2006-035505

Auslandsaufenthalte

III Graduate School on Physics at Colliders
7-11 Januar 2008, Torino, Italy

PSI Summerschool on Particle Physics
13-19 Juli 2008, Zuoz, Switzerland

Physics at One Loop
14-21 September 2008, Svit, Slowakei

HEPTOOLS Midterm Meeting
9-12 Marz 2009, Lisbon, Portugal

MC4LHC: from Parton Showers to NNLO
4-8 Mai 2009, CERN, Switzerland